SECOND NATIONAL COMMUNICATION
ON CLIMATE CHANGE

Climate Scenarios for Peru to 2030

PNUD

GLOBAL ENVIRONMENT FACILITY

Senamhi

CLIMATE SCENARIOS FOR PERU TO 2030

SENAMHI
National Meteorology and Hydrology Service
Numerical Prediction Center – CPN
http://www.senamhi.gob.pe

Authors: Guillermo Obregón,
Amelia Díaz
Gabriela Rosas
Grinia Avalos
Delia Acuña
Clara Oria
Alan Llacza
Richard Miguel

Year: 2009

Edition: SENAMHI

The present publication is part of the Vulnerability and Adaptation Component within the framework of the Second National Communication on Climate Change to the UNFCCC, financed by the GEF and Coordinated by the Ministry of Environment of Peru.

Ministry Environment – MINAM
Av. Guardia Civil 205, San Borja, Lima.
Telephone: (51 – 1) 2255370 - Fax:2255369
http://www.minam.gob.pe

National Meteorology and Hidrology Service – SENAMHI
Jr. Cahuide 785 Jesús María
Telephone: (51 – 1) 6141414 (central) and 6141408 (CPN)
http://www.senamhi.gob.pe

Legal Deposit:

Design	: Q&P Impresores
Graphic Director	: Ricardo Eslava Escobar
Digital edition	: Hugo Negreiros Bezada
Style	: Carlos Canales Zubizarreta
Printing	: xxxxxxxxxx
First Edition	: January 2009
First Issue	:

Printed in Perú
2009

PERÚ | Ministry Environment -MInAM | National Meteorology and Hidrology Service - SENAMHI

SECOND NATIONAL COMMUNICATION ON CLIMATE CHANGE

Climate Scenarios for Peru to 2030

MINISTRY OF ENVIRONMENT

Dr. Antonio José Brack Egg
Minister

Vice-minister for Strategic Development and Natural Resources
Eng. Vanessa Vereau Ladd
Project National Director

General Director for Climate Change, Desertification and Water Resources
Eduardo Durand López-Hurtado
Alternate National Director

Executive President SENAMHI
Mag. FAP (ret.) Wilar Gamarra Molina

EXECUTING UNIT OF THE PROJECT

General Coordinator: **Jorge Álvarez Lam**

Vulnerability and Adaptation Coordinator: **Laura Avellaneda Huamán**

Inventories and Mitigation Coordinator: **Rafael Millán García**

Communications Coordinator: **Luisa Gómez Elías / Jenny Chimayco Ortega**

Administrator: **Kelvin Orbegoso Contreras**

Assistant: **Ruth Camayo Suárez**

PNUD

PRESENTATION

ACKNOWLEDGEMENTS

The working team wishes to express its appreciation:

To Dr. Guillermo Obregón, prominent scientist, who has an outstanding career from the Centro de Previsión del Tiempo y Pesquisas Espaciales – CPTEC Brazil, for sharing his knowledge and invaluable experience to develop the present study and for providing his important comments and suggestions and permanent encourage for the work done.

Reiterate our appreciation to the National Center for Atmospheric Research – NCAR of the United States of America, for providing the information used as basis for the generation of regional scenarios, which have been the essential information to develop this study.

The Max Planck Institute – MPI from Germany, for providing climate scenario information from the ECHAM model.

The Scientific Modeling Center form the University of Zulia, in Venezuela.

The University of Zulia, Deputy Director of the Scientific Modeling Center of Venezuela.

Eng. Juan Guerrero, advisor from the Regional Government of Ancash, for his valuable and important contributions to the development of the study on the Santa river basin.

The group of the Project Execution Unit of the Ministry of Environment and to the implementing agencies of the SNCCC.

Amelia Díaz Pabló
Technical-Administrative Director of the Project
National Meteorology and Hydrology Service

INDEX

CHAPTER 1

INTRODUCTION

INTRODUCTION

The IPCC Fourth Assessment Report (AR4 as per its English acronym, IPCC 2007) unequivocally points out, unlike the Third Assessment Report (TAR, as per its acronym in English, IPCC, 2001), that the climate systems is warming up; also, this anomaly is the response to human activity because of the increase of greenhouse gases emissions (GHG). The certainty of this statement implies a series of questions about the consequences these processes of global scale will cause at a regional and local level in each country, with a higher or lower level of vulnerability. Global climate change will undoubtedly generate severe impacts on less prepared societies, affecting the sustainable development of their socio-economic activities in the future.

Peru is aware of this problem, more and more intense extreme events have been frequently observed in the last decade, such as the snowfalls in 2004 in the southern part of the country, that caused severe economic loss, or floods in San Martin in December 2006, or the early frosts in Huancayo in 2007; that even though we can't directly relate them to climate change, they give us a good perception that climate variability is been modified. On this matter, national studies indicate that there are some pronounced diminishing trends in precipitation in some regions of the country, such in the Mantaro River basin, that registers a diminish from 5 to 54mm/decade; or opposite situations, such as the increase of rainfall observed in the Urubamba River basin, with values that range between 7 to 85 mm/decade; these results, based on the observation of almost 40 years of records, are indicators of possible changes in climate patterns that are directly or indirectly related to global warming (PRAA, 2007)

On this matter, there are also some other processes that we know are directly related to the increase of global temperature: glacial retreat. At a global level, Peru has more than 75% of the tropical glaciers, witnessing the accelerated retreat of some of the most important glaciers at national level, Pastoruri, in the central mountain range, Chachani, Coropuna and Misti in Arequipa. The critical part of this glacier vanishing is that most of them, besides being unique high mountain ecosystems, are mainly a source of water for a series of socio-economic demands in all of the surrounding basins: for human consumption, generation of electric power, agriculture, industry etc.

The regional impacts of global climate change are not completely known, the uncertainties associated to the knowledge of climate are so large in the case of our country for its Andean character. The Andes Mountain Range generates in our territory a vast diversity of climates and microclimates that respond to global climate change in several different ways; besides, considering that a significant part of our territory does not have observations of meteorological variables for long periods of time, the certainty to know how does climate works at high mountain regions or the Amazon region is not very conclusive.

Lately, however there has been made significant progress in the scientific and technological field to improve our understanding and modeling of climate system, which will allow us to know better its current situation and estimate its future situation in a more reliable way.

Progress has been made in improvements by incorporating physics-mathematic into models (atmosphere general circulation models) and nowadays, it allows us to have available basic information for the assessment of vulnerability and adaptation in regions vulnerable to climate change impacts. The GCMs simulate the dynamics of the climate system, considering the different GHGs emissions scenarios; generating at the same time different climate scenarios. To carry out these processes a solid capacity in computing is required, that only the most important World Climate Modeling Centers have; but in order to be able to use them in the evaluations of vulnerability it is necessary to take some intermediate steps, since the information coming form these GCMs have a very low spatial resolution that ranges form 100 to 300 Km which represents a

serious limitation for the Andean countries, due to the complexity of its topography, analysis at regional and local scales are required. The intermediate steps imply the use of a series of methodologies to obtain the required details, based on the global information of the Global Circulation Models (GCMs), obtaining regional climate scenarios that would describe the impacts of climate change associated to the proper characteristics of the area under study, such a basin, a department or a district. Finally, this generated information is important to develop better vulnerability assessments and to establish the most adequate adaptation measures for planning socio-economic activities that might be affected in the future.

In this sense, inter-institutional studies, such as the National Program for Capacity Strengthening to Manage the Impacts of Climate Change and Air Pollution (PROCLIM- 2005) and regional studies, as the Regional Andean Program for the Adaptation to Climate Change (PRAA-2007) executed by the National Environment Council (CONAM), the current Ministry of Environment, have allowed to generate useful information to determine the present and future vulnerability in specific regions; and adaptation measures according to the local characteristics of the areas under study, as the IPCC states in its AR4, in which it recognizes the importance of generating regional information.

The present study aims at generating detailed information on the possible impacts of climate change, to attend the requirements of the different national socio-economic sectors that need information on the current and future climate conditions and how it determines the changes in their own sectors, i.e., in agriculture, transportation, availability of electric power, economy, etc. The present analysis, made at national level, will provide information concerning the trends and indicators of extreme climate events , extreme temperatures and precipitation based on the last 40 years and their behavior in the future, based on CO2 emissions scenarios, considering the A2 scenario as the most pessimist of all. It is important to state that each step in the elaboration process of regional climate scenarios considers an uncertainty aspect, for both the limited knowledge on climate variability and for the methods used to generate information at regional level, which in turn adds some errors in step of the process, for this reason, the generated results must be used adequately as climate projections, under the assumption of a dramatic greenhouse gases emission. Finally, these results will allow to improve our knowledge on the vulnerability of our country and to guide policy makers on adequate adaptation measures to face climate change at national level and this way contribute to the Millennium Development Objectives.

1.1 OBJECTIVES

The objectives of the present study are:

- Determine the current climate trends at national level based on observed data.
- Estimate the climate projections at national level TO the year 2030, based on global climate scenarios, using statistical and dynamic downscaling techniques for the A2 emission scenario (high emissions).
- Evaluate extreme indicators for rainfall and temperature, both observed and simulated to the year 2030.

1.2 THEORETICAL FRAMEWORK

Climate is a description in terms of mean values of temperature, humidity, rainfall and wind variability, of a certain location or region, in a relatively long period of time, such as 30 years, according to the World Meteorological Organization. Also, it is the result of a complex interaction between the five components of the climate system: the atmosphere, the biosphere, the hydrosphere, the cryosphere and the land surface. They maintain a natural dynamics generating variations at different time scales, events as El Niño/La Niña

that lasts several years or events as the glacial age, that lasts much longer periods of time as thousands or millions of years and are possibly interrupted only by natural causes, such as volcanoes eruptions and variations in solar emissions or by human activity.

The United Nations Framework Convention on Climate Change (UNFCCC) defines climate change as a change of climate which is attributed directly or indirectly to human activity, and in the last decades the scientific community has found evidence of a relation between climate change and the increase in greenhouse gases emissions (GHGs) caused mainly by industrialized societies because of the use of fossil fuels. This Chapter gives the reader some information on the current and future trends of global climate, based on the IPCC Fourth Assessment Report (2007).

1.2.1. Current situation of climate change at global level

In 2007, the IPCC concluded that it is "very likely" (higher than 90% of probability) that the increase of greenhouse gases generated by human activities have caused most of the increases observed in the global average temperature since the middle of the XX century, and that it is "extremely unlikely" that it has been caused only by climate variability without forcings. It has been observed that the concentrations of carbon dioxide in the year 2005 exceeds by far, the natural range in the last 650 000 years, as it has been determined by the ice caps (see figure 1). Fossil-fuel burning and the change in land use, are the main drivers behind the increase of greenhouse gas emissions into the atmosphere, originating the intensification of the GHGs concentration.

FIGURE 1

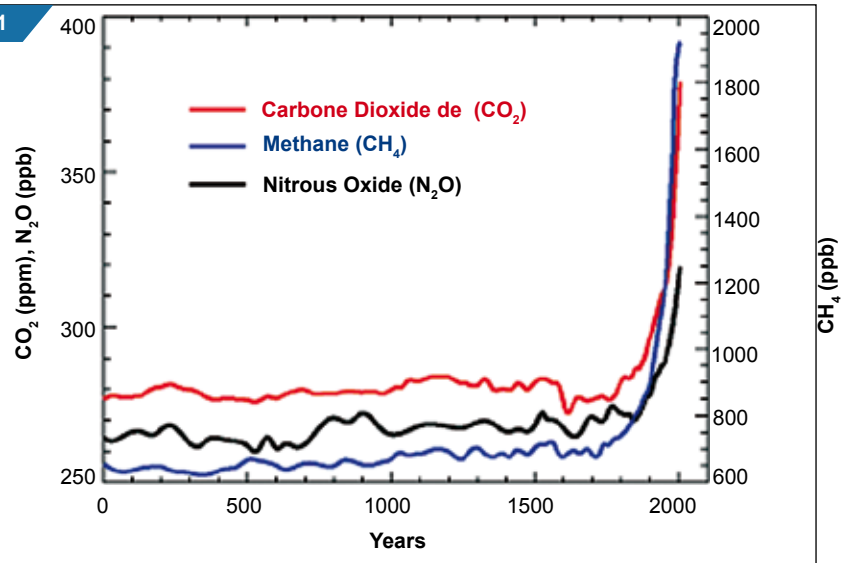

Atmospheric concentrations of long-duration GHGs in the last 2000 year. The units in ppm and ppb, indicate the number of GHGs molecules per million or billion of air molecules, respectively, in a sample of atmosphere. Source IPCC, 2007.

Better and more comprehensive observations and studies have allowed to estimate that in the last 100 years (1906-2005) global temperature has increased in 0,74 ºC, and the warming rate is getting higher (see Figure 2). From the very beginning, when information records started to be made (1850) it has been determined that the warmest 15 years have occurred during the last 20 years and 11 years occurred since 1995. Further scientific analysis have confirmed that the second half of the 20th Century was the warmest 50-year-period during at least the last 1 300 years in the Northern Hemisphere. However, it is important to specify that the warming rate does not uniformly rise over the whole planet. For example, during the last century, the arctic temperatures increased twice as much the rate of the global average index and Europe has warmed at least 1 ºC in the last century, at a faster pace than the global average.

FIGURE 2

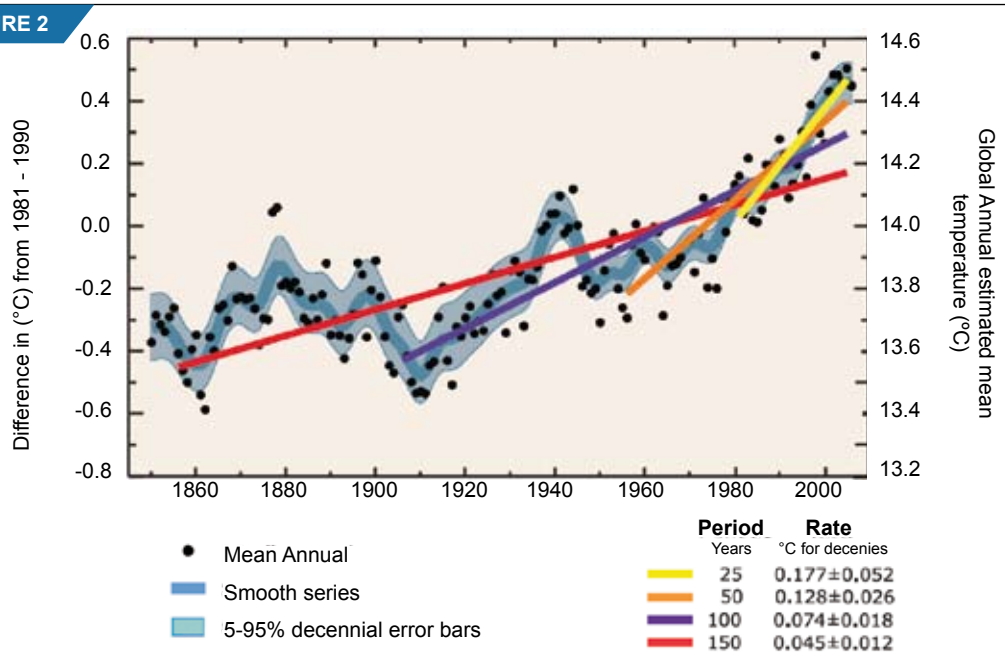

Global annual mean temperature (black dots) including application of linear adjustment to the information. The left axis shows anomalies in average temperature for the period 1961 to 1990 and in the right axis it is observed the estimates of current temperatures, both expressed in ºC. The linear trends are shown during the last 25 years (yellow), 50 year (orange), 100 years (purple) and 150 years (red) (IPCC, 2007).

According to observations made since 1961, the air temperature and ocean warming is causing the continuous increase of sea surface temperature, confirming that the oceans have been absorbing more than 80% of the heat added to the climate system, contributing to rising sea levels (see Figure 3), due to either the increase of the ocean water volume or the ice melting in the poles, determining and increase of 17 cm during the 20th Century.

The acceleration in the melting processes of ice coverage is very significant, mainly in the North Pole and Greenland, as well as it is the reduction of mountain glaciers and snow coverage at global level (see Figure 4).

FIGURE 3

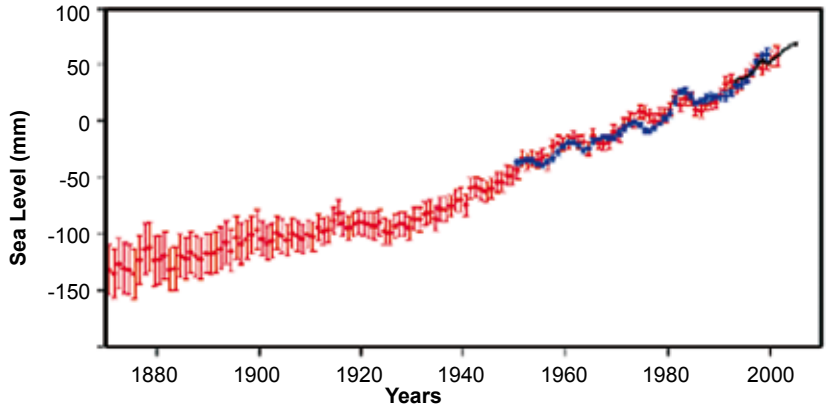

Anomalies at sea level, observed by satellite and direct data. Source IPCC, 2007

FIGURE 4

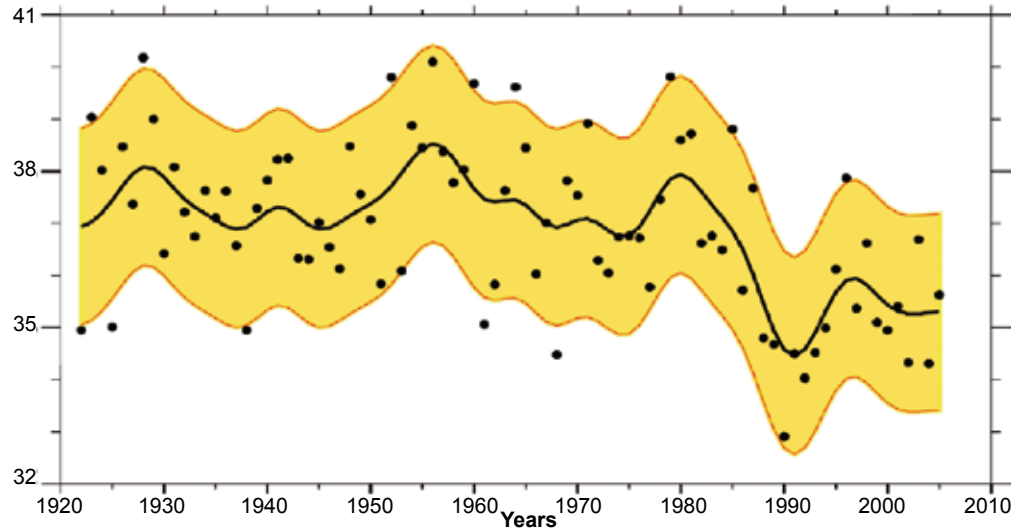

Changes in snow cover in the Northern Hemisphere, from March to April, based on the snow cover index in a station and satellite information.

Extreme climate events have increased, and climate patterns have changed: heat waves and other extreme weather events, such as the variations in the atmospheric circulation models, storms trajectories and rainfall, can be now explained, in a retrospective way, because of climate change caused by human activities.

1.2.2. Climate prospective at global level until the end of the XXI Century

In the future, the Earth will continue to warm up. This statement is based on the results obtained from the different climate models that were considered by the First IPCC Working Group in its last report on future climate projections. These projections indicate that during the XXI century, mean temperature in the Earth will increase between 1,1 ºC and 6,4 ºC (see Figure 5). The climate projections consider the SRES emissions scenarios (Special Report on Emission Scenarios) of the IPCC (2000), in which there is a range of possible CO2 concentrations, in response to human activities in relation to its environment. In this sense, there are scenarios that range form the more optimistic one that considers a stop in global emissions up to the most pessimist one in which current emissions trends are maintained.

The IPCC projects as "very likely" that in the next three decades there will be an approximate warming of 0,2 ºC if GHGs emissions are not reduced The best estimations used to calculate the average air surface warming, at a global level, range from 1,8 ºC (for a range of 1,1 to 2,9 ºC) for the more optimistic scenario (B1 scenario) and up to 4 ºC (for a range of 2,4 to 6,4 ºC) for the most pessimistic (A1F1 scenario). Unlike the previous report of the IPCC, the new assessment considers a larger number of climate models that have developed some improvements in their climate estimation processes with a greater realism and complexity, as well as, the new information about climate system.

Also it has been estimated that the increase in temperature will be higher over large continental masses in the Northern Hemisphere, where it could exceed 4 ºC, while in the large ocean extensions of the Southern Hemisphere, an increase of less that 1 ºC is expected (see Figure 6).

Special Report on Emissions Scenarios – See summary in SENAMHI, 2005 http/www.ipcc.ch

FIGURE 5

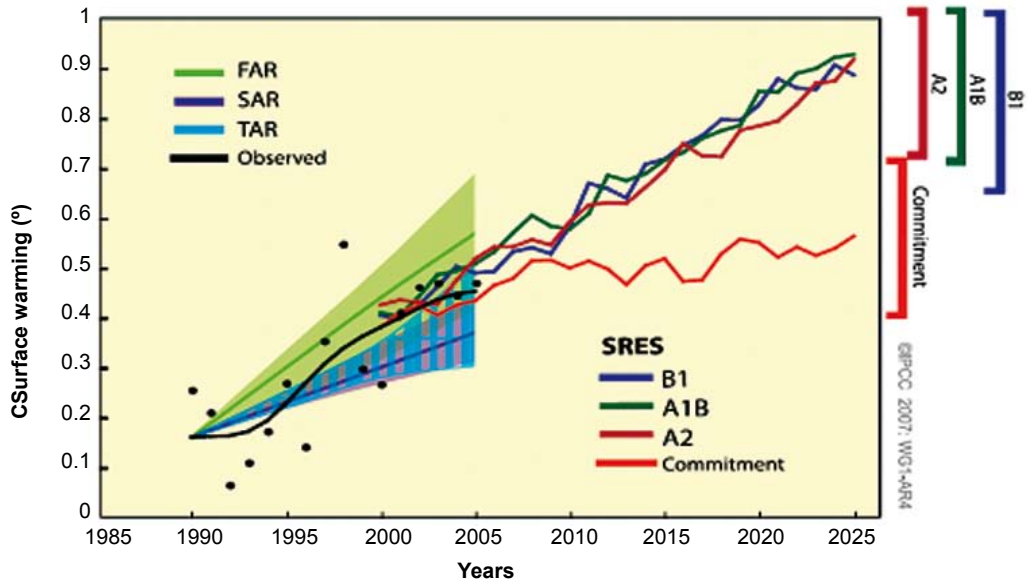

Projections of global warming models compared to some observations made up to 2005, shown in black dots the lines correspond to projections up to 2025. Source IPCC, 2007.

FIGURE 6

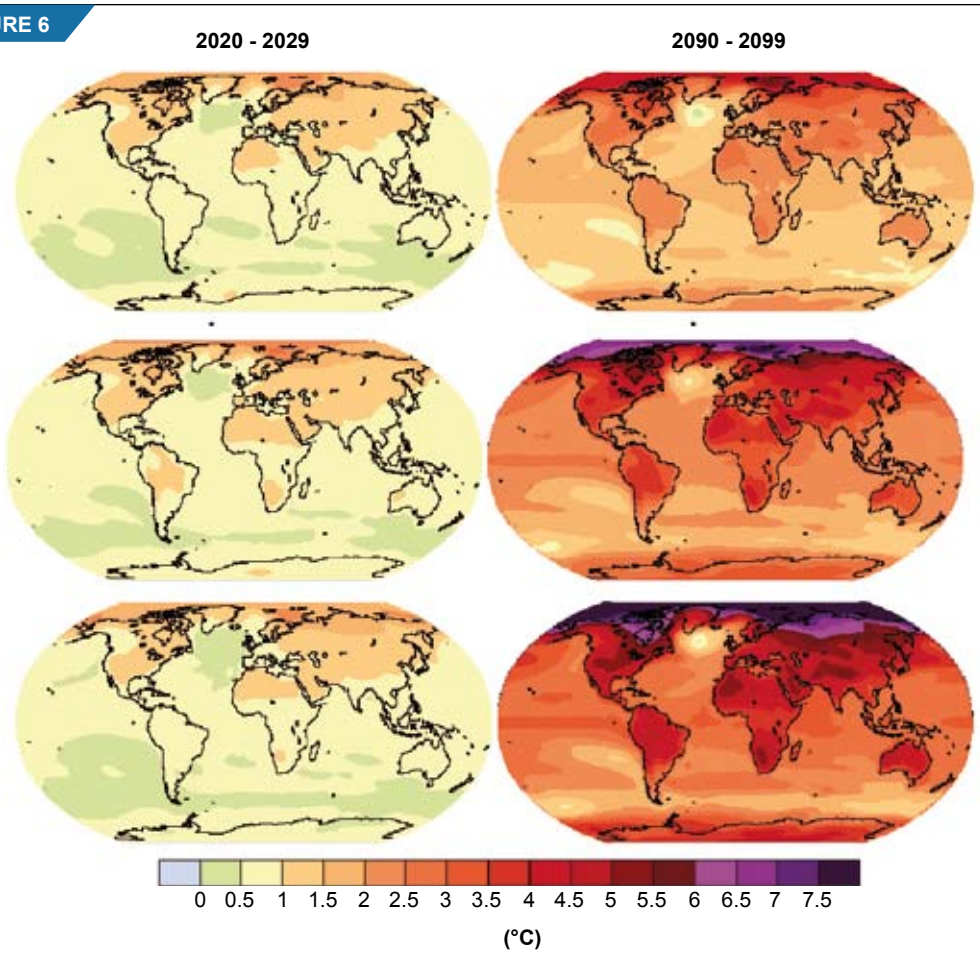

Average projections multi-model AOGCM for the B1 (up) and A1B (middle) and A2 (down) SRES scenarios averaged over decades form 2020-2029 and 2090 to 2099. Source IPCC, 2007

About sea level rise, most of the models project an increase that ranges from 18 to 37 cm for the most favorable scenario and 28 to 59 cm for the least favorable or pessimist one up to 2100, where thermal expansion itself, due to ocean warming, contributes in 70 to 75% (see Figure 7). Uncertainty associated to these projections is smaller than those in the Third Assessment Report (TAR) of the IPCC, because there is more registered information about the loss of glacier mass that has helped to improve the estimation of thermal expansion.

FIGURE 7

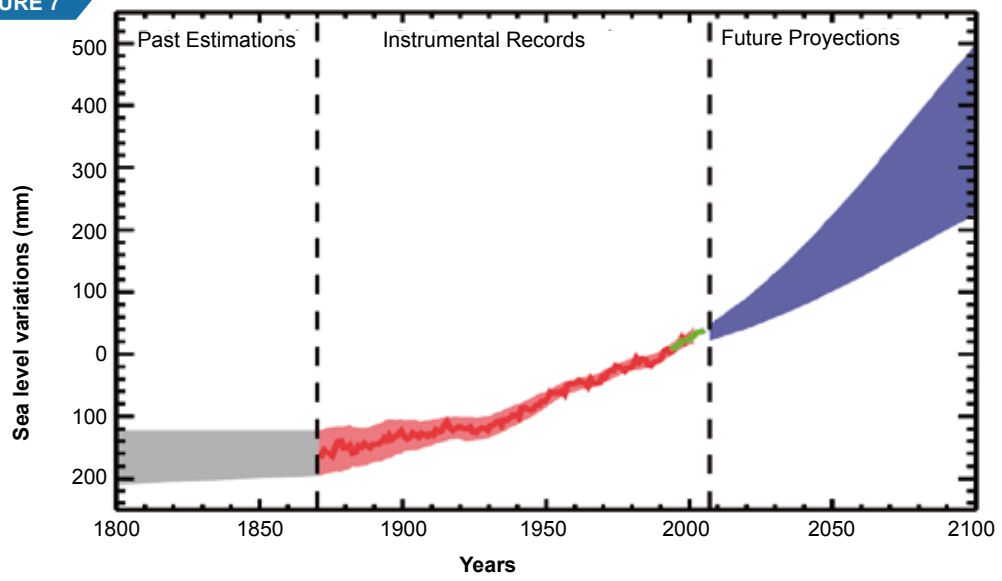

Chronological series of global mean sea level (deviations of the mean from 1980 to 1999) in the past and its future projection. There are no global measurements of sea level before 1870. The grey-shaded portion shows uncertainty concerning the variations rate of sea level, estimated at a long term. The red line is a reconstruction of global mean sea level based on tide measurements, and the red shaded portion shows the variation range starting at the curve. The green line shows global mean sea level observed with a satellite altimeter. The blue shaded portion represents the range of the projections of the models for the A1B scenario of the SRES in the XXI Century, compared to the mean between the years 1980 to 1999 and it has been estimated independently from the observation.

During the XXI Century, the ice cover in the Arctic Region will continue shrinking, as well as mountain glaciers and snow cover. Ice cover like the one in Greenland will continue to shrink, contributing to sea level rise. Current models indicate that the loss of ice-mass will occur more rapidly than anticipated, because of the projected global warming. However, current climate models cannot explain the dynamics observed of the ice flux at a global level and up to this moment there is not the necessary consensus.

According to the IPCC, it is likely (66% of probability) that typhoons and hurricanes will increase in intensity. Regarding precipitation, it is very likely that it will increase at high latitudes, while it is possible that it will decrease in most of the subtropical regions.

1.2.3. Reliability of numerical models to project future climate change

There is considerable confidence concerning the fact that climate models provide credible quantitative estimates about future climate change, particularly, at continental scale and above. This confidence originates from the fact that models are based on accepted physical principles and their ability to reproduce the observed features of current climate and past climate changes. The confidence in model estimates is higher for certain climate variables (for instance: temperature) than for others. (for instance: precipitation).

The IPCC indicates that there are three reasons to be confident on the use of models for climate projections.

- The first reason comes from the fact that fundamental principles of these climate models are based on physical laws: conservation of mass, energy and momentum

- The second reason is based on the ability of these models to simulate important aspects of current climate. Models have proved to have an important ability to represent many main characteristics of average climate. Also, these patterns have been used to evaluate the implication of GHGs forcing in the observed global warming during the last 50 years (see figure 8)

FIGURE 8

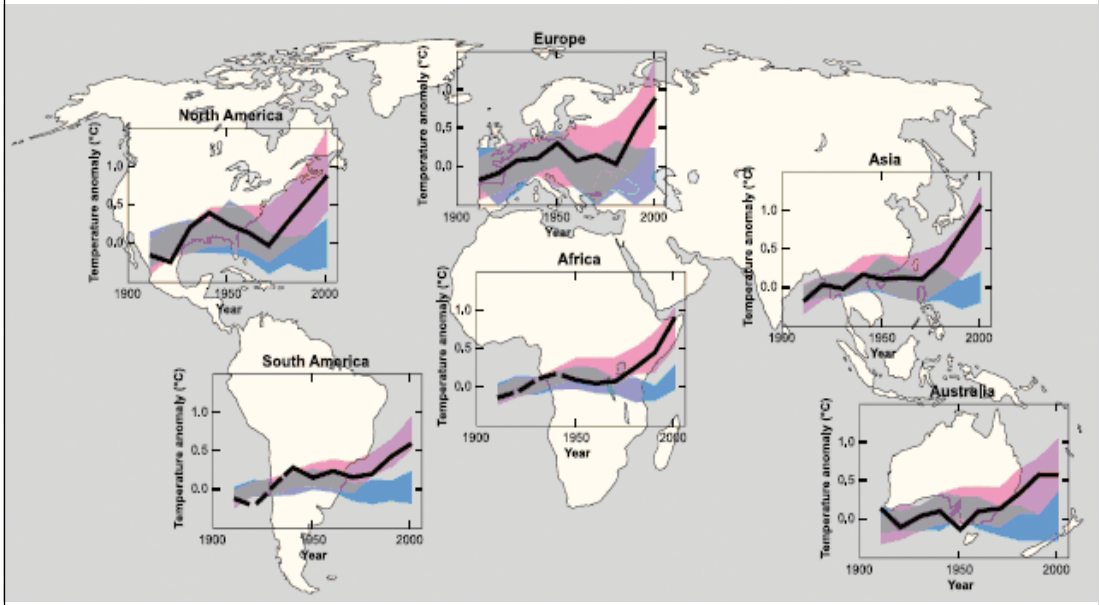

Continental comparison made on observed changes in surface temperature with results simulated by means of climate models using natural and anthropogenic factors. Averages from 1906 to 2005 are observed, in which the light blue lines show the results of the model using natural factors, the pink lines using natural and anthropogenic factors and the black thick line corresponds to observations, so the effectiveness of the climate model can be appreciated. Source IPCC , 2007

- A third reason originates from the ability of models to reproduce features of past climates and climate changes. Models have been used to simulate the climate in ancient times, such as the middle part of the Holocene Warm Period 6,000 years ago, or the Last Glacial Maximum of 21,000 years ago.

Nevertheless, models still show some significant errors. Although, they are generally greater at smaller scales, there are still some important problems at a larger scale. For example, there are some deficiencies in the simulation of tropical precipitation El Niño / La Niña Southern Oscillation and Madden-Julian Oscillation. The main reason for most of these errors is that several important small-scale processes cannot be represented explicitly in models.

1.2.4 Dealing with uncertainty

Dealing with uncertainty was a subject addressed by the IPCC in a transparent way in order to be able to distinguish the different levels of confidence on scientific knowledge and the probabilities of specific results that would be obtained in the assessment reports on climate change.

There are two primary kinds of uncertainty: value and structure. The uncertainty in value arises when values or specific results cannot be totally interpret and they are calculated using statistical methodologies, estimates are obtained in a probabilistic way. The uncertainty in structure occurs when it is not possible to interpret all the processes that regulate the values or results and the determination on the exactness of a result is made on confidence criteria of all the authors.

The IPCC provided an uncertainty guidance note that distinguishes levels of confidence on the scientific knowledge and the probabilities of specific results. This way, the authors can express with certainty that a situation is unlikely to happen (for example, to throw the dices two times and obtain a six twice) or that it is as likely as it is unlikely (for example, to toss a coin and get heads or tails). Confidence and probability are different concepts; but, in the practice they go together.

The terms used to define the scale of confidence are based on the ones described in the uncertainty guidance note:

Terminology of confidence levels	Scale of confidence
Very high confidence	9 out of 10
High confidence	8 out of 10
Medium confidence	5 out of 10
Low confidence	2 out of 10
Very low confidence	1 out of 10

The universal terms used to define the likelihood of a result, provided that the result can be calculated in a probabilistic way, are:

Terminology of likelihood	Likelihood of the result
Virtually certain	> 99% probability
Extremely likely	> 95% probability
Very likely	> 90% probability
Likely	> 66% probability
More likely than not	> 50% probability
About as likely as not	To 33 of 66% probability
Unlikely	< 33% probability
Very unlikely	< 10% probability
Extremely unlikely	< 5% probability
Exceptionally unlikely	< 1% probability

CHAPTER 2

PERU: PHYSICAL AND SOCIAL CONTEXT

PERU: PHYSICAL AND SOCIAL CONTEXT

When we refer to Peru, it is inevitable to avoid mentioning that we are looking at a country with a complex geography, mainly due to he elevations of the Andes Mountain Range and the currents of the Pacific Ocean, all of which constitute different climates and landscapes, that are reflected in the coastal dessert, the Puna or high Andean plateau or the tropical jungle region in the Amazon basin, all of them, converging into a territory with a great variety of natural resources.

2.1. LOCATION

Geographically speaking, Peru is located in the central western part of South America, immediately below the equatorial line between 0º01'48" and 18º21'03" south latitude, 68º39'27" and 81º19'34,5" west longitude and it has a total area of 1'285,215.6 Km2 (Ponce de León, 2000).

It is the twentieth largest country in the planet and the third one in South America. It is bordered to the north by Ecuador and Colombia, to the east by Brazil, to the southeast by Bolivia, to the south by Chile and to the west by the Pacific Ocean. It is worth mentioning that according to our new Constitution, the maritime sovereignty of Peru extends up to 200 miles offshore.

2.2. GENERAL CHARACTERISTICS

2.2.1. Peruvian Sea

The Peruvian sea is heterogeneous because of the confluence of two sea currents, each one with different characteristics. The Peruvian Current or Humboldt Current, a cold water current that flows northward, up to 5º south latitude, determining a temperate non-tropical climate in the coastal region and a warm water current called El Niño that permanently influences the northern coast of the country and temporarily further south.

The presence of these currents determines up to four marine zones off our coastal region:

- *The Cold Sea* of the Peruvian Current, its location starts at 5º south latitude to the central part of Chile, with relatively low temperatures.
- *The Tropical sea*, north of 5º south latitude, with warm temperatures
- *The Ocean zone,* west of the Peruvian Current, with warm temperatures
- *Transition zone,* between the cool tropical sea, where the warm and cold waters meet off the coasts of Piura and Lambayeque.

2.2.2 Andes Mountain Range

The presence of this large mountain range, along the territory determines the geographical heterogeneity of Peru, consisting of:

a. Three large continental landmasses: the coast, between the sea and the Andes Mountains; the mountain region, as a mountain mass; and the Amazon region, east of the Andes.

b. Three hydrographic basins: the Pacific, the Atlantic and the Titicaca.

c. Different zones in the mountain region such as: the bleak upland, north of the Porculla ravine, the Andean plateau in the central and southern region, and the high Andean plateau, in the surroundings of the Titicaca Lake basin.

The altitudinal distribution of the Andes Mountain determines different vertical layers, from sea level and the Amazon jungle up to the high mountain range, in the western and eastern slopes. Because it is wider towards the southern region, an arid area is originated in the mountain region towards the west and a humid area towards the east.

The complex division of the Andes mountain range causes a huge local heterogeneity in the distribution of precipitations, originating some arid zones in the inter-Andean valleys that lay parallel to the mountain ranges.

2.3 LATITUDINAL LOCATION

The latitudinal location of the Peruvian territory, from almost the Equatorial line to a little further up 18º South Latitude, is responsible for causing ecological variations such as the duration of day and sunlight hours (shorter to the south in the winter). The conjunction of the latitude with the altitude of the Andes Mountains and the Sea Currents, determine an important variation of climate conditions and vegetation from south to north in the coast, in the slopes, and over the Peruvian Amazon region.

2.4 POPULATION AND DEMOGRAPHIC GROWTH

Total population in Peru amounts to 28 million 220 thousand 764 inhabitants (INEI 2007)*.
Its increase, measured by the average annual growth rate, refers that it has shown an annual average growth for the period 1993-2007 of 1,6 % which confirms the diminishing trend observed in the last 46 years. Between the 1981 and 1993 census, the population growth was 2,0% per year, this rate was higher in the inter-census period between 1972-1981 (2,6% per year).

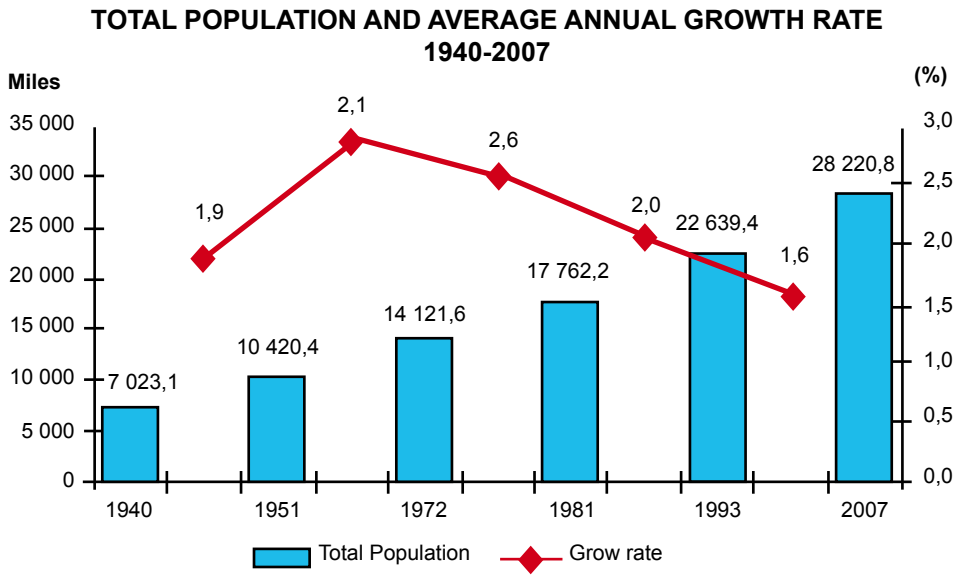

Fuente: INEI- Censos Nacionales de Población y Vivienda, 1940, 1961, 1972, 1981, 1993 y 2007.

* National Statistics and Computing Institute.

2.5 ECONOMICAL ACTIVITIES AND GDP IN PERU

The economy of Peru is mainly based on mining, fisheries, agriculture, construction and trade. Most of the exportations are raw material or primary elaborated material (69.5%), followed by secondary elaborated products or industrial products (29,6%) and a minimum percentage for exports of services or tertiary production (0,9%).

The GDP is an economical indicator that involves the addition of all the productive activities and services of a country, and as such, it serves as a reference how the economic life of a nation is going. According to the information provided by the National Statistics and Computing Institute (INEI), in Peru the evolution of the Gross Domestic Product in the last 10 years shows an intensified activity and currently it already exceeds 60 billion dollars. For example, the growth in 2003 was 4% with regard to the previous year.

Recently, the Ministry of Economy and Finance presented the Multi-annual Macro-economic Framework 2008-2010 (MMM, 2007) which shows the rates that the main macro-economical variables would reach in the next annual periods.

GDP GROWTH 2000-2010

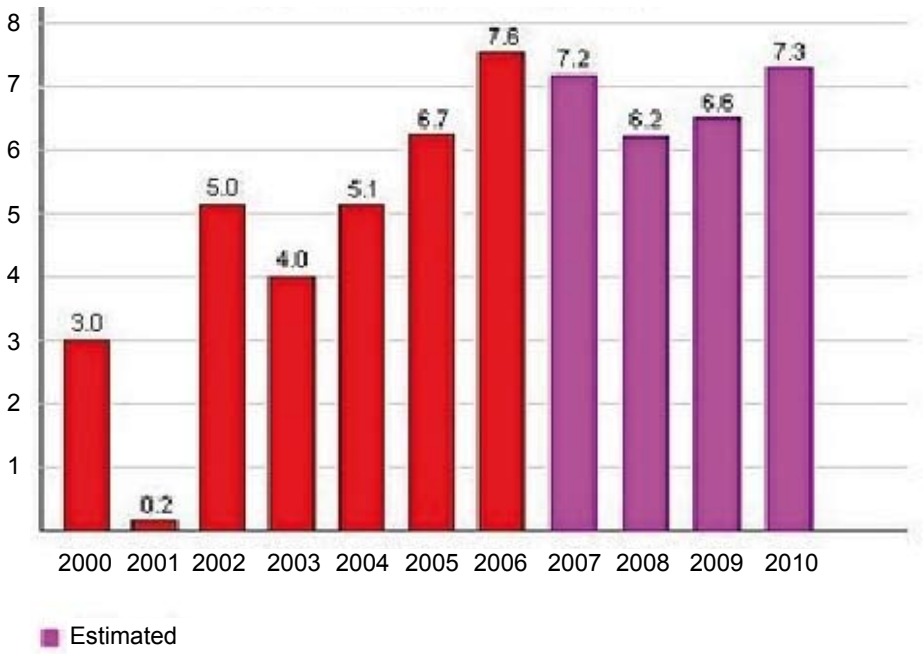

Source: Ministry of Economy and Finance, 2007

Concerning the GDP, it is expected a 7,2% growth in the year 2007, 6,2% in 2008, 6.6% in 2009 and 7,3% in 2010. On this matter, except for small variations, it is expected that economy might keep registering high growth rates. Peru requires an annual average rate of 7% in order to substantially reduce poverty and to quickly head towards development; if these estimates are reached the country would be getting closer to the adequate rate.

2.6 CHARACTERISTICS OF CLIMATE IN PERU

2.6.1 Classification of climate in Peru

The climate classification of Peru (SENAMHI 1988) has been elaborated considering factors that determine the climate, such as latitude, altitude, the Andes Mountain Range, the Peruvian Current (cold waters), the South Pacific Anticyclone and the continentality.

The basic information of this classification is based on 20 years records (1965-1984) of meteorological data, on which all the climate indices were established according to the Climate Classification System of Werren Thornthwaite. According to this classification, Peru has 27 different types of climate in the whole territory, that range from semi-dry climate zones, cold with rainfall shortage like in Puno in the southern part of the country; up to rainy climate zones, warm with plenty of rainfall such as in Iquitos in the northern part of the country. However, in general, three geomorphological and climatological units can be clearly distinguished: the coast, the mountain and the jungle regions. The coast, a plain area situated between the coastline and the Andean foothills, is a dry region with scarce rainfall, except for the northern zone during the El Niño events; the mountain is a steep region due to the Andes Mountain, that because of its altitude and uneven topography it has a diversity of climates that range from the temperate to polar; and finally there is the jungle, an almost plain region characterized for having a exuberant vegetation, with plenty of rainfall originated from convective clouds. (See map 03 Appendix 1).

2.6.2. Multiannual variation of extreme temperatures and precipitation

In general, the highest temperatures occur in the northern part of the coast and low jungle. Also, the lowest temperatures are registered in the highlands, especially in the high Andean plateau. In the central and southern part of the coast there is scarce or almost no rainfall; in the mountain region there is moderate rainfall and in the northern and southern part of the jungle there is heavy rainfall.

Multi-annual average maximum temperature reaches up to 32 ºC in the northern coast (Ricaplaya) and most part of the low jungle, while in the central and southern part of the mountain region the lowest maximum temperature values are registered, reaching up to 12 ºC in Pillones and Ilave (See map 01 Appendix 2).

Multi-annual average minimum temperature reaches values of -7 ºC in the high Andean plateau and 22 ºC in the northern part of the jungle. In the northern part of the coast, on average, it reaches 21 ºC; in the central and southern part of the coast values oscillate between 12 ºC and 17 ºC; in the northern part of the mountain region values varies between 3 ºC and 10 ºC; in the southern part of the mountain region minimum average temperatures oscillate between -7 ºC to 10 ºC, while in the jungle values oscillate between 16 ºC and 22 ºC (See map 02 Appendix 2).

Total multiannual rainfall in the northern coast reaches values that vary from 22 mm/year to 260 mm/year. Conversely, in the central and southern coast annual rainfall does not exceed 10 mm/year. In the northern mountain region, accumulated rainfall oscillates between 360 mm/year to 1 370 mm/year; in the central mountain region, accumulated rainfall, varies between 270 mm/year to 1 200 mm/year, while in the southern mountain region these values oscillate between 250 mm/year to 870 mm/year, the heaviest rainfall occur in the eastern part of the Andes Mountains. In the jungle, accumulated precipitation in one year, show values that oscillate between 1 000 mm/year to 5 800 mm/year, being the highest accumulated values registered in Pongo de Caynará (San Martin) with 4 300 mm/year, Francisco Orellana (Loreto) with 3780 mm/year, Tingo María with 3 500 mm/year and San Gabán with 5 800 mm/year. (See map 03 Appendix 2).

Multi-quarterly or seasonal average maximum temperatures show configuration similar to multiannual average maximum temperature, with the difference in the highest values for the northern coast form the period between December and January (summer) with a value of 33 ºC in the meteorological station of Ricaplaya and in the jungle in the months for September to November (spring) with a value that reaches 33 ºC in the meteorological station of Iñapan. Maximum temperatures registered in the summer for the mountain and jungle region are slightly lower than the values showed during the spring (See maps 4,5,6 and 7 Appendix 2).

In the Peruvian coast, for the period December to February (summer) multi-quarterly or seasonal minimum temperature values oscillate between 15 ºC and 20 ºC; while the lowest value registered in the summer occurs in Imata (Arequipa) with -2,4 ºC; also, the jungle shows values that oscillate between 18 ºC and 22 ºC in the summer. On the other hand, for the period June-August (winter) in the central and southern coast, temperature varies between 9 ºC and 14 ºC, while in the central and southern mountain region, these values change between -13 ºC and 7 ºC, and in the jungle minimum temperature values oscillate between 16 and 21 ºC. (See maps Nº 8,9,10 and 11 Appendix 2).

For the period December-February, rainfall in the central and southern coast, shows accumulated values that reach 5 mm, while in the northern coast it amounts up to 110 mm for the whole quarter. In the mountain and jungle regions the heaviest rainfall occurs in this same period, with accumulated values that varies between 50mm and 500 mm, the lowest rainfall occur in the western slope of the Andes Mountains, in the jungle with accumulated values that for this quarter reach up to 2 400 mm/year. (See map Nº 12 Appendix 2).

Multi-quarterly rainfall for the period March-May, registers accumulated rainfall values that significantly decrease in the whole Peruvian territory in relation to the previous quarter, except for the northern jungle, where rainfall keeps its values. On the other hand, the driest period, corresponds to the quarter from June – August , where the accumulated rainfall for the coast is less than 5 mm, in the mountain region up to 100 mm and in the jungle up to 900 mm. In the period September – November, rainfall slightly increases in the mountain and jungle regions with regard to the previous quarter (See map Nº 13,14 and 15 Appendix 2).

2.6.3. Temporal and spatial variation of extreme temperature and rainfall in extreme events: El Niño/La Niña

Diaz. A. (SENAMHI 2007) says that El Niño- Southern Oscillation (ENSO) is a perturbation of the Ocean-Atmosphere Systems in the Equatorial Pacific, with important consequences for climate at a global level, since it alters the global patters of atmospheric circulation, precipitation and temperature. The ENSO, has a strong and direct influence over a large tropical and subtropical area of South America (Garreaud and Aceituno 2007) through the tele-connections, that are the changes in the global atmospheric circulation induced by the ocean-atmosphere anomalies in the Equatorial Pacific. The ENSO cycle has two phases: a warm or positive phase (El Niño) which occurs in intervals of 4-5 years and a cold or negative phase (La Niña); there are also transition periods characterized by sea surface temperature values close the its climate mean values. Transition from the El Niño to La Niña tends to be quick, while the transition from La Niña to El Niño tends to be gradually. Both transitions are influenced by intraseasonal variability (Madden-Julian Oscillation, mean latitudes blockings, low and high pressure systems, tropical storms, etc.) according to Kousky and Higgin (2007).

The variations in climate that occur in Peru from one year to another, known as interannual variability is mostly determined by the presence of the ENSO, and the extreme events associated to it, which cause large economic loss because its direct or indirect impacts. In the following paragraphs the main impacts

of the ENSO on the thermal and pluvimetric regimens at national level, for this reason the El Niño warm events of 1982/83 and El Niño 1997/98, have been analyzed; both are considered the most intense events during the last century; also one cold event: La Niña of 1988/89, considered as one of the most intense of the negative phase of the ENSO.

a. El Niño 1982/1983

The average maximum temperature during the period between June 1982 and May 1983 reached up to 33 ºC in the northern coast; 24 ºC to 32 ºC in the central and southern coast; 14 ºC to 22 ºC in the mountain region and 32 ºC in the jungle region. When considering the quarterly average the highest maximum temperature values occurred in December 1982 to May 1983, reaching an average of 35 ºC in the northern coast. In the mountain and jungle, the highest values occurred in the quarter between September and November. See Maps Nº 16, 17, 18, 19 and 20 Appendix 2.

Minimum temperature in the coast reached values above its multiannual average and especially in summer and autumn seasons. In the mountain region, the isotherm settings are similar to the multiannual values, the values registered in the southern mountain region were lower than -14 ºC (Imata) also the ones for the quarter corresponding to June-August. In the jungle, minimum temperature, on average, showed values between 28 ºC and 32 ºC, with very slight variation with respect to multiannual estimates. See maps Nº 21, 22, 23, 24 and 25 Appendix 2.

Accumulated precipitations between the period starting June 1982 to May 1983 showed significant anomalies in the northern part of the country. This way, in the Ricaplaya station, where the multiannual average between June and May is 257 mm, during the same months of the period 1982/83, an accumulated value of 5,051 mm was registered; representing and anomaly of 1,860%. In the northern part of the mountain and jungle region, precipitation was higher than normal for the same period. See maps Nº 26, 27, 28, 29 and 30 Appendix 2.

b. La Niña 1988/89

It is considered that La Niña started in June 1988 and ended in May 1989. In the northern coast maximum average temperature oscillated between 28 ºC and 32 ºC, values that were close to multi-annual averages. While in the central and southern coast, averages oscillated between 23 ºC and 29 ºC, which was slightly lower than normal. In the mountain and jungle region there were no significant differences with regard to climate values. Concerning quarterly variation of maximum temperature, the most significant variation was observed in the coast, where average values reached up to 33 ºC in the summer and 19 ºC in the winter., while in the mountain region the highest values were observed in the quarter between September and November. In the jungle, during the quarters between June-August and September-November, maximum temperature reached an average of 34 ºC. See maps Nº 31, 32, 33, 34 and 35 Appendix 2.

Minimum temperature showed significant variations in the central and southern coast, where minimum average temperature reached 7 ºC in Ica for the quarter between June –August and when La Niña was in its initial phase. In the jungle, minimum temperatures were between 18 ºC and 21 ºC, which represented values slightly lower than their multiannual averages. In the mountain, minimum temperature between June-August was lower than -13 ºC and in locations situated above 4000 masl, except for the areas close to the Titicaca Lake, where the decrease in temperature was moderate due to the thermo-regulating effect of the lake. For the quarter between June-August the southern jungle showed and average value of 16 ºC. See maps Nº 36, 37, 38, 39 and 40 Appendix 2.

Precipitation was higher than its total multiannual value, reaching 650 mm (Ricaplaya) 2 100 mm (Quiruvilca) and 6 700 mm (Pongo de Caynarachi) in the northern coast, northern mountain region and northern jungle respectively. Also in the southern mountain region (Capachica) registered values of 1 100mm. In the other regions, precipitation was lower than multiannual values. The quarterly accumulated values showed the highest precipitation during the quarter between December-February and the lowest precipitation during the June-August quarter. See maps Nº 41, 42, 43, 44 and 45 Appendix 2.

c. El Niño 1997/98

The coastal region showed maximum and minimum temperatures that exceeded their multi-annual average values up to 4 ºC, in the central coast 33 ºC was registered as an average value of maximum temperature in the summer.

The values of maximum temperatures in the coast were higher than 28 ºC; while in the mountain region average values of maximum temperatures did not show any important variation with regard to normal climate, and in the jungle, a larger area was observed with maximum temperatures exceeding 32 ºC. See maps Nºs 46 to 50 in Appendix 2.

Minimum temperatures show higher values than normal (up to 4 ºC) in the coast, in the mountain and jungle regions the behavior of minimum temperatures was similar to the multi-annual averages. In the jungle minimum temperatures lower than 15 ºC were registered, for the quarter from June to September. See maps Nº 51 to 55, Appendix 2.

Accumulated precipitations between June 1997 and May 1988 were intense in the northern coast, with values up to 3 900mm in Lancones; in the northern mountain region, values up to 4 000 mm in Santo Domingo, Piura. In the southern coast accumulated values registered up to 45 mm in Punta Atico, Arequipa. In the central mountain region, rainfall amounted 2 000 mm in Choclococha, (high zone of Huancavelica); and in the jungle, rainfall accumulated value of 8700 mm in San Gabán (between Puno,Cusco and Madre de Dios). In the remainder part of the country, precipitations were lower than total multi-annual values. In the quarters December to February and Marcho to May, occurred the heaviest precipitations in the whole territory. The period between June and August registered less precipitations. See maps Nº 56, 57, 58, 59 and 60, Appendix 2.

CHAPTER 3

NATIONAL CLIMATE TRENDS

NATIONAL CLIMATE TRENDS

Detecting climate change in climate series and indices of climate extremes in Peru, besides being an important scientific result, is a real need in order to establish some basic climate parameters to evaluate the effects of climate change in Peru. These parameters will constitute fundamental basis for future planning of the different activities carried out in our society.

Several studies on the climate trends of total annual precipitation, in some representative stations in the mountain and jungle regions of Peru, for the period 1951-2000 (Obregón and Marengo, 2006), show that the registered trends are not statistically significant at the 5% level, and in the northern mountain and jungle regions there was an increase in precipitations and in other regions there was some diminish; with higher values in the southern mountain region than in the central mountain region. Another study on this same issue, Obregón (2006), points out that there is a need to homogenize temporally all the series used in any study of this kind. The main reason is due to the presence of almost decadal or longer oscillations that modulate precipitation in the different regions in Peru, rather than to the presence of long-term monotonic variations (gradual). These oscillations agree with the variability of the ocean system and/or the atmospheric circulation, such as the North Pacific Oscillation (NPO), Antarctic Oscillation (AAO) respectively.

Another study with a large amount of data (1964-2000), carried out by Sanabria and Zevallos (2006), for five zones distributed in the coast and southern mountain region of Peru, indicates some variations in maximum and minimum temperature between 3 to 4 ºC/decade in the high Andean plateau and in the coastal zone for maximum temperature these values are 0,2 to 0,3 ºC /decade and for minimum temperature they are from 0,2 to 0,5 ºC/decade. Also, they show that annual precipitation in the high basins in the northern coast and in the high Andean plateau increased from 0,1 to 0,3 mm/decade. Conversely, in Huancavelica and Ayacucho it decreased 0,2 mm/decade.

As part of the World Climate Research Program (WCRP) of the World Meteorological Organization (WMO), the subprogram of Climate Variability and Predictability (CLIVAR) carried out several studies on climate extreme indices for temperature. The results of this research (Vincent et al. 2005) identified the occurrence of a positive trends in the frequency of warm nights (TN90P) and negative trends in the frequency of cold nights (TN10P) and for the period 1960-2000 for Peru, in the daily thermal amplitude there were found no results on climate extremes.

Recent studies on temperature and precipitation trends, as well as climate extremes were carried out in the Department of Arequipa (Marengo et al. 2006 and Obregón et al. 2008). In general, the results show that temperature trends (1971-2006) are positive, non significant, with higher values registered for minimum temperature in the months of autumn. Similarly, precipitation does not show significant values, but it does show a regionalization of the trends. At the same time, this research confirm the trends observed by Vincent et al. (2005), in the climate extremes of temperature, but with a large record of observations (1940.2006) for the high regions in Arequipa (Imata). Conversely, in the analysis of the climate extreme trends in precipitation, at a long term, it is observed that they are modulated by some kind of oscillation larger than interannual variability.

The present chapter based on historical observed data at national level for the period 1965-2006 has the following objectives: 1. Detect climate changes, determining their trends and extreme indices. 2. Analyze the drought as a climate extreme.

The results of the present Chapter will serve as the fundamental basis of knowing the complex climate variability at long term, from a global point of view, as well as a tool for identifying vulnerable regions to climate change and consequently for planning and development management.

3.1. DATA

To carry out studies on the detection of climate change, is necessary that temporal climate series used are enough long, continuous and homogenous. This premise will provide great advantage because the most representative statistics will be obtained, and with them it will be possible to characterize climate phenomena more accurately. This way, the observed data are turn into the base of any tentative detection of climate trends or any other kind of analysis related to climate change.

It is essential to have good quality data for this kind of estimates and analysis, so it is necessary to prepare most adequately the data series that will be used, by means of a detailed quality control. Another point for this kind of study which is made to highlight regional features is to be sure to have an adequate spatial distribution within the area of study.

3.1.1. Used basic data

The basic information that was used in the present report is based on the daily observations of precipitation and minimum and maximum temperature from the database of the National Meteorology and Hydrology Service of Peru – SENAMHI, for the whole territory. The observation periods vary quite a lot. The detailed information that was used from the pluviometric and climatological stations is in Map 1 Appendix 1.

3.1.2. Quality control and how to fill in data

a. Daily data

The source of errors in any kind of data can be classified in three categories:
19 Internal consistency
2) Random and;
3) Non-homogeneous

The internal consistency errors can be, for example, when there is a transposition of the observations (for instance 35mm for 53mm). Contingent errors may occur due to a mistake in the electronic communication, deterioration of sensors of the measuring instruments and other reasons, which are some times difficult to be noticed. Finally, the errors of non-homogenity mainly occur when there are changes in the observation practices and they can be detected because of some discontinuities, trends in the data records, etc.

As a first step in the quality control process and selection of key stations to make the analysis, the following principles were considered:

1) Daily continuity of each time series, for precipitation and temperature, independently from each other.
2) Graphic analysis of the evolution in time of the selected variable.
3) Daily, monthly and seasonal analysis of the average and variance of the series.
4) Analysis of outlier values.

Using the first type of analysis the common period was determined from1965 to 2006, because most of the stations had observational records corresponding to this period, so it was chosen as the basic period of data to be used. This also meets the need to have temporally homogeneous records in order to make the estimates and facilitate the corresponding analysis on the climate extreme indices and subsequently, to obtain the temporal series of the climate variables to make the estimates and analysis of the trends to fulfill the objectives of the present report.

Then, from the other two kinds of analysis made in the previously selected stations for the period already chosen, the assumed data errors were detected and separated when the stations showed some inadequate distributions, different form the ones observed in adjoining stations. Finally, the values that exceeded 2,5 times the variance showed in the adjacent station were separated.

Considering all these analysis, the key stations were selected, with daily data to make the estimates of the extreme climate indices. Then, the main condition for the final selection of the key stations was that the time series of each variable should have more than 90% of valid, continuous daily data for the period between 1965 and 2006 (42 years) or, up to 85% of discontinued data, but they had to have data corresponding to the beginning and end of the period. This way, 99 stations with daily precipitation data were selected.

b. Monthly data

Even though many studies have been made about the climate in Peru, there is not a comprehensive study about the quality of the data used to prepare them. All the observed records show some kind of discontinuity, that need to be worked on, in order to get representative data, and where possible, complete them, trying to get close to reality, in order to obtain reliable and realistic results of what climate variability really is in Peru, using the historical data series.

In order to select the key climatological stations for total monthly precipitation and monthly mean temperature, initially, all those stations in which the missing and discontinued monthly data were less than 12% (60 months) from the whole monthly series for the period 1965-2006, were considered. However, it was necessary to increase the number of stations with precipitation and temperature series, those that showed up to 15% of missing monthly data. This was done specially in some departments where there was very little or no information, this was the case of some stations with lack of information of precipitation in the city of Iquitos, and that initially didn't comply with the required characteristics. For many stations, the lack of monthly data was crucial in order to be selected, because in most cases there were incomplete records to estimate the climate indices.

The next step was to complete the monthly data for each one of the selected series, as aforementioned. So, to make these studies the interpolation method called Kriging and the first-order auto-regressive statistical method (AR1) were used.

The Kriging method was used when there was enough data (for more than 3 points in the grid) within a radius of ± 0,5º latitude/longitude. In this case, from the existing data, an estimated and specific value was determined for the missing data, as shown in Figure 9, and the complete series for precipitation, indicating the missing data, as shown in Figure 10.

Where there was no data within a radius of ± 0,5 º, related to the missing data, or when a station didn't have one near to be correlated with, the auto-regression method was used to fill up to three (3) continuous missing data. In order to apply this method, the data is initially standardized to remove certain signals as the annual cycle and linear trends as well; and the missing data is estimated, then the time series is reconstructed. This method can be made several times until the missing data is totally completed.

An example is shown in Figure 11, in which 7 pieces of missing information were completed, representing 2,8% of the total existing information. From this new series, shown in Figure 12, again the missing data are estimated. In the case, the total missing data are not completed, other criteria can be used; such as the harmonic analysis in case of temperature; this way the total data are completed with or without using the closest station for correlation purposes.

The time series, with completed data, were subject to the following final analysis, in order to determine the homogeneity of each one of the climate variables:

FIGURE 9

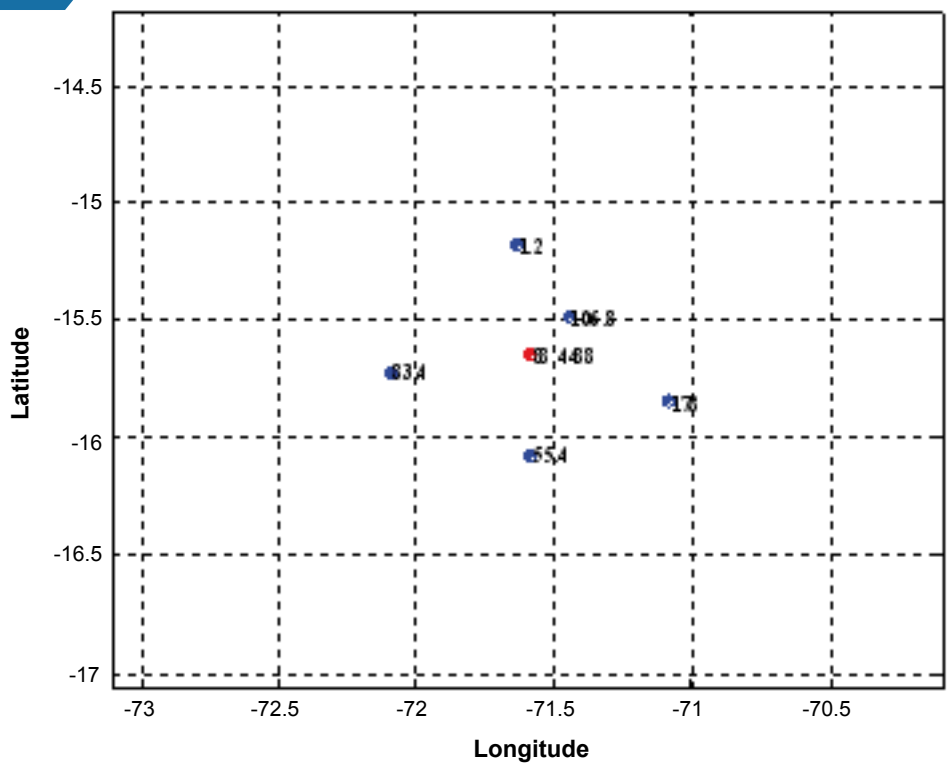

Example of interpolation using the Kriging method. Blue dots represent observed data. Red dots represent estimated data based on the others (blue dots)

FIGURE 10

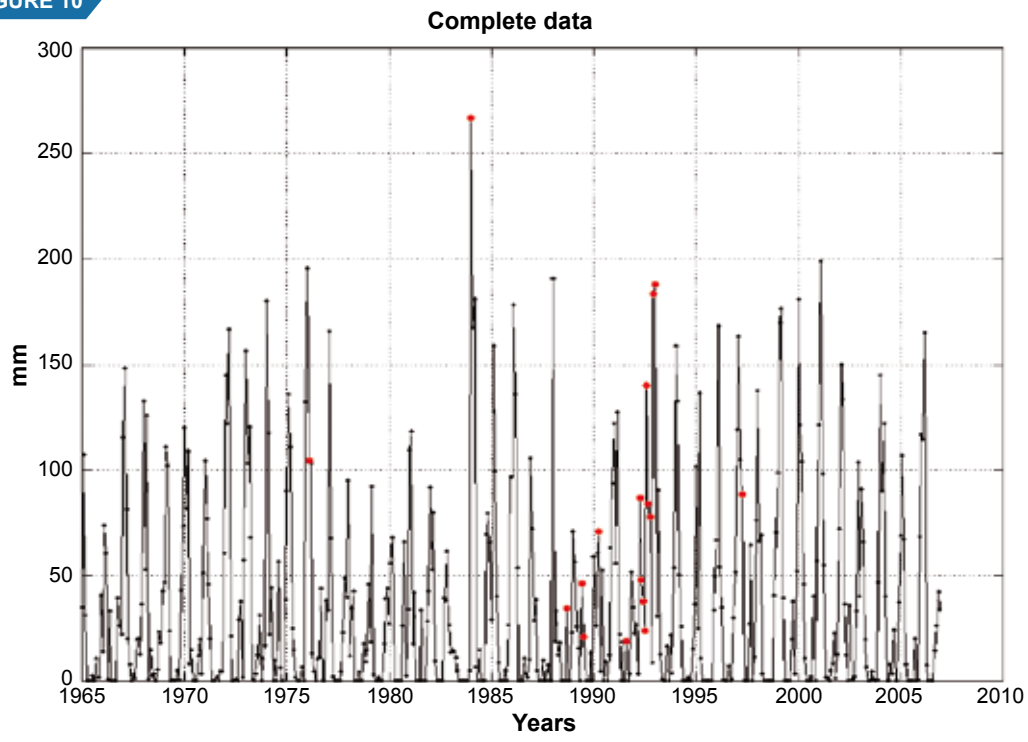

Example of interpolation using the Kriging method in precipitation series. Red dots represent complete data estimated based on the adjacent observed data series..

1) Analysis of partial averages and accumulative deviations from the average.
2) Selection of the best correlated series (homogenous)
3) Application of the double mass method

Removing heterogeneity, when it is observed, consists of correcting the part in which heterogeneity is detected by means of the double mass curve. Following this procedure, deduction of the heterogeneity of temporal evolution of the climate series can be done by a graphics analysis. Also, some uncertain values can be easily found, since they are related to discontinuity, trends and singularities for a determined period. In addition, changes in the average can be easily noticed in long series. The adjustments just described not only remove inconsistencies; but, also they fairly reduce or eliminate the deviation in the whole time series.

When all the adjustments were finished, 64 stations for total monthly precipitation were selected. This is shown in Figure 13a and described in Table 2.4. Also 29 stations with monthly average maximum and minimum temperature data. The distribution of the last two data series is shown in Figure 13 b-c and described in Tables 2.5 and 2.6, respectively.

FIGURE 11

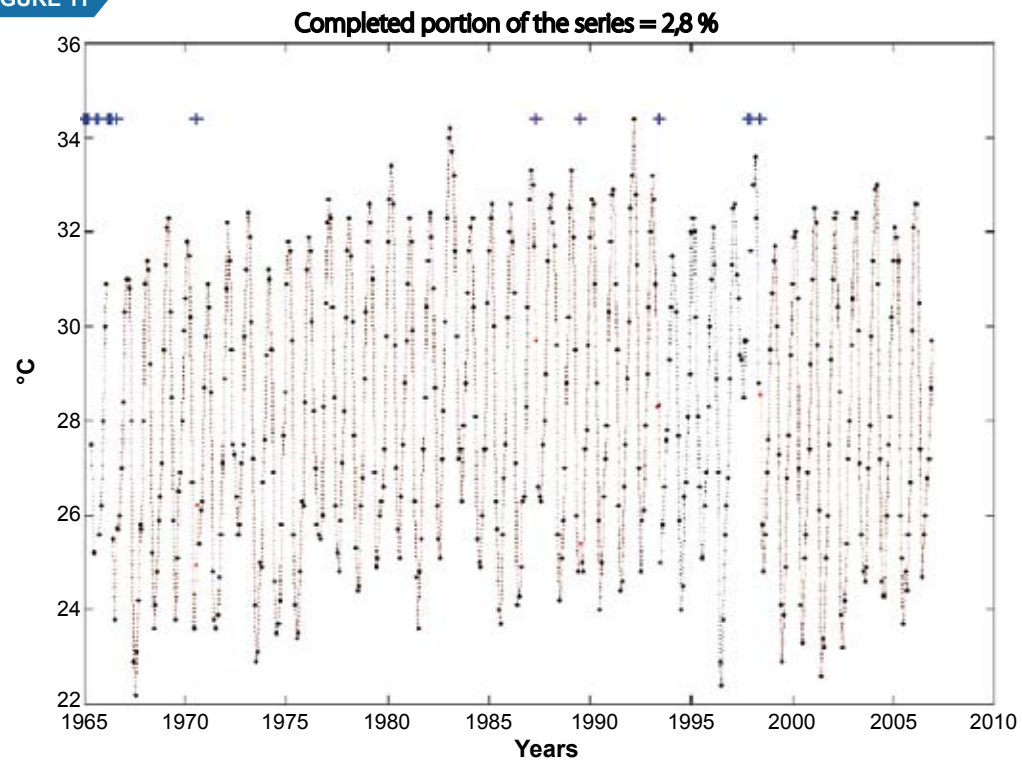

Example of an interpolation using the auto-regression (AR) method to complete data in temperature series. The black dots represent the observed data. The crosses in blue indicate the amount of missing data. The red dashed line represents the size of the series used to generate the AR1 parameter to estimate the data represented in red. The data is estimate based on the other (blue points).

FIGURE 12

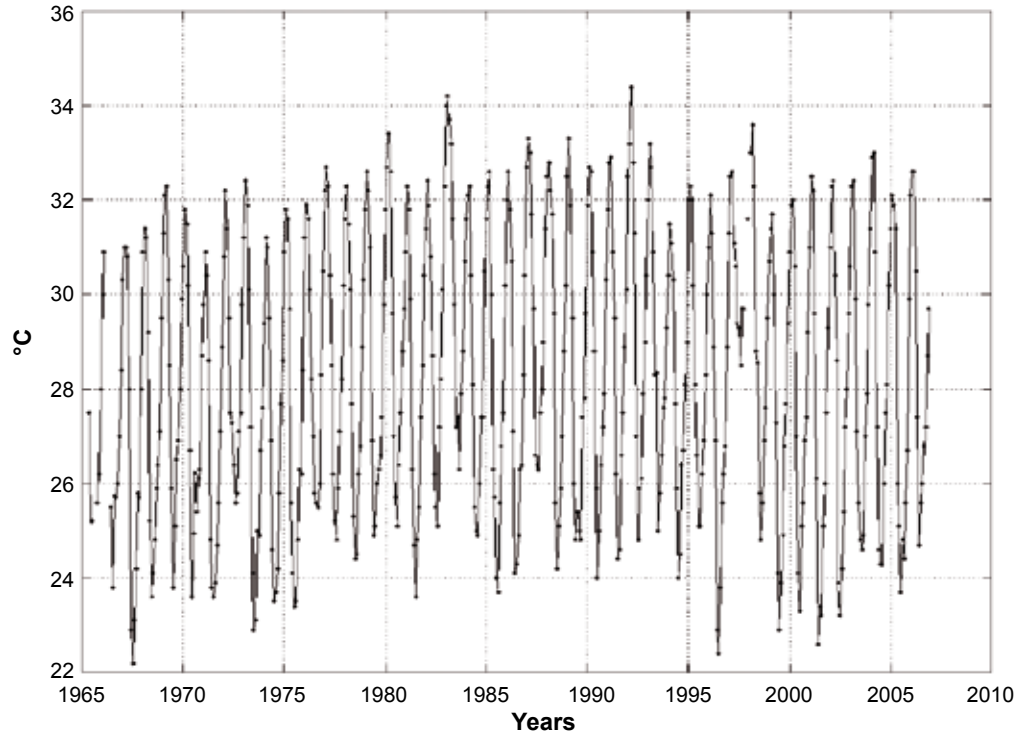

Final data series of maximum temperature, completed using the auto-regression method (AR1)

METHODOLOGY

3.2.1. Estimation of linear trend

The magnitude of the estimated linear trend of a temporal series, called slope (ratio of a variable per time unit), can be estimated using as a base the least squares of the estimated slope "ß" using the linear regression method. However, when "ß" is estimated this way, it can be significantly biased from the real slope value whenever there are some discrepancy values "outliers" in the time data series to be estimated (Gilbert, 1987). For this reason a very simple procedure is used developed by Sen (1968) and extended by Hisch et al. (1982).

In this method, the slope of the temporal series trends is obtained estimating N" = n(n-1)/2 estimated slopes using:

$$S_e = \frac{x_j - x_i}{j - i}$$

Where, xj and xi are the values of the data at time j and i, respectively, and j > i. N' is the number of data pairs of the series in which j is > i. The median of these N' values of Se, is the estimated slope value of the time series, called Sen's slope.

Due to the high variability both temporal and spatial, of precipitation; it is necessary some kind of standardization in dealing with these estimates, basically to analyze the spatial distribution of trends. This

FIGURE 13

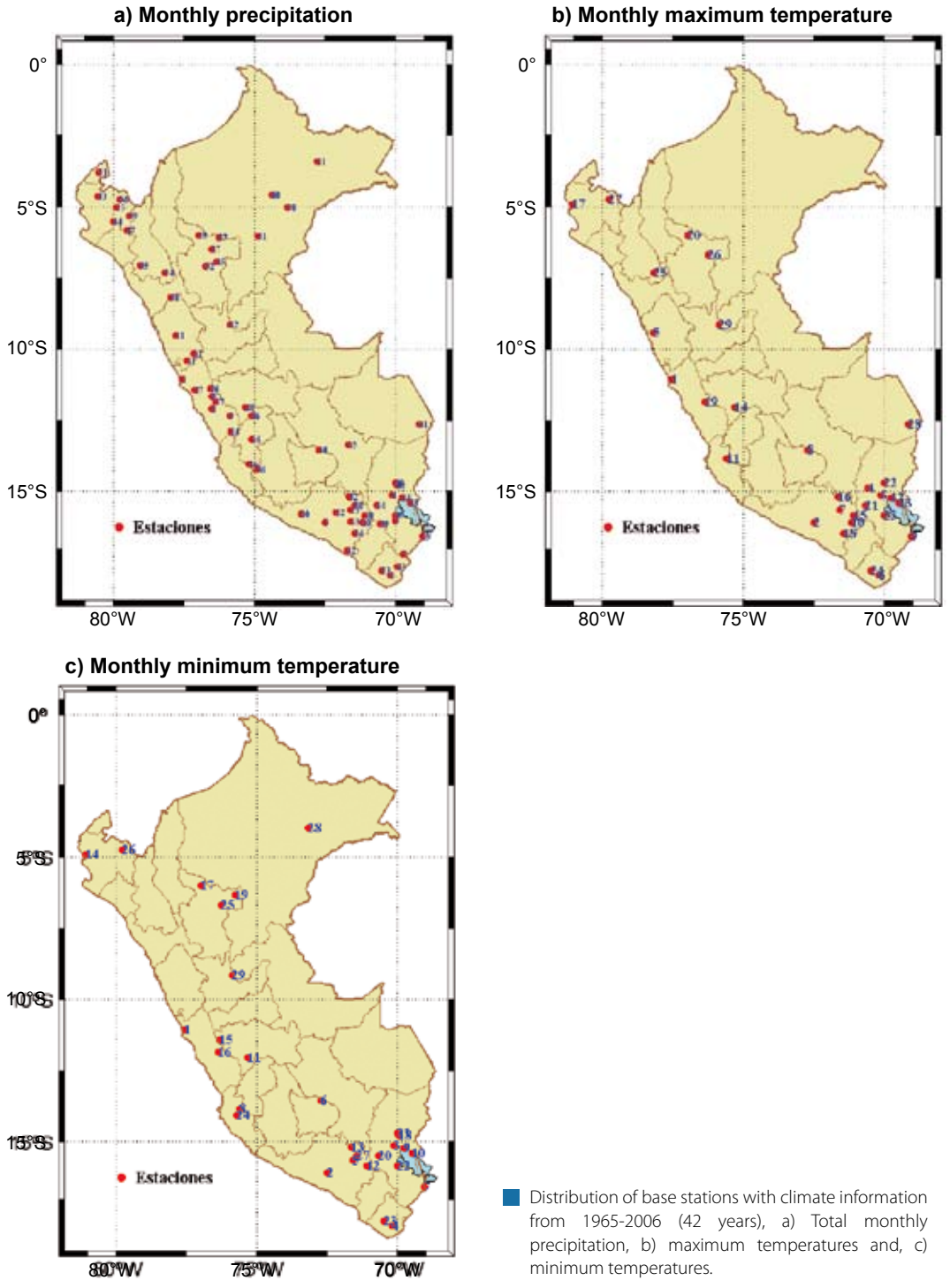

Distribution of base stations with climate information from 1965-2006 (42 years), a) Total monthly precipitation, b) maximum temperatures and, c) minimum temperatures.

way, to obtain a better analysis and understanding of the spatial distribution of precipitation trends, the present report shows the percentage of the linear trend for each time series in relation to the average corresponding to the period under study.

This parameter is computed as follows:

$$T = \frac{se * nd}{\overline{x_i}} * 100$$

Where, se is the estimated slope of the time series done by means of the Sen method, $\overline{x_i}$ is the average of precipitation for the whole period, and nd is the number of data (years or months) of the data series that are being considered. For example, nd is equal to 42 years for precipitations (1965-2006). The linear trends of maximum and minimum temperatures were expressed in ºC /decade.

3.2.2. Determination of the statistical significance of the linear trend

Determining the statistical significance of linear trends of precipitation, temperatures and climate indices, the non-parametric test Mann-Kendall is used. The advantage of using this test is to know how to use the relative magnitude of the values of the time series, filtering extreme values, instead of using real values. At the same time, it is necessary to keep in mind that in this test the data needs to comply with certain conditions, such as: they must be random variables, independent and identically distributed (iid). In conclusion, the autocorrelation of the series needs to be null.

These conditions restrict its application in climatological series, such as precipitation, due to the strong monthly and seasonal dependence. Then, it must be taken into account the characteristics of this test when it is going to be applied to climatological series, such as precipitation, for the total annual series, total or averages of a station or some specific month that can be considered as independent. More details on this methodology can be found in Kendall (1975), Hirsch and Slack (1984) and Gilbert (1983).

The null hypothesis (HO) states that the x1, x2, x3 ….. xn are independent random variables and identically distributed (iid). The statistical test of Mann-Kendall (S) is given by:

$$S = \sum_{i=1}^{n-1} \sum_{j=i+1}^{n} sgn(x_i - x_j)$$

Where, the sgn function is:

$$\begin{aligned} sgn(xi - xj) = 1, &\quad sí \quad xi - xj > 0, \\ = 0, &\quad sí \quad xi - xj = 0 \\ = -1, &\quad sí \quad xi - xj < 0 \end{aligned}$$

For the series larger than 10, the statistic (S) is close to normal distribution, when the following correction is made S= S-sgn (S). Considering the null hypothesis and there is no repetition of values in the series, the variance of (S), [Var(S)] is defined as:

$$Var(S) = \frac{n(n-1)(2n+5)}{18}$$

And with the correction, due to repetitions, the variance stays as:

$$Var(S) = \frac{\left[n(n-1)(2n+5) - \sum_{p=1}^{g} t_p (t_p - 1)(2t_p + 5) \right]}{18}$$

Where g is the number of groups with repeated data and tp is the number of data in the worst group. Then S and Var (S) are used to estimate statistical Z, with normal standardized distribution:

$$Z = \frac{S-1}{[Var(S)]^{1/2}}, \quad \text{if} \quad S > 0,$$

$$Z = 0, \quad \text{if} \quad S = 0,$$

$$Z = \frac{S+1}{[Var(S)]^{1/2}}, \quad \text{if} \quad S < 0$$

The positive (negative) values of Z indicate the ascending (descending) trend. In order to improve the interpretation and to deepen in the linear trend analysis, the trends of the climate variables of precipitation, total annual and seasonal were estimated; and for temperatures, the annual and seasonal averages were estimated as well. Regarding the climate indices trends, only the annual values were considered. For the present study, the seasons of the year were defined as follow: spring (SON), summer (DJF), autumn (MAM) and winter (JJA).

If the null hypothesis (HO) is truth, the statistical Z has a normal standard distribution. To test, the ascending trends as well as the descending trends, at the significance scale α, HO is accepted if the absolute value of Z is lower than Z1-α /2 (two-side test). The value of Z1-α /2 is chosen a priori once we know the direction of the trend. This value, α, in all the test made for the present report, is 0,05 (5%).

3.2.3. Determination of climate extreme indices

To estimate the climate extreme indices, daily data of precipitation and maximum and minimum temperature are used. The indices used in the present report are based on the methodology of Frisch et al. (2002) and are used in the IPCC report (AR4) (Trenberth et al. 2006) to define variations of extreme values of future climate. In table 1 each one of the definitions of the indices estimated for the present report are described.

These indices do not represent extremes considered as rare which can possible affect the statistical processing and the significance of the trends due to the small number of events registered in the historical record. Some of these indices are based on a fixed threshold value, making it easy to understand their impacts. Other indices are based on percentiles which allows to make comparisons between seasons.

3.2.4. Standardized Precipitation Index (SPI)

The methodology used in the analysis of drought in the present report, is the Standardized Precipitation Index (SPI). The SPI is used because it provides a simple value to measure the intensity of the drought, as a measure of the probability of occurrence, for any time scale. This value reflects the impact of the drought on the availability of the water resources.

Its temporal invariance is another important feature of the SPI, it allows that long term or short term events may be captured with the same methodology; it is possible to experiment drought conditions on certain time scale, while it experiments humid conditions on another time scale. This makes de SPI a very versatile tool to report conditions of precipitation.

Table 1 Indicators of climate extremes

Indicator	Name of indicator	Definition	Unit
CDD	Consecutive dry days	Maximum number consecutive days with RR< 1mm	days
CWD	Consecutive humid days	Maximum number consecutive days with RR>=1mm	days
R10mm	Number of days with Intense precipitation	Number days in a year in which PRCP>=10mm	days
R20mm	Number of days with Very Intense precipitation	Number of days in a year in which PRCP>=20mm	days
R95p	Very humid days	Total annual precipitation in which RR>95 percentile	mm
R99p	Extremely humid days	Total annual precipitation in which RR>99 percentile	mm
RX1day	Maximum amount precipitación en un día	Monthly maximum precipitation in 1 day	mm
RX5day	Monthly maximum precipitation in 5 days	Monthly maximum precipitation in 5 consecutive days	mm
TX10	Cold days	Annual percentage in which maximum temperature is TX< 10 th percentile in relation to the climatology from 1971-2000	days
TX90p	Warm days	Annual percentage in which TX > 90 th Percentile in relation to the climatology	days
TN10p	Cold nights	Annual percentage in which minimum temperature is TX< 10 th percentile in relation to the climatology from 1971-2000	days
TN90p	Warm nights	Annual percentage in which TX > 90 th Percentile in relation to the climatology	days

The Standardized Precipitation Index (SPI) was originally established as a method to quantify and define the conditions of drought (McKee et al, 1993 and 1995), then it became a valid tool for all the studies on water availability, for either long or short duration (Hayes, et al, 1999). The estimate of the SPI values is based on the distribution of precipitation over relatively long periods of time (preferably more than 50 years). From the monthly precipitation records from 1965 to 2006 (42 years) for 64 stations distributed all over Peru, the total monthly values of precipitation for each station were accumulated quarterly and annually; then, they were adjusted to a Gama distribution of probabilities, a condition that is necessary to apply the SPI (Mc Kee, 1993, Abramowitz and Stegun, 1972) in order to determine monthly, quarterly and annual values. This distribution is then transformed in normal standard, so that the mean equals zero and the deviation is standard, i.e. the unit.

The SPI values correspond to the standardization of the total gama-transformed precipitations for which an index equal to zero indicates that there was no deviation in the values of precipitation, relative the average precipitation for the analyzed period. The positive values of SPI indicate that precipitation exceeds the average, and negative values indicate that precipitation is less than the average. So, drought periods are characterized for showing negative SPI values (Table 2)

Table 2 The SPI and intensity of drought

SPI	Severity of the drought	Probability
> 0	Humid	50%
-0,99 a 0	Slight	34,1%
-1,49 a -1	Moderate	9,2%
-1,99 a -1.5	Severe	4,4%
<= -2	Extreme	2,3%

Source: McKee, 1993.

The gama distribution is defined in the publication (Wu et al. 2005) and is established by means of the following equation:

$$G(x) = \frac{1}{\mathrm{b}\ \Gamma(\mathrm{a})} \int_0^x x^{\mathrm{a}-1} e^{-x/\mathrm{b}} dx$$

Where:

G (x) – accumulated probability
β– parameter of scale
a – parameter of form
x – random variable (monthly precipitation)
Γ [α] – gama function

The parameters α and β are estimated $\mathrm{a} = \frac{1}{4A}\left(1+\sqrt{1+\frac{4A}{3}}\right)$ and $\mathrm{b} = \frac{\bar{x}}{\mathrm{a}}$. Where:

$A = \ln(\bar{x}) - \frac{\sum(\ln(x))}{n}$, being n the number of observations (Lloyd-Hughes and Saunders, 2002).

After estimating the accumulated probability G(x), being x the monthly, six-monthly and annual precipitation, the value of Z (standardized precipitation) was determined for the same probability, this way the SPI is obtained.

3.2.5. Tele-connections of droughts in Peru

The large scale atmospheric systems that modulate weather and climate and produce precipitation in Peru are diverse and associated to local geographical conditions, resulting in the different regimens of observed precipitation.

It is well known that the warm phase of the ENSO phenomenon causes anomalies in precipitation over the southern part of Peru, and floods in the northern coast (Quinn and Neal, 1992). This way, this seasonal relation between the SPI and the monthly anomaly of sea surface temperature of the El Niño 3.4, which is an index of the ENSO event, intends to confirm the effect of the warm events of the ENSO in producing negative anomalies in precipitation, and determining the variability in the intensity of these

connections in Peru. On the other hand, there are some studies on the impact of PDO on precipitations. The results of the work done by Obregón and Marengo (2006) show that precipitation in the central and southern mountain region is strongly modulated in a decadal scale by the Pacific Decadal Oscillation. The purpose is to disseminate these results and to determine the existence of consistent possible tele-connections; both spatial and seasonal. Also, the difference in the sea surface temperature (SST) between the Southern and Northern Tropical Atlantic (TSA – TNA) defined by Rajagopalan et al (1998), is associated with the latitudinal position of the Inter Tropical Convergence Zone (ITCZ) and it shows high inter-annual and decadal variability. If the main source of atmospheric humidity for the jungle and mountain regions in Peru is the Atlantic Ocean, it is expected that the transport of humidity from the Tropical Atlantic mainly related to the interannual variability of the SST dipole between the southern and northern tropical Atlantic; causes some effect on the distribution of precipitation and drought events in Peru.

a) Simultaneous correlations

In order to determine these possible connections between large scale patterns, that modulate the occurrence of precipitation during the seasons of the year, and consequently cause drought in Peru, simultaneous correlation analysis were made between temporal and seasonal series of the SPI and the indices of the El Niño Southern Oscillation (ENSO) event, the Pacific Decadal Oscillation Index (PDO) and the standardized difference between the SST of the northern and southern Tropical Atlantic (TSA-TNA). The seasonal series for each one of the ocean/atmosphere indices and for the SPI, were estimated as standardized anomalies, computed from the mean monthly values for each season of the year.
Simultaneous correlation indicates the linear relation that exists between two variables, x(t) and y (t), during a period of time (N). The magnitude of the correlation coefficient (r) indicates a useful measure of the variability rate in which both variables are associated. In case the correlation coefficient is statistically significant, there is the possibility of an inherent physics relation. The correlation is defined in the following way:

$$r = \frac{\frac{1}{N}\sum_{t=1}^{N}(x(t)-\bar{x}).(y(t)-\bar{y})}{S_x S_y}$$

Where, x(t) and y (t) are the temporal series of a N size with averages $\bar{x}$ and $\bar{y}$,and standard deviation Sx and Sy respectively

b) Statistical Significance of Correlations

The statistical significance of correlations is estimated using the effective number of DOF of the time series, which is obtained by the method suggested by Davies (1976), as follows:

$$N_{\not e} = \frac{N}{T_d}$$

Where, $N_{\not e}$ is the effective number of independent observations, N is the size of the time series and Td is the characteristic time scale.

In the present study, to estimate T_d it is assumed that the series are the results of auto-regression processes AR1 or red-noise processes, in a way that:

$$T_d = \frac{1+\mathrm{r}_x(1)\mathrm{r}_y(1)}{1-\mathrm{r}_x(1)\mathrm{r}_y(1)}$$

Where: $r_x(1)$ is the autocorrelation of the base series X and $r_y(1)$ is the autocorrelation of the second series Y.

Then, the significance of the correlations at 95% is obtained by means of the two-tailed t-test, based on the null hypothesis, zero correlation.

3.2.6. Analysis of the Principal Components (PCA)

The analysis of the principal components (PCA) is a multivariate statistical technique used to examine the spatial-phase structure of the climate /atmospheric variables that have several dimensions, so it is convenient and necessary to reduce these dimensions to smaller ones, in which most of the variability proportion can be represented.

In studies made with observed data and data from modeling, both meteorological and climatological, the PCA is quite known and frequently used. More details can be found in many references (for example, Richman 1986; Preisendorfer , 1998; Von Storch and Navarra, 1995; Von Storch and Zwiers, 1999).

In the present report, the PCA is used to determine the spatial/temporal patterns of droughts in Peru, based on temporal series of 64 quarterly SPI (agrometeorological droughts) computed as indicated in item 3.1. The reason for using quarterly series is because they have continued values, different form monthly values that have a lot of null values as a consequence of prolonged dry periods.

The computing of the PCA was done from the diagonalization of the dispersion matrix or correlation C (MxM) obtained from the data matrix of the Standardized Precipitation Index (SPI), both monthly and normalized. X(NxM) where M=64 corresponds to the number of SPI series (pluviometric stations) and N= 504 is the number of months of the period used for the present study (1965-2006). From the matrix C groups of patterns are determined mutually orthogonal that include the matrix E (MxM) and the corresponding matrix of expansion coefficients Z (NxM), whose columns are mutually orthogonal. The patterns are denominated "empirical orthogonal functions". EOF (or auto-vectors) and in this case, they represent the spatial pattern, and the expansion coefficients are referred to as "principal components" –PC or temporal series of the coefficient matrix Z. It must be emphasized that the first empirical orthogonal function e1 is the linear combination of the input variables xj that explain the larger fraction of the combined dispersion of the X's. The second e2 is the linear combination that explains the larger fraction for residual dispersion and it continues like this.

In any PCA it is important to determine how many EOF/PCA represent the signal and how many of them are "noise" and also the statistical unit of each autovalue (EOF), that is determined by separating their corresponding auto-values . It was also demonstrated that when the autovalues in the neighborhood have similar magnitudes, it occurs an effective degeneration in which two or more EOFs are mixed. To make a diagnosis unity and determine the number of most representative EOFs in the analysis, the North rule (1984) is used. This rule determines that for autovalues in the proximities, not to be subject to mixing, the separation between an autovalue and the adjacent ones, $A\beta = \lambda\alpha - \lambda\beta$ must be larger that its sampling error ($\lambda\partial\alpha = \lambda\alpha\ (2/n)\ ½$). This way, they are part of the degenerated "multiplet" and their EOFs are a mixture of the true EOFs.

3.2.7. Wavelet Analysis

The wavelet analysis facilitates a local assessment of the amplitude and phase of each harmonic, contrary to what the traditional Fournier's transform, which gives the ampleness and mean phase of each harmonic throughout the period. This way, the OT is useful to detect non-stationary signals or episodic fluctuations.

Also, the OT provides an adaptive window to time-frequency that automatically enlarges when it focuses on high frequency oscillations and it shrinks for low frequencies. These features are the most adequate in the signal analysis with multi-scale components. For this reason, the OT is considered to be ideal for the analysis of the series that are highly non-stationary with episodic characteristics and multi-scale, as the temporal series of the drought patterns in Peru are expected to be, as result of the PCA.

The Wavelet decomposes a continuous function $f(t)$ in terms of a group of waves $\psi_{r,s}(t)$. Each wave is derived from a basic function $\psi(t)$ by means of the transference (r) (change position) and expansion (change scale)

$$\psi_{r,s}(t) = \frac{1}{\sqrt{s}}\psi\left(\frac{t-r}{s}\right)$$

The wavelet follows the $f(t)$ function, defined as the integral of:

$$W(r,s) = \frac{1}{\sqrt{s}}\int \psi^{*}\left(\frac{t-r}{s}\right) f(t)dt$$

Where: ψ^{*} is the conjugated complex of ψ. The $1/\sqrt{s}$ factor of the integral is used to normalize the energy of each wave. This equation essentially shows the transformed of the $f(t)$, function, of the temporal domain, for the $W(r,s)$ function in the transfer domain and of the scale , or in the r-s domain. For a given wave, there is usually a relation that transfers r for the time t, and the scale s for the frequency f, allowing to obtain the relation $W(r,s) \rightarrow W(t,f)$. In conclusion, the wavelet decomposes the function $f(t)$ in the time-frequency space, t-f.

There are a lot of basic functions used to generate several waves. In the present study the most complex function of Morlet (Morlet et al. 1982a, 1982 b). This function consists of a plain wave modulated by a Gaussian envelope. The generated waves are called Morlet waves. The similar pattern to waves of this wavelet is particularly adequate for the analysis of the oscillations of the time series of each significant pattern determined in the PCA of the monthly standardized precipitation indices (SPI) for Peru. Morlet's basic function is expressed as:

$$\psi(t) = e^{iw_0 t} e^{-t^2/2}$$

Where, wo is the non-dimensional frequency and it ha a value of 6 to meet the condition of admissibility (Morlet's basic function must have zero as the mean value and it has to be located in both spaces: time and frequency) the generated waves are:

$$\psi_{r,s}(t) = \frac{1}{\sqrt{s}} e^{iw_0\left(\frac{t-r}{s}\right)} e^{-\left(\frac{t-r}{s}\right)^2/2}$$

The relation between the space r-s and the space t-f for the Morlet wave (Torrenco and Compo, 1998) are:

$$f = \frac{w_0 + \sqrt{w_0^2 + 2}}{4\pi s}$$

The temporal series of each spatial patterns of the SPI, determined by the PCA will be subject to the Wavelet analysis with the purpose to determine the oscillations in the different scales, which are typical of each one of them and, with this estimate their relation with the interannual variability of droughts.

3.3 RESULTS

In the present item the detection of climate change and the national extreme climate indices are analyzed in detail.

3.3.1 Linear trends of precipitation

Linear trends of total annual precipitation, estimated in percentages, in relation to the average value for the analyzed period (1965-2006) for 64 station distributed throughout the country, are shown in Figure 14. The observed extreme values reach percentages from -94%, in the Juancito station, Department of Loreto, up to + 70% in the Ricaplaya station, Department of Tumbes.

For the northern coast of Peru an increase in the total annual precipitation is observed for the last 42 years (1965-2006). This characteristic extends towards the central coast (northern part of Lima) and the northern jungle of Peru. Then, the positive trends continue in the entire central mountain region and reach the southern mountain region, in Puno, especially in the highest areas of Arequipa and Tacna. The extension of these positive trends towards the northern jungle are observed in some isolated stations, in the middle of other station with negative trends, specially those in the jungle region of the Department of San Martin. In the northern jungle (Loreto) negative trends are observed, focused on Juancito station. Conversely, in the central jungle (Tingo María) and southern jungle (Tambopata) the trends are positive.

Also, in the central and southern part of the coast and the western side of the mountain region some non-significant positive and negative trends are observed, without a visible regional pattern. It is worth mentioning that between the southern part of Arequipa and Tacna these trends are emphasized negatively, reaching intense negative values between -82% and -84%, which are statistically significant. For what has been observed about the mountain and southern jungle, apparently there is some kind of regional climatological precipitation pattern, especially in the Departments of Puno, Arequipa and Madre de Dios.

FIGURE 14

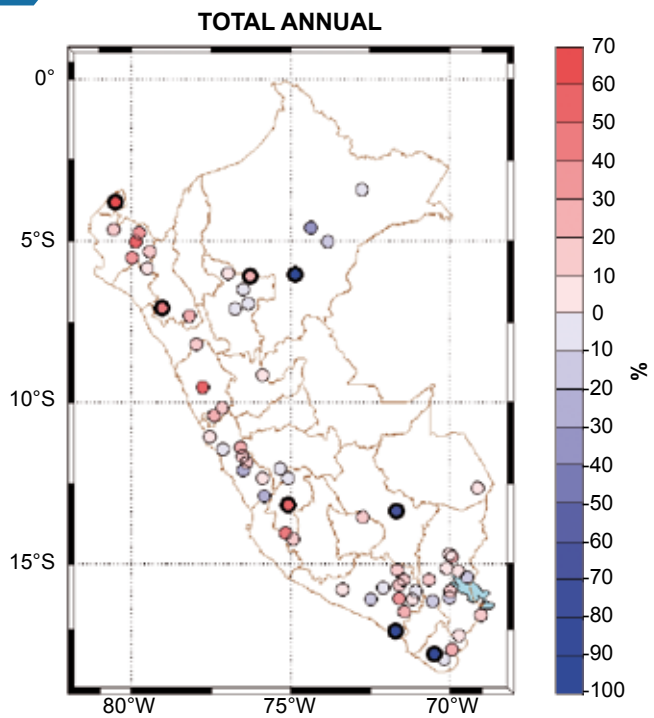

Linear Trend of total annual precipitation in %, relative to the multiannual average (1965-2006). Trends with statistical significance at a rate of 5% or less than the Test Mann-Kendall, are indicated in black

Colquepata (Cusco) is a location with a significant negative trend, it shows -68%. La lack of data corresponding to the central mountain and jungle region in Peru, does not allow neither to get nor to make any kind of relation between the recorded negative trends in the northern jungle or further down to the Department of Cusco, since any conclusion made on this matter, will have no argument because of the lack of observations.

The best way to obtain a clear idea between interannual variability of total annual precipitation and its relation to linear trends is by means of a temporal distribution of total annual precipitation during the period under study. Figure 15 shows the interannual distribution of precipitation and its trend in four stations distributed in the country that may be representative of the regional characteristics of precipitation; they are located in the northern coast (Sondorillo), northern jungle (Juancito) central mountain region (Huayao) and southern mountain region (Puno).

Total precipitation over Sondorillo is less than 700mm and they show a slight constant increase throughout the 42 years (17,7% of the total average). Interannual variability does not present any clear signal related to El Niño / Southern Oscillation (ENSO). The station located at Juancito is characterized for an intense diminish in precipitation; statistically significant of -40mm/year (-93% of the average), mainly form the 70's decade up to the end of the 1990's. Then there is an intense increase in precipitation that goes from an average value of approximately 1 000 mm from 1995 to 2000, to a peak of more than 3 000 mm in 2002. The interannual variability does not show any modulation related to the ENSO phenomenon or to another event of a longer period.

The Huayao and Puno stations show inverse trends with lower values that are not statistically significant. Both stations register identical interannual variability, with low precipitations in the years 1983 and 1992; apparently associated to the positive ENSO events and high precipitations in 1984 related to the La Niña cold phase.

The temporal distribution of the total annual precipitation in the four stations, show the complexity that occurs in Peru. In the northern coast, there is apparently a constant increase of precipitation during the last 42 years, according to what has been observed in the Sondorillo station. In the northern jungle, where the interannual variability of precipitation is low, the main characteristic seems to be the important diminish in precipitation from the 60's decade up to end of the last century, when it occurred a sharp increase related to the ENSO event, then it seems to gradually go down . On the other hand, in the mountain region, both central and south, the effect of the ENSO event seems to modulate with higher intensity the interannual variability of total precipitation, and the values and trends are relatively low.

The main characteristic of the annual distribution of precipitation over most part of Peru is seasonality, with maximum values recorded during summer months and minimum values recorded in the winter time. This characteristic requires making seasonal analysis to detect climate change for precipitation, for instance computing the trends of the seasonal total values for precipitation.

The distribution of seasonal trends of precipitation in Peru, for the spring (SON), summer (DJF), autumn (MAM) and winter (JJA), are shown in Figure 16 a-d. The trends are estimated in % relative to the seasonal average of the whole period under study (1965-2006).

The spring season (Figure 16 a) shows trends with extreme values between -146% and +87%, as the values observed in Sama Grande (Tacna) and in Huaros (Lima), respectively. The spatial pattern during spring (SON) keeps several characteristics of the observed distribution in the total annual trend distribution (Figure 14) in the northern jungle, including the Departments of Loreto, San Martin, in the central coast (Ancash and Lima) and in the southern mountain region in the Departments of Huancavelica and some isolated stations in the Departments of Cusco and Abancay. In the northern mountain region, larger differences are observed, where negative trends prevail, and in the souther mountain, specially in the high part of Arequipa and Tacnawhere precipitation trends are negative (opposite to what is observed in total annual values).

FIGURE 15

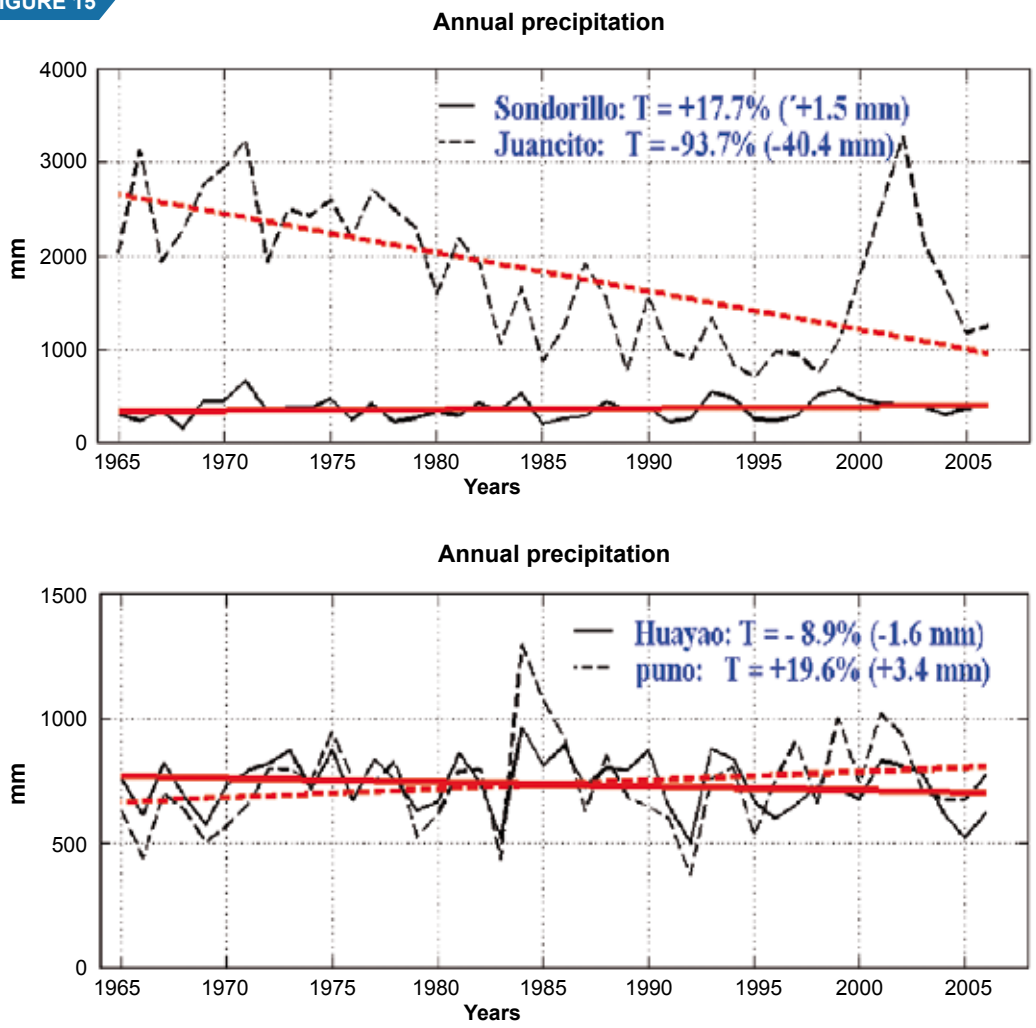

Temporal distribution of total annual precipitation (1965-2006) in mm at the Sondorillo (northern coast) Juancito (northern jungle) Huayao (central mountain region) and Puno (southern mountain region) stations. The best adjustment of linear trends is shown in the red lines.

During the summer season (DJF) seasonal precipitation trends (Figure 16 b) are very similar to the total annual. These slopes can be explained because during this season the highest precipitation values are registered, and they are proportional to the total annual value for the whole country. The difference between the annual patterns and the summer ones seem to be more noticeable in the absolute values of the trends than in the direction, increase or diminish. The extreme trends reach -88% minimum values in Juancito (Loreto) and the maximum of 72% in Rica Playa (Tumbes), which are the same station that show extreme values in total annual records.

In the autumn (MAM) and winter (JJA) seasons (Figure 16 c-d) the patterns of the total precipitation trends do not substantially change in relation to what has been observed in the total annual and the summer season. The extreme values in the autumn are observed from -98%, registered in Pampa Blanca (Arequipa) to +72% registered in Choclococha (Huancavelica). The winter months values range from -152% in Carania (Lima) to +98% in Choclococha (Huancavelica).

The distribution of the trends during the autumn season is very close to the one in the summer, with some differences in the northern jungle, Department of San Martin, and in the central mountain region,

FIGURE 16

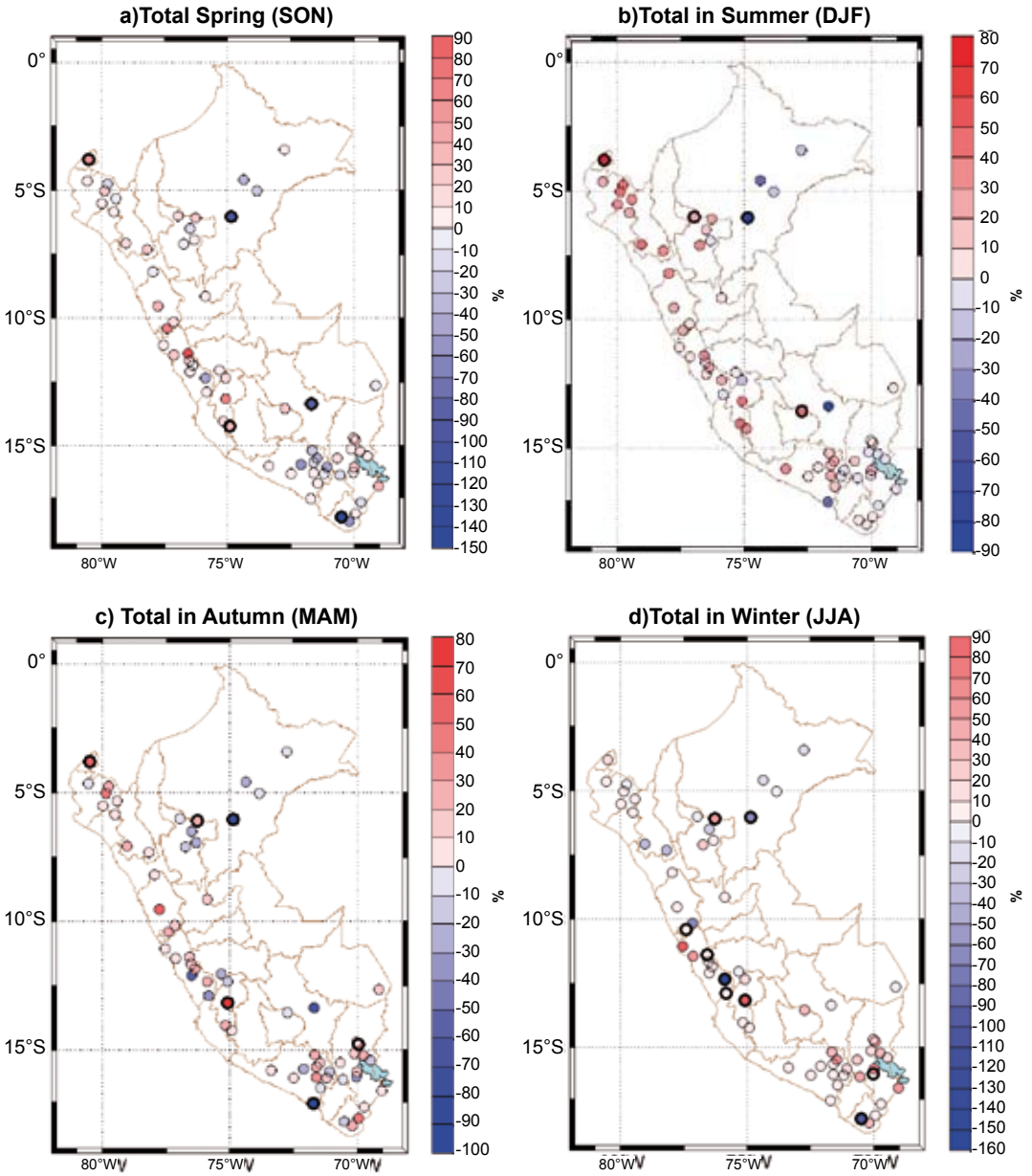

Linear trend of total seasonal precipitation in %, relative to the multiannual seasonal average (1965-2006) a) spring (SON), b) summer (DEF), c) autumn (MAM) and d) winter (JJA). The trends with statistical significance at a 5% level or less (test Mann-Kendall) are indicated in black circles.

where there happens to be some opposite trends in certain places. The spatial winter pattern (Figure 16 d) seems to be similar to the one in the spring along the coast, mountain and northern jungle; and, in the southern region also there is a similar pattern as in the summer months. Conversely, the coast and the central mountain show a very characteristic pattern, prevailing positive trends and some are statistically significant, especially in the western side of the Andes Mountains. In the middle of these locations there are some others that are scattered, with negative trends.

The temporal distribution of seasonal precipitation in the spring (SON) in the northern coast (Sondorillo) and northern jungle (Juancito) (Figure 16 a) has similar characteristics to the distributions of the total

annual values, with intense negative trends in Juancito and quite weak in Sondorillo. The interannual variability is moderate and, apparently, there are no signals of the effects of the ENSO events during the whole period under analysis. Conversely, in the central (Huayao) and southern (Puno) mountain region, interannual variability is very high, particularly from 1975 to 1985, but the trends follow the same direction of the total annual values.

The behavior of these temporal series does not have any evident and continuous signals of the effects of the ENSO phenomenon. However, they seem to be modulated during these months by a larger oscillation because the interannual variability changes quite a lot before 1975 and after 1985.

During the summer (DJF) total distributions of the stations located in the coast and northern jungle (Figure 17 b) show interannual variability and trends very similar to the annual totals. In these months it is possible to observe some signals of the ENSO phenomenon of 1982/83 in two stations. There is also a substantial diminish in Juancito and a slight increase in Sondorillo. In other ENSO events , there is practically no evident signal . In the stations of the central and southern mountain region, the interannual variability is similar to the annual total and very different from the spring months. There can be seen an apparently oscillation at a longer scale than the interannual. The events that occurred in the positive phase of the ENSO phenomenon of 1982/83 and 1991/92 are evident in both stations, causing a shortage in precipitation.

The stations located in the coast and northern jungle show similar distributions to the ones observed in the annual total, and in the stations located in the central and southern mountain region are similar to the ones observed during the months of spring, with high interannual variability, especially during the period under study. Also, during those months, the stations in the central and southern jungle, seem to show more sensibility to the warm events of the ENSO, in relation to the stations located in the coast and northern jungle, as it can be seen in the strong events of 1982/83 and 1991/92. Figure 17c shows the temporal distribution of precipitation in the months of autumn (MAM).

In the winter months (Figure 17 d) precipitations over the northern coast are practically none, and shows no particular characteristic. The distribution in Juancito registers little interannual variability and a strong relation with the extreme events of the ENSO, such as in the case in 1982 and, especially in the winter of 2002, when precipitation reached more than 1 000 mm. In the central (Huayao) and southern (Puno) mountain region precipitation shows high interannual variability and the ENSO signal seems weakened due to other intense events such as the ones in 1981 and 1990. But, it seems that there is some larger oscillation that modulates precipitation in these two regions, that becomes evident in the high variability before 1975 and after 1985, an inverse behavior to the one observed during the spring months. This way, the reason for the negative (positive) trends in Huayao (Puno) seems to be associated to these oscillations that basically modulate the intensity of the interannual variability.

3.3.2. Linear trends of maximum temperature

The spatial distribution of the trends of annual maximum mean temperature (Figure 18) shows that there is a predominance of positive values, statistically significant, at 5 % in the whole country. The extreme values are: -0,26 ºC /decade, registered in Pampahuta (Puno) and +0,52 ºC/decade registered in San Marcos (Cajamarca).

Between 1965 and 2006 (42 years) it can be observed that in almost the whole territory of Peru there was an increase in the annual maximum mean temperatures, and their trends showed values statistically significant almost in every location in the mountain and, apparently in the southern jungle, where the trends are significant. In some very regionalized places, some diminish in annual maximum temperature was registered, as in a location in Puno, coastal zone of Piura, San Martin and Tingo María. In the northern jungle (San Martin) the negative trend is statistically significant.

FIGURE 17

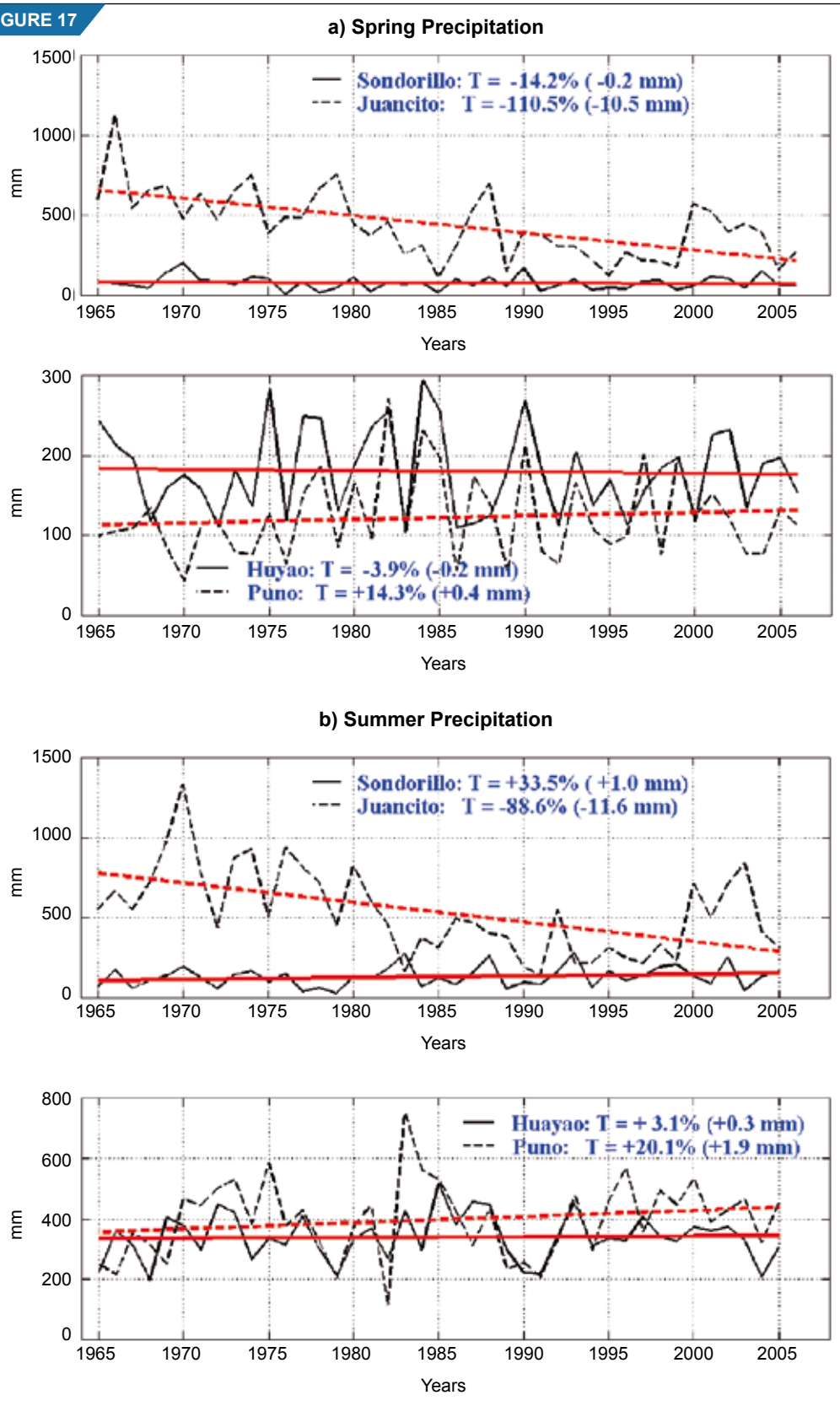

Temporal distribution of total seasonal precipitation (1965-2006) in the stations of Sondorillo (northern coast), Juancito (northern jungle), Huayao (central mountain region) and Puno (southern mountain region). a) Spring (SON), b) summer (DJF), c) autumn (MAM) and d) winter (JJA). A better adjustment of the linear trends is indicated in red lines.

FIGURE 17

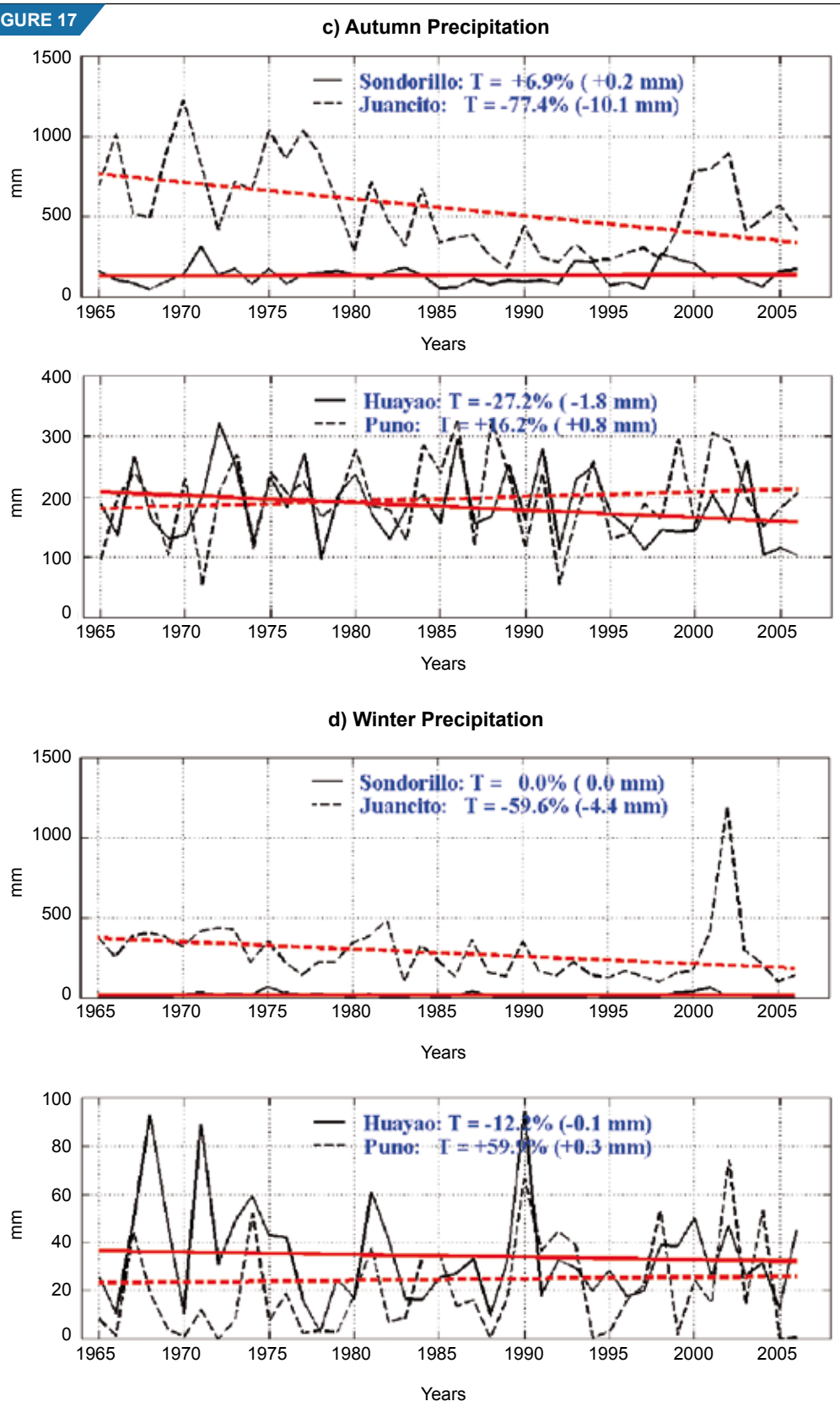

Temporal distribution of total seasonal precipitation (1965-2006) in the stations of Sondorillo (northern coast), Juancito (northern jungle), Huayao (central mountain region) and Puno (southern mountain region). a) Spring (SON), b) summer (DJF), c) autumn (MAM) and d) winter (JJA). A better adjustment of the linear trends is indicated in red lines.

FIGURE 18

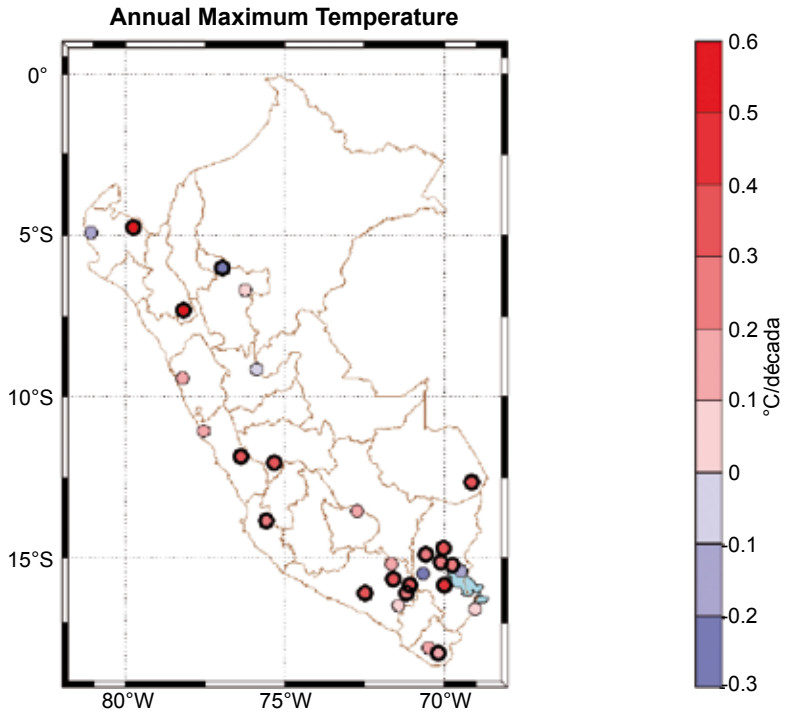

Spatial distribution of annual maximum mean temperature (°C/decade) estimated for the period 1965-2006. The trends with statistical significance at 5% or less in the Mann-Kendall Test are indicated in black circles.

As it was done for precipitation, for maximum and minimum temperatures some representative stations were chosen, from which a clear idea of variability and temperature trends could be obtained, for the period under study (1965-2006). Figure 19 shows the temporal distribution of the annual maximum temperatures of three selected stations that better characterize la northern jungle, central and southern mountain region. Two stations (Puno and Matucana) show positive trends, contrary to what the station in the jungle region (Moyobamba) does. The temporal variation of annual maximum mean temperature in the three stations characterize for presenting monotonic alterations (gradual continuous change). This feature is associated to low interannual variability, and apparently, is not modulated by longer periods and the variations among them are not within the phase. It seems that maximum temperature variability in these stations is independent one form each other.

The only station that seem to be affected by the impact of the ENSO is the Puno station, as it is shown in Figure 19, where it can be observed slight alterations in temperature during the warm events of 1982/83 and 1997/98.

The spatial distribution of the seasonal maximum mean temperature trends (Figure 20 a-d) shows similar patterns to the one of the annual maximum mean temperature (Figure 18). The lowest values of the seasonal trends are registered in the summer season (DJF) and autumn (MAM) in the northern jungle, in Moyobamba with 0,39 and -0,33 °C/decade respectively. The maximum seasonal value was registered in the winter time (JJA), in Piura, in the location called Sausal de Chulucan, with +0.67 °C/decade.

In the spring time (SON) and in the summer (DJF) the positive significant trends, include the whole territory of Peru, except for some isolated regions, as in the coast of Piura, San Martin and Puno where the trends are negative. The autumn spatial pattern is identical to the annual one. The same thing occurs with the winter pattern, except for the negative trends observed in all the stations of the northern jungle (San Martin and Tingo María).

FIGURE 19

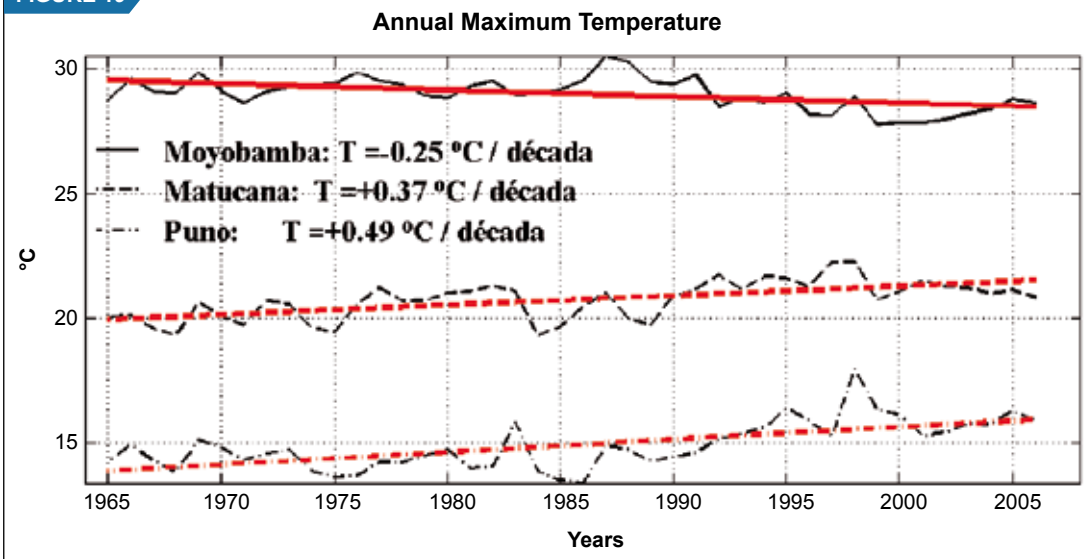

Temporal distribution of anual máximum mean temperatura (1965-2006) of the Moyobamba station (northern jungle), Matucana (central mountain región) and Puno (southern jungle) A better adjustment of the linear trends is indicated in red lines.

The temporal distribution of seasonal maximum temperatures of the three stations which are characteristic of the northern jungle and central and southern mountain region (Figure 21 a-d) shows the monotonic trend during the four seasons. The Moyobamba station (northern jungle) shows low variability in all the seasons of the year and it does not register any signal of the ENSO phenomenon. However, during the autumn and winter seasons, it shows little cycles with slight positive anomalies at the end of the 80's decade and negative anomalies at the end of the 90's. The distribution of the stations in the central and southern mountain region shows that during summers the interannual variability is larger than in any other season and it occurs in a synchronized way throughout the whole period under analysis. Another observed characteristic is the direct relation existing between the warm events of the ENSO and the maximum temperatures in Puno and slightly in Matucana, particularly during the summer and autumn, as it is observed during the events of 1982/83 and 1997/98.

3.3.3. Linear trends of minimum temperatures

A spatial distribution of the annual minimum mean temperature trends in Peru, for the period 1965-2006, is shown in Figure 22. Also it can be observed the predominance of the positive trends. Also, some positive statistically significant inclinations are observed in the southern mountain region, Department of Arequipa and Tacna, in the northern coast and northern jungle. Conversely, negative values are registered in the central mountain region and in Puno, in the areas surrounding the Titicaca Lake. The minimum value of the trend was registered in Puno, in the El Progreso location with -0.28 ºC /decade and the maximum value in Piura, in the La Esperanza location, with +0.48 ºC /decade. This pattern shows, in a mean term, a distribution of the trends with values in the same direction of the maximum temperature pattern over most part of Peru. The largest difference is observed in Puno, where the majority of the station in areas close to the Titicaca Lake register significant negative trends.

The temporal distribution of annual minimum mean temperatures in representative stations in the northern (Moyobamba) and southern (Puno) jungle, shows opposite directions regarding the central mountain (Matucana) see Figure 23. These trends are exactly opposite to those observed in the distribution of the annual maximum temperatures (Figure 19). Minimum temperature in Puno gradually increases in the middle of the low interannual variability, without the presence of any anomaly due to the presence

FIGURE 20

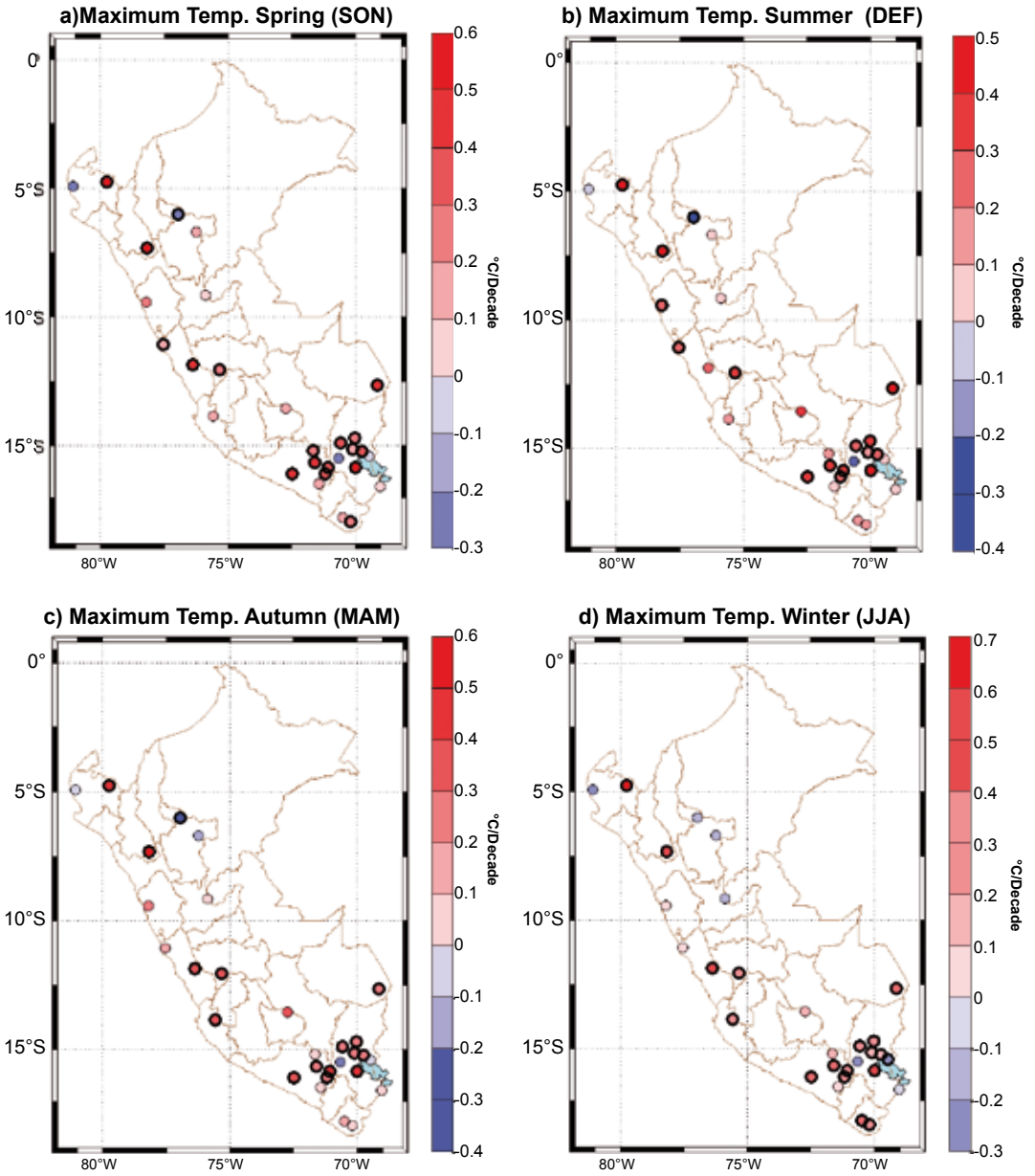

Spatial distribution of the trends of seasonal maximum mean temperatue (ºC / decade) estimated for the period 1965-2006), a) spring (SON), b) summer (DJF), c) autumn (MAM) and d) winter (JJA). The trends with statistical significance at 5% or less (Test Mann-Kendall) are indicated in black circle.

of the ENSO event. On the other hand, the annual series minimum temperature in the northern jungle and central mountain region, besides having opposite trends, they show opposite periods of interannual variability as well. This way, in the northern jungle los interannual variability is observed between the beginning of the 1980's up to 2006, after and apparent oscillation of a larger scale, observed since the beginning of the period under study, apparently associated to a strong negative anomaly occurred during the ENSO event of 1976/77, and in the central mountain region this characteristic reverses, with a very weak interannual variability from the beginning up to the end of the 1980's, then it becomes similar to the one observed in the northern jungle, before the decade of de 1980's. All this, apparently is associated to the warm event of 1982/83 that caused positive anomalies, and to the presence of very intense negative anomalies occurred in 1999.

FIGURE 21

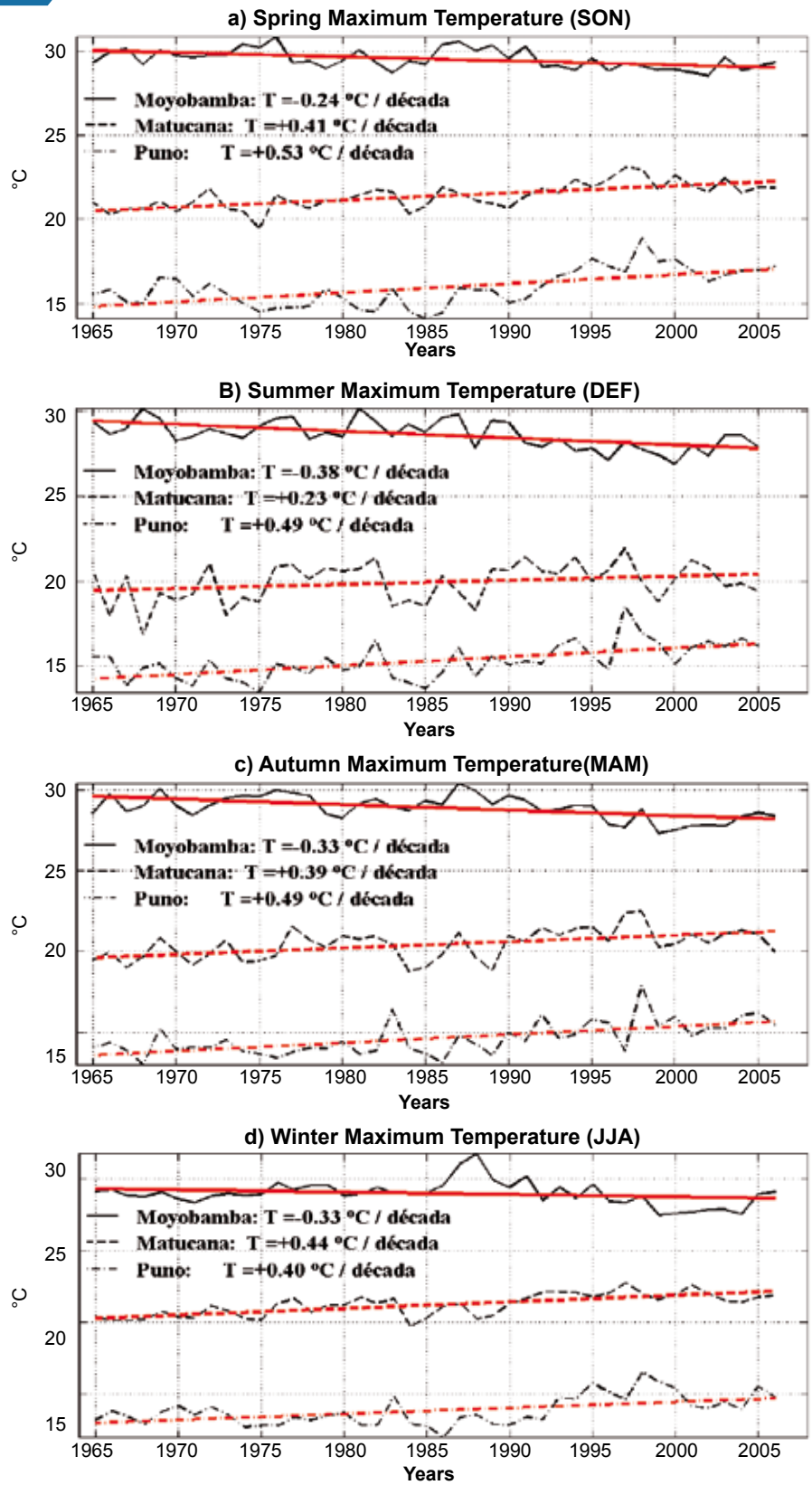

Temporal distribution of seasonal maximum mean temperature (ºC /decade), estimated for the period 1965-2006) of the Moyobamba (northern jungle), Matucana (central mountain region) and Puno (southern mountain region) stations, a) spring (SON), b) summer (DJF), c) autumn and d) winter (JJA). The better adjustment of the linear trends is indicated in red lines.

FIGURE 22

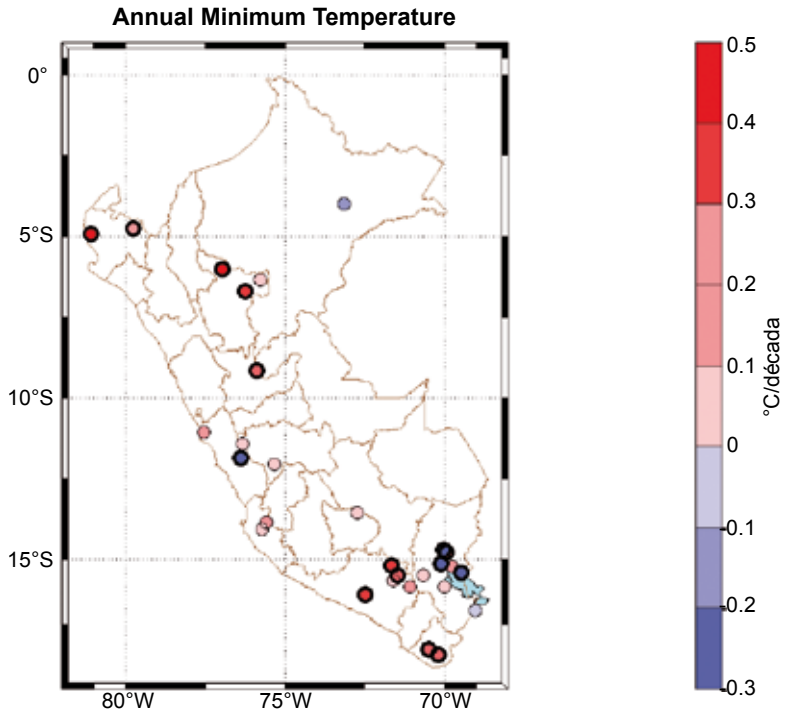

Spatial distribution of annual minimum mean temperature trend (ºC /decade) estimated for the period 1965-2006. The trends with statistical significance at 5% or less (Test Mann-Kendall) are indicated in black circles.

The spatial distribution of the seasonal trends of minimum mean temperature (Figure 24 a-d) shows a less persistent behavior than the observed in the seasonal distribution of the maximum temperature trends, station after station. These differences are more noticeable in the coast and central mountain region, than in the northern jungle and southern mountain region, where the persistence during the year is greater. While the trends range vary approximately around 1,5 ºC/decade in spring and autumn, the higher range of seasonal variation is observed in the winter months, when it reaches 1 ºC /decade, as a result of the extreme values. These values are observed from -0.63 ºC/decade, registered in El Progreso (Puno) up to +0.91 ºC /decade, registered in La Angostura (Arequipa).

Another characteristic that is necessary to point out is the bipolar behavior between the stations situated in the highlands of Arequipa and those located in Puno, particularly in the northeastern part of the Titicaca Lake. While in the high areas of Arequipa and Tacna the trends are positive and statistically significant, in Puno happens to be that trends are negative and statistically significant. Also, during the year, the trends in Puno are less persistent than the observed in the highlands of Arequipa.

The temporal distributions of seasonal minimum mean temperatures of the three representative stations (Figure 25), shows that the variability of minimum temperature in the northern jungle (Moyobamba) and the central mountain region (Matucana) are identical to the annual totals, particularly during the spring an summer months.

The high interannual variability observed in Moyobamba before the years 1980 , associated to the occurrence of negative anomalies during the warm event of the ENSO of 1977/78, is present throughout the year, with a very intense value during spring (SON). Also in the station located in the mountain (Matucana) shows positive anomalies, very similar in the four seasons related to the effects of the ENSO 1991/92 and negative anomalies during the four seasons related to the ENSO 1997/98.

FIGURE 23

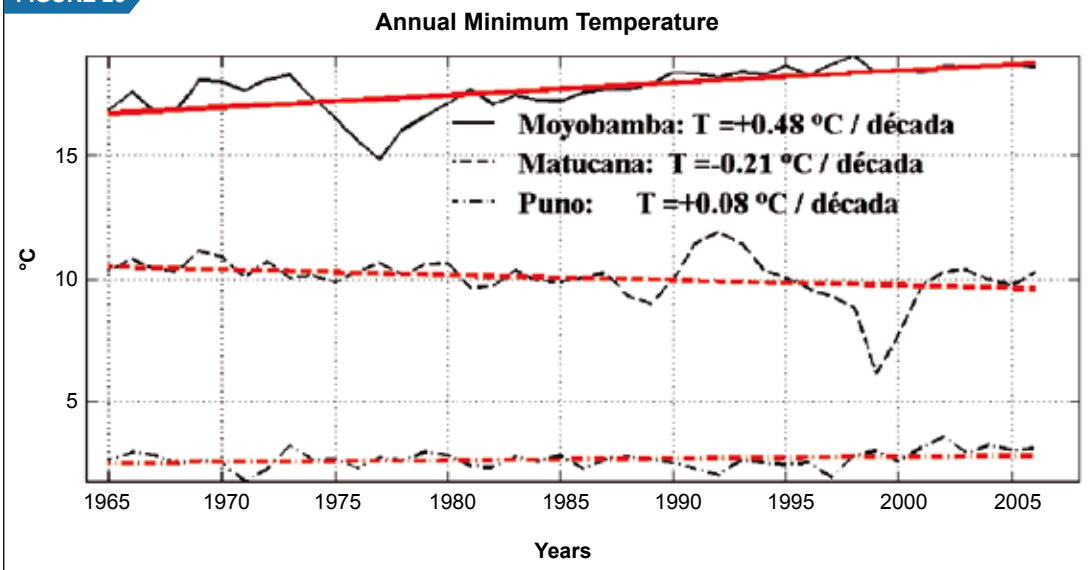

Temporal distribution of annual minimum mean temperature (1965-2006) in the Moyobamba (northern jungle), Matucana (central mountain region) and Puno (southern mountain region). A better adjustment of the linear trends is indicated in red lines

3.3.4 Trends of the diurnal cycle in Peru

The trends, in the difference between the maximum and minimum temperature, called diurnal cycle (diurnal amplitude of extreme temperatures) estimated for mean annual and seasonal values for the 23 stations are shown in Figure 26 and 27, respectively.

The slopes in the annual mean diurnal cycle (Figure 26) show values between -0,74 ºC/decade in Moyobamba (San Martin) up to +0,62 ºC /decade registered in El Progreso (Puno). Most of the stations show statistically significant values. In the stations located in the northern jungle negative trends are observed, that is, a diminish in the diurnal amplitude of temperatures; which seems to be more the result of the weak positive trend or negative trend observed in the annual maximum mean temperature in this region than due to the positive trends of the annual minimum mean temperatures. Also the negative trend registered in the northern coast is due to the same mechanism observed in the northern jungle.

In the mountain region, except for the highlands in Arequipa and Puno, positive trends are observed and most of them are statistically significant. The increases in the diurnal cycle, except for the ones located over the central part of Puno, in the areas adjacent to the Titicaca Lake, are basically due to the higher positive trend of annual minimum mean temperatures observed in this zone. The maximum trends registered in the central part of Puno, opposite to the ones observed in the northern jungle, seem to be a mixture between the intense positive trends of the annual maximum mean temperature and the negative trends or weak positive trends of the annual minimum mean temperatures.

In the high zones of Arequipa and Puno, the weak positive trend and the negative trend of the maximum temperatures, compared to the intense positive trends of minimum temperatures, are the main reason for the occurrence of negative trends of the annual cycle. This same mechanism can also explain the negative trends observed in the stations in Tacna.

The seasonal distributions of trends of the diurnal cycle (Figure 27 a-d) show a very similar pattern to the one of the trends of the annual diurnal cycle (Figure 26). The minimum value was registered in the summer months (DJF) in the location of Moyobamba (San Martin) with -0,92 ºC/decade (Figure 27 b)

FIGURE 24

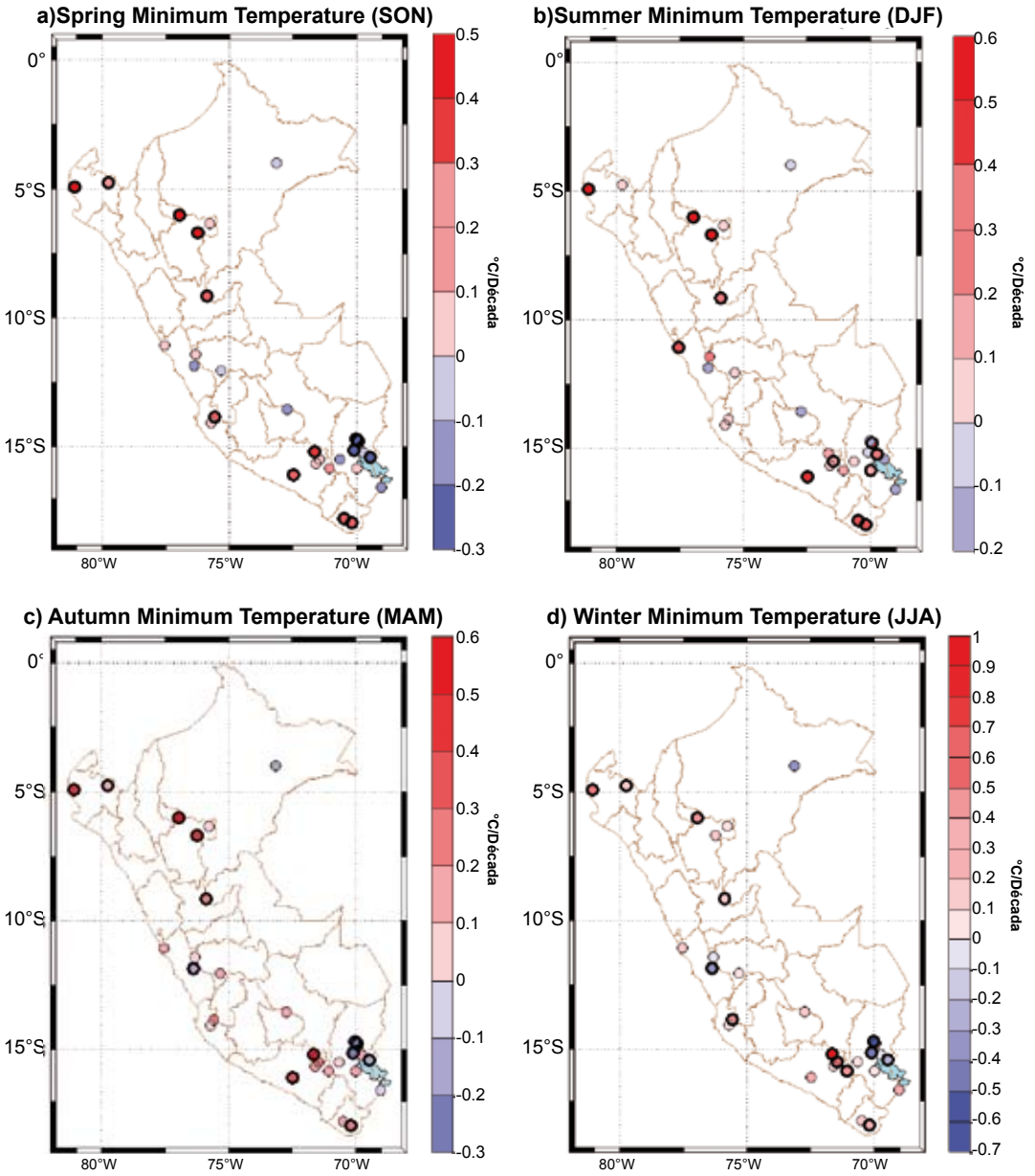

Spatial distribution of seasonal minimum mean temperature trends (ºC/decade), estimated for the period 1965-2006. a) spring (SON), b) summer (DJF), c) autumn (MAM)y, d) winter (JJA). The trends with statistical significance at 5% or less (Test Mann-Kendall) are indicated in black circles.

and the maximum value was registered in the winter in La Angostura (Arequipa) with +0,85 ºC/decade (Figure 27 d). In the northern jungle the negative trends observed during the four seasons of the year are due to the occurrence of intense negative temperatures or weak positive trends of the mean maximum temperature.

In the mountain and the coast regions, especially in the spring (SON) and autumn (MAM) seasons, the patterns of the trends are similar to the ones of the annual cycle, also for the same reason explained in the case of the annual cycle. In the winter (JJA), see Figure 27 d, in the southern zone of Puno and in Tacna, statistically non-significant positive values are observed. In the Department of Tacna occurs because

FIGURE 25

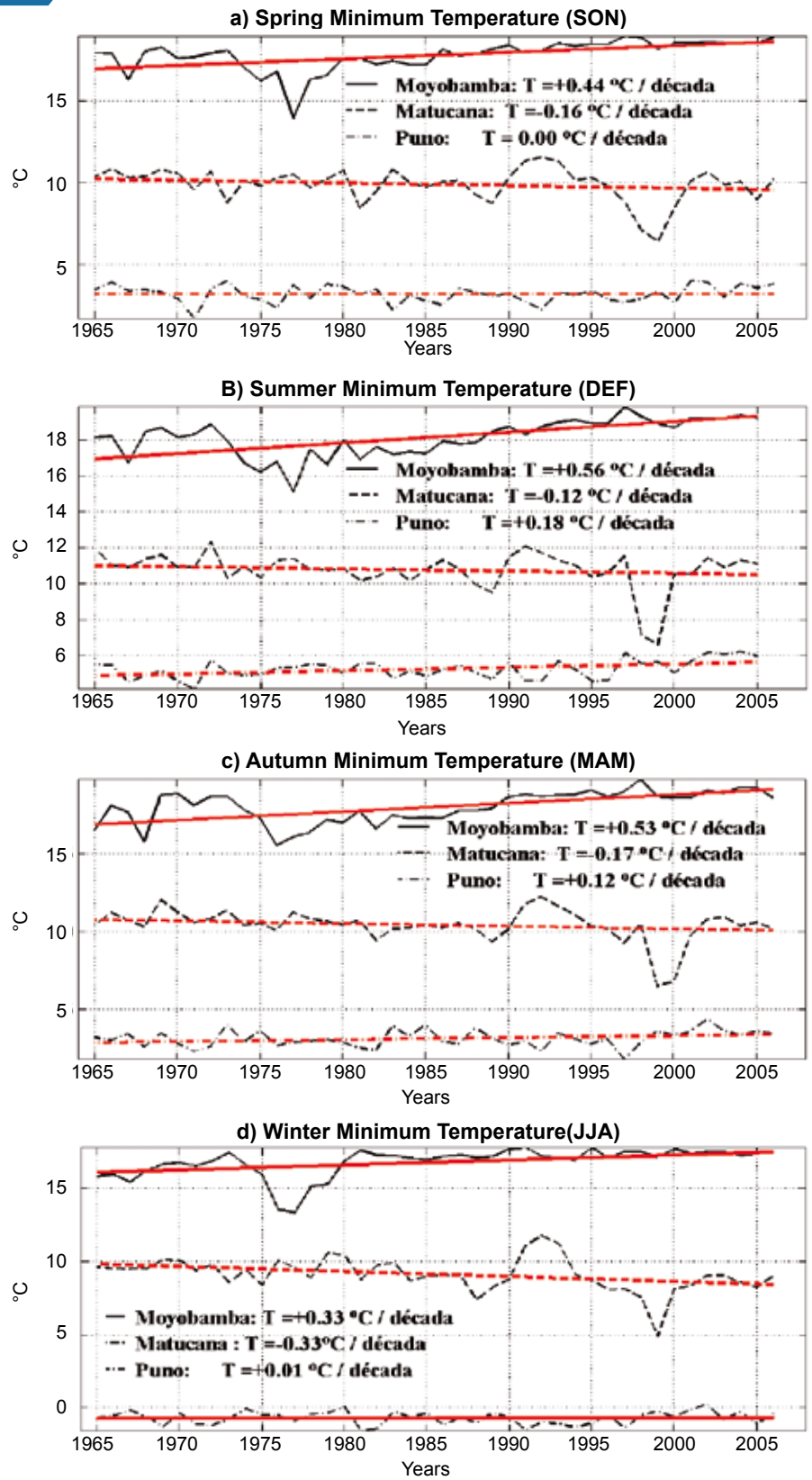

Temporal distribution of seasonal mean minimum temperature (ºC /decade) estimated for the period 1965-2006 for the stations of Moyobamba (northern jungle), Matucana (central mountain region and Puno (southern mountain region), a)spring (SON), b) summer DJF, c) autumn (MAM) and winter (JJA). The best adjustment of the linear trend is indicated in red lines

FIGURE 26

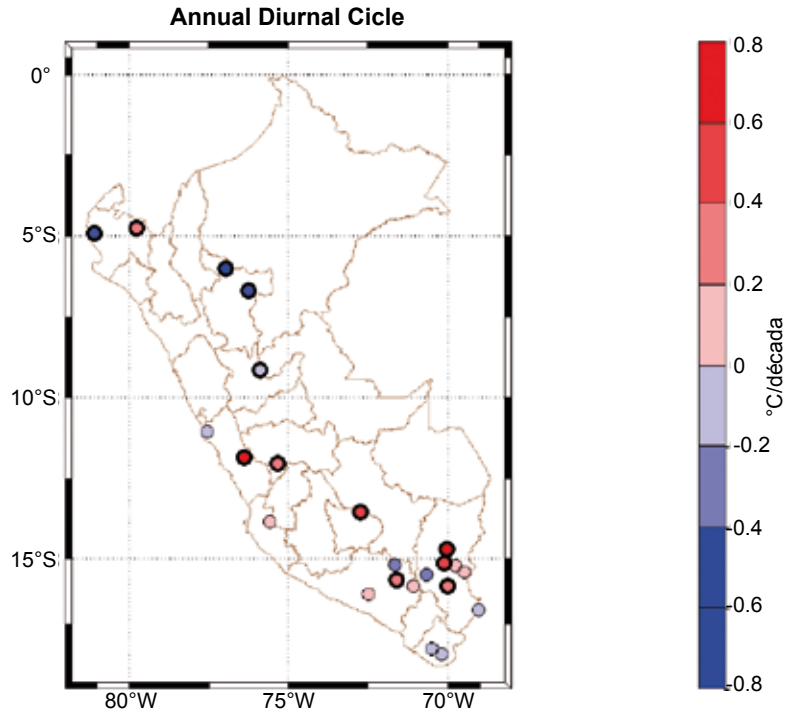

Spatial distribution of the annual diurnal cycle trends (ºC / decade) estimated for the period 1965-2006. The trends with statistical significance at 5% or less (Test Mann-Kendall) are indicated in black circles.

the maximum mean temperature trend in the winter are higher than the minimum mean temperature trend, and in the southernmost part of Puno occurs because the maximum mean temperature trend is negative, while the minimum temperature trend is positive.

3.3.5. Linear trends of the Extreme Climate Indices

3.3.5.1. Extreme Climate Indices of precipitation

The distribution of the trend of the annual precipitation daily intensity index (SDII) is shown in Figure 28. This index, in simple terms, indicates the average intensity per day of the precipitation occurred during one year and the trend shows the possible variation at a long term, the increase SDII (+) or diminish SDII (-) of the intensity of the rainfall in total terms. The values of the trends are relatively low, ranging between ± 0,2 mm/day/year, which means a increase of diminish of 8mm in the intensity of precipitation occurred in the last 42 years.

This index seams to characterize an apparent regionalization of precipitation in Peru. This is based on the signs of the trends, that possibly reflect the large scale effect joined to the own regional orographic characteristics. For example, the positive values, statistically significant, are scattered along the coast and northern mountain region, and in the high zones of Arequipa, Tacna and Puno. On the other hand, negative values, statistically significant are grouped in the coast and central mountain region, in the northern jungle and in the southern mountain region (Pacific Ocean Drainage Area)

FIGURE 27

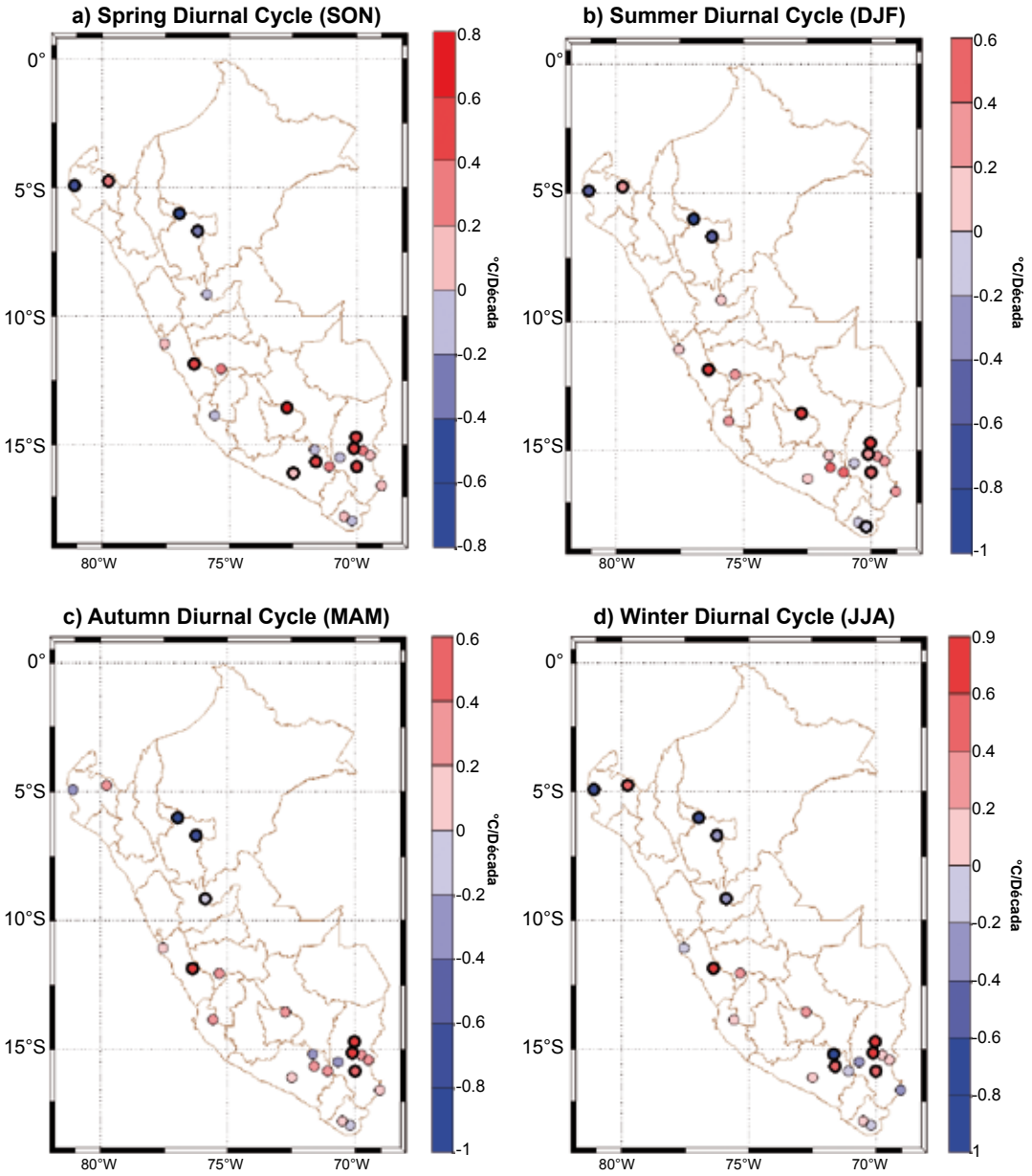

Spatial distribution of the trends of the seasonal diurnal cycle (ºC /decade) estimated for the period 1965-2006 a) spring (SON), b) summer (DJF), c) autumn and d) winter (JJA). The trends with statistical significance at 5% or less (Test Mann-Kendall) are indicated in black circle.

The trends of the indexes of maximum number of consecutive dry days (CDD) and consecutive days with precipitations (CWD), shown in Figure 29 a-b, can be interpreted as indicators of drought and floods, respectively. The trends of the CDD index show a spatial distribution very similar to the trend of the SDII index in the coast and northern mountain region, which can be interpreted as the existence of some kind of direct relation between these indices.

This relation indicates that the higher the CDD is, the SDII is higher too; or viceversa, that is to say; the more prolonged the dry period is, the intensity of the precipitation is higher. Conversely, in San Martin, Tingo Maria and Loreto the CDD trends, are opposite to the SDII index, which indicated that besides being a decrease in the intensity of precipitations there is also an increase in the period of days without any rainfall.

FIGURE 28

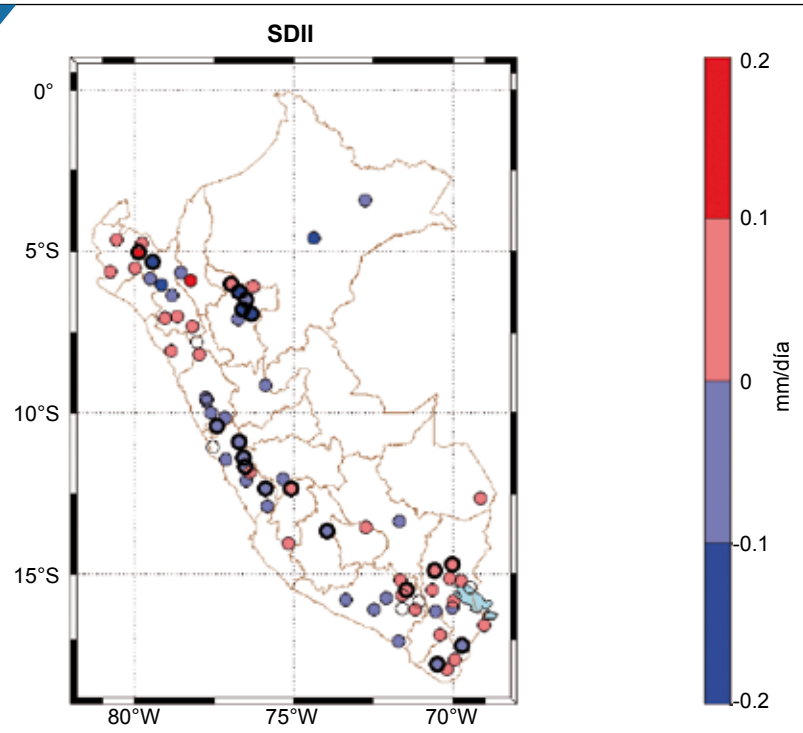

Spatial distribution of the trend of the precipitation daily intensity index (DSII) (mm/day/year) estimated for the period 1965-2006. The trends with statistical significance at 5% (Test Mann-Kendall) are indicated in black circles.

In the central mountain region prevails positive trends of the CDD with some statistically significance trends, opposite to the SDII index. These characteristics could be interpreted as the decrease in the intensity of precipitation, at the same time the occurrence of an increase of number of days without rainfall, originating as a result a decrease in total precipitation; but this is what it is not verify in the analysis of the item 3.3.1. (Figure 14). This result is because there are other parameters that need to be considered in this analysis, such as the existence of extreme precipitation. The southern region shows a prevailing of positive values of CDD and SDII, which seems to have the same behavior as in the coast and northern mountain region, particularly in the high zones of Arequipa and Puno.

The distribution of the CWD index trend shows a prevailing of null values where the trend is practically zero. These values are distributed more frequently in the southern mountain region and in the northern jungle (San Martin). The positive values prevail over the northern and central mountain region, and they extend towards the northern and central jungle, where a statistically significance trend is registered (Tingo Maria).

In the southern mountain region a mixture of trends, with positive and negative values, is observed, without any defined spatial pattern, registering an extreme value of 0,48 days/year, in Pampa de Arrieros (Arequipa). Thus, this index indicates the existence of a regional pattern that includes the northern and central mountain region, where apparently there is an increase in the days without precipitation, because the trends are not statistically significant, and most of the trends show values lower than 0,2 days/year (a total of 8 days in 42 years), which has practically a non-consistent significance. On the other hand, the trends observed in the southern mountain region indicate that the local characteristics are predominant in these places.

The trend of the maximum precipitation registered in one day and the maximum total accumulated during 5 consecutive days are represented by the RX1 day index and the RX5 day index (Figure 30 a-b) respectively. These indexes indirectly indicate the intensity of precipitations registered and are related,

FIGURE 29

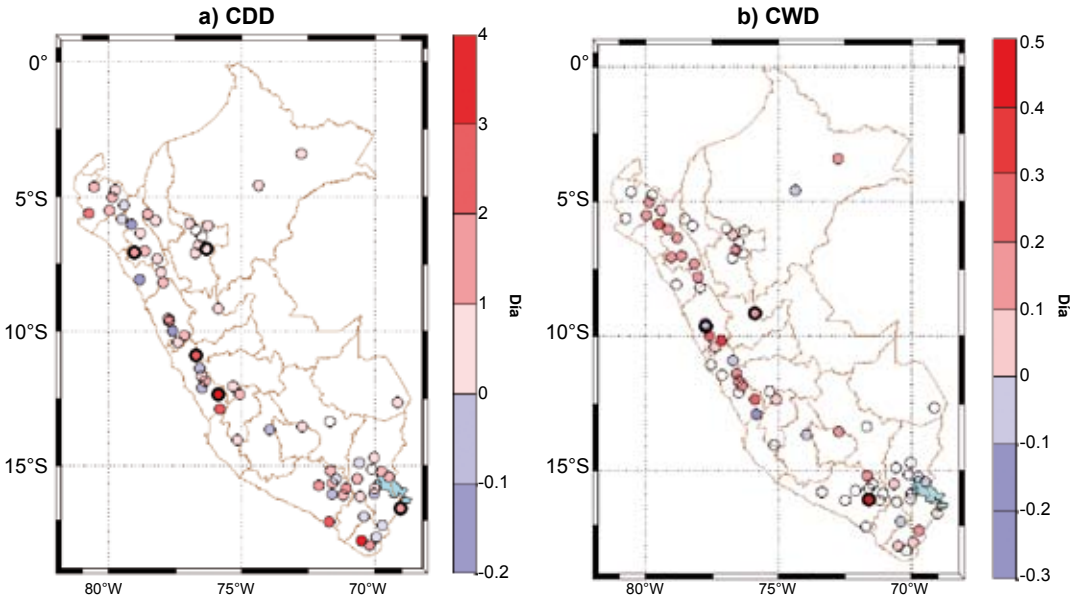

Spatial distribution of the trends of the indexes of : a) Maximum number or consecutive days without precipitation (CDD) and b) Maximum number of consecutive rainy days (CWD) estimated for the period 1965-2006. The trends statistically significant at 5% Test Mann-Kendall, are indicated in black circles. The white circles indicate void trends (0,0 day).

some way, with the probable occurrence of floods. Particularly, the RX5 day index is very important as an indicator of possible landslides and/or floods, since the persistency and amount of precipitation are basic conditions for soil saturation.

The spatial distribution of the RX1 day trend (Figure 30) is similar to the SDII index trend (Figure 28) over the whole country. This indicates a direct relation between these two indices, which shows hat the observed trend in the SDII index are basically due to the intensity of the daily precipitation. The exceptions are observed in the stations located in San Martin and Tingo Maria, where the trends are just the opposite. In these regions, on one side, there is an increase in the intensity of daily precipitation in the southern jungle (although they are not statistically significant) and a decrease in he northern part of jungle (where there is a station with statistical significance) which is related to the CDD index trends. This indicates that there is an opposite action from some mechanism that generates the precipitations over these region or at least two different types of mechanisms; but at the regional scale, in the Department of San Martin, it seems hat the orography plays a very important role in the intensity of the registered precipitations.

The trend of the index of maximum accumulated precipitation in five days (RX5day) (Figure 30 b) shows a pattern similar to the one observed for the maximum precipitations trends registered in one day (RX1-day), with slightly higher values. Also it is observed that the RX5 day shows positive trends statistically significant in the jungle and negative over the mountain region; this does not occur in the RX1day distribution, where negative and positive statistically significant trends are observed mainly over the mountain region.

The patterns of the trend for these two indices, besides indicating some stressed differences of certain mechanisms that generate precipitation over the jungle region, they also indicate that the intensity of the precipitation over the mountain and coast region of Peru are quite regionalized. Another fact, that is worth mentioning, is the intensity of precipitations, which are probably originated by the influence of some typical regional factors (orography, geographical location) that respond to large scale mechanisms that generate these precipitations.

The trends show a polarity between the mountain and the northern jungle in both distributions, with increases over the northern mountain region and a decrease in the northern jungle. In the central mountain region a predominance of the negative trends of the RX1 day is observed, and in the southern mountain a predominance of the positive trends. In the southern mountain region, apparently the local characteristics do not seem to modulate the trends in accumulated precipitations in one day or five days.

The trends of moderate precipitations (R10mm) and the trend of intense precipitations (R20mm) can be observed in Figure 31 a b. In the distribution of the R10mm index trend it is observed that most of the stations located in the western side of the Andes Mountains do not show any kind of trend. This index

FIGURE 30

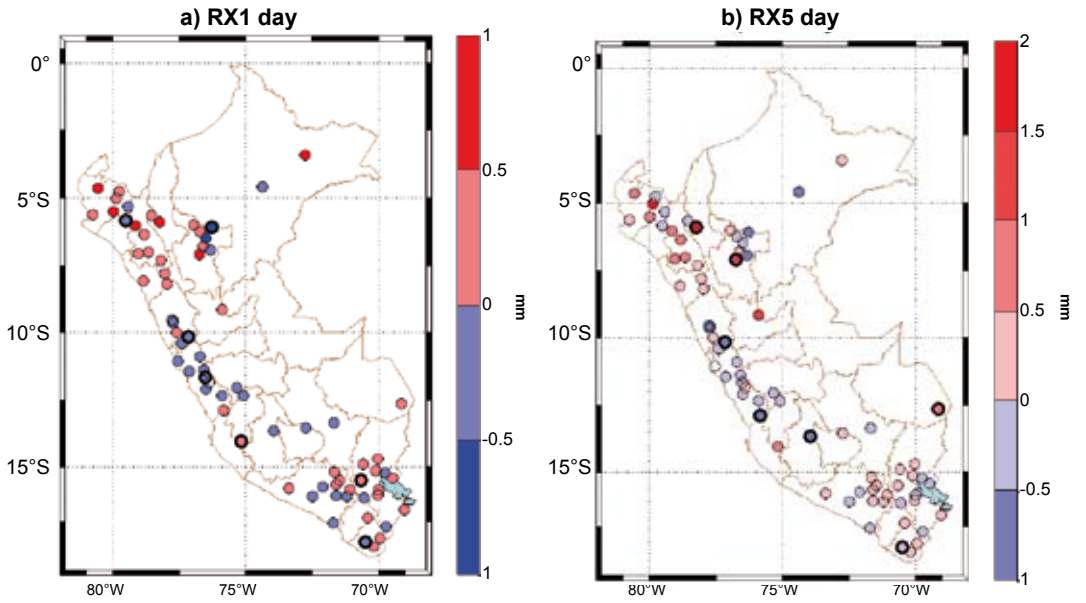

Spatial distribution of the trends of the indexes: a) maximum accumulated precipitation in one day (R1day) and , b) maximum accumulated precipitation in 5 consecutive days (RX5day), estimated for the period 1965 – 2006. The trends with statistical significance at 5% or less test Mann-Kendall, are indicated in blank circles. The white circles indicate void trends (0.0 mm/day).

increases in the distribution of the Rx5day, there is a predominance of stations without any trend during the period of the present analysis for the whole country.

It is also observed that the patterns of the two distributions in the mountain region and northern jungle, as well as in the southern mountain region, are very similar, with some stressed regionalized trends. The values of the maximum trends of these two indexes are very close, which means that there is an increase or diminish in the days with moderate rainfall and heavy rainfall over the same regions, in similar proportions, except for the fact that they are more consistent in he northern jungle, also because the statistical significant values are present in both distributions. All this indicates that the local characteristics are the ones that modulate this kind of event in these regions.

The trends of the number of very rainy days (R95p) and extremely rainy days (R99p) are described in Figure 32 a-b. The distribution of trends of very rainy days follows a pattern similar to the index trend R10mm with stations that present null trends, mainly along the western slope of the Andes Mountains. The contrast between the trends of the stations located in San martin and the northern mountain region, are less noticeable in this distribution, since there are some positive significant trends in both regions. Also the positive trends registered in the southern part of Peru are more homogeneous that the ones

FIGURE 31

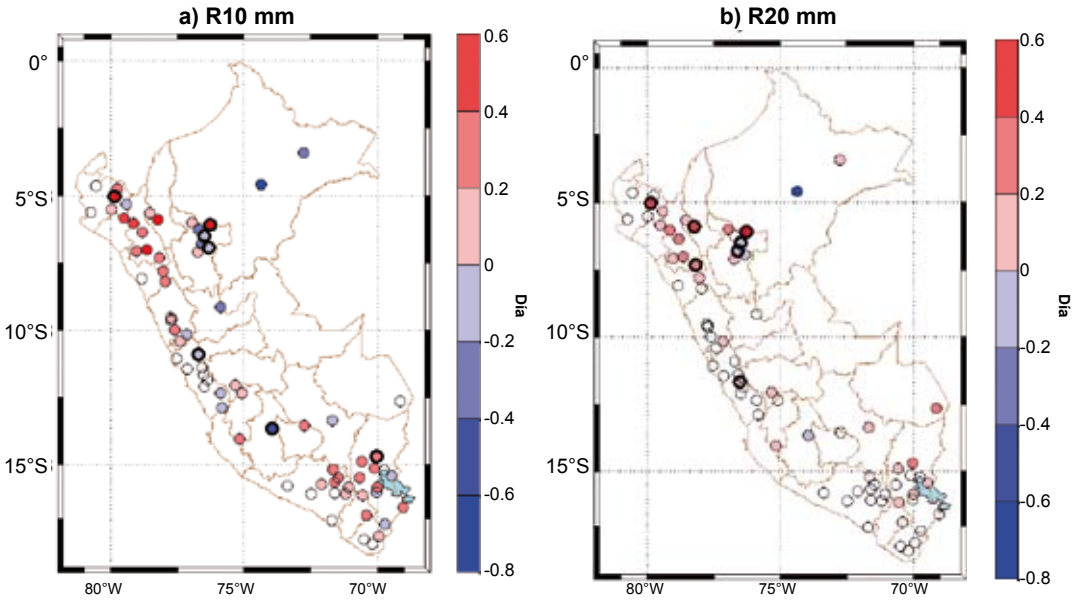

Spatial distribution of the trend of the indexes of the amount of days with occurrence of: moderate precipitation (R10mm) and b) heavy precipitations (R20mm), estimated for the period 1965-2006. The trends with statistical significance at 5% or higher Test Mann-Kendall are indicated in black circles, the white circles indicate void trends (0,0 mm/day).

observed in others distributions, which indicates a regionalization of precipitations regardless of the orographic factors.

Another characteristic observed is the presence of negative significant trends in all the central mountain region, indicating more evidently that this is also another region that presents its own characteristics, apparently modulated by large scale effects, more than it is because of geographical factors.

Concerning the trends in the extremely rainy days (Figure 32 b) there is predominance of null values over the whole country, there are very few stations where positive trends prevail, and they are distributed over the northern mountain region central and southern jungle and southern mountain region. Only one station is observed in the central mountain region. The trends indicate that in mountain and in the western side of the northern jungle there were some significant increases in extreme precipitations. The same thing happened in the central zone of Puno.

3.3.5.2. Extreme Climate Indexes for /OF maximum temperature

The trend of the index that indicated the number of very cold days (TX10p) shows a predominance of negative values, statistically significant, distributed over the whole mountain and southern jungle regions of Peru, except for three locations in the southern mountain region, which shows positive values distributed as follows: one located in Cusco and two in Puno. In the jungle region positive values are observed in San Martin and Tingo Maria. This pattern indicates that there was a decrease in the number of days with maximum temperatures lower than the percentile 10% and means that during the period of analysis, cold days gradually decreased particularly in the southern mountain region.

The trend pattern corresponding to warm days (TX90p) (Figure 33) describes a model that is exactly opposite to the one for the colds days. The difference is that most of the positive trends of this index show statistically significant values. The intensity is similar over all the mountain region and southern jungle.

FIGURE 32

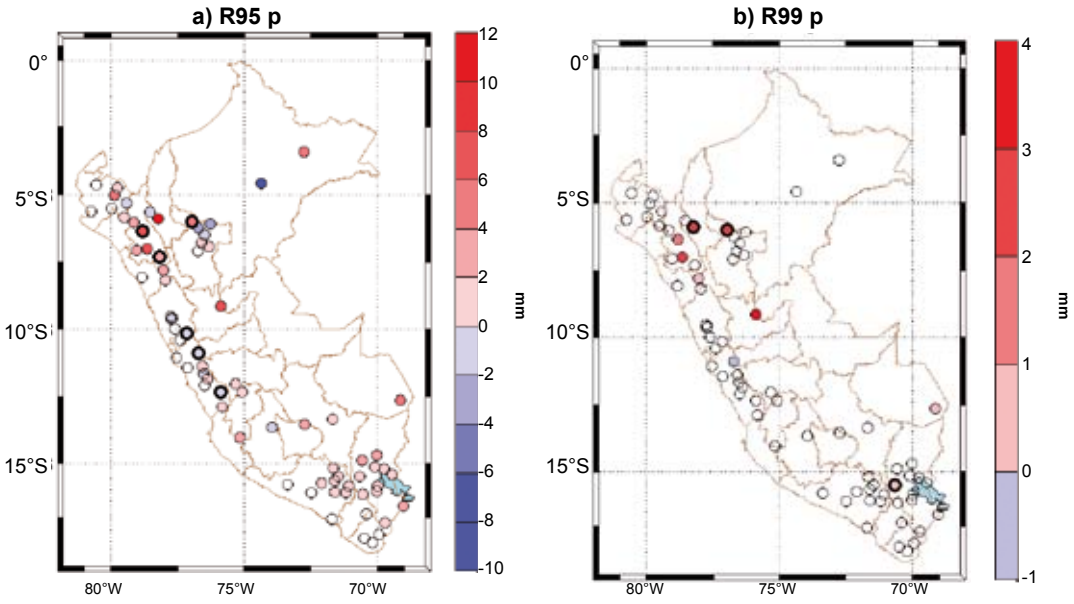

Spatial distribution of the trends of climate extreme indices for precipitation a) very rainy days (R95p), percentile 95% and b) extremely rainy days (R99p), percentile 99% estimated for the period 1965-2006, based on the climatology of 1971-2000. The trends with statistical significance at 5% or less Test Mann-Kendall, are indicated in black circles. The white circles indicate void trend (0,0 mm/day).

FIGURE 33

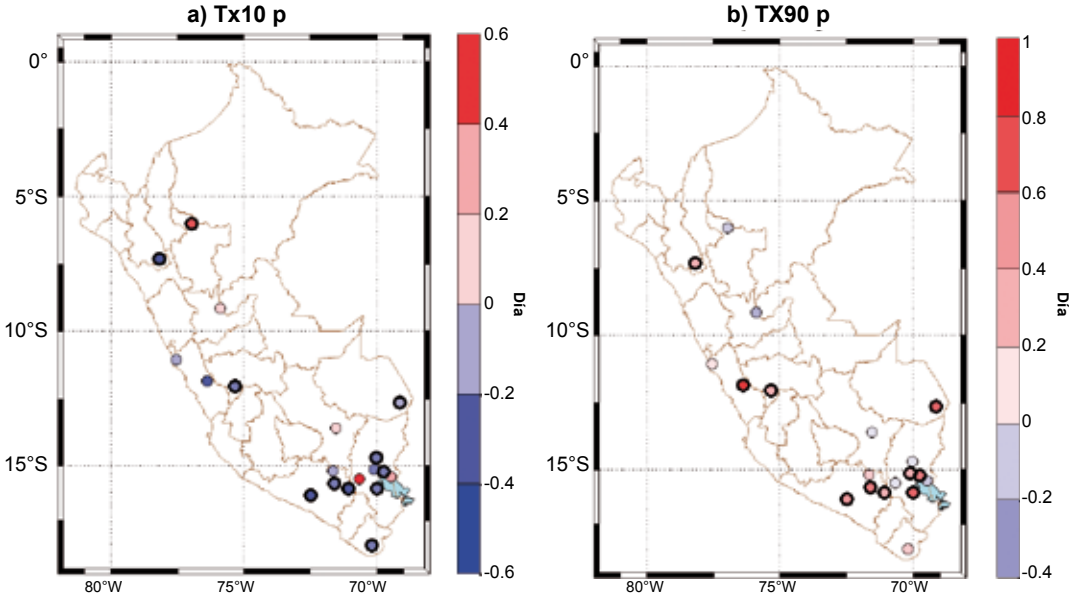

Spatial distribution of the trends of climate extreme indices for maximum temperature, a) cold days (TX10p), percentile 10% and b) warm days (TX90p), percentile 90% estimated for the period 1965-2006, based on the climatology of 1971-2000. The trends with statistical significance at 5% or less Test Mann-Kendall are indicated in black circles.

It is important to highlight that both indices of extreme maximum temperature do not show any sign of the thermo-regulating influence of the Titicaca Lake. The values of the observed trends in Cusco and the central and northern jungle, as well as in Puno, are apparently due to regional effects that modulate the energy balance day after day, from which the maximum temperature is a result.

3.3.5.3. Extreme Climate Indexes for Minimum Temperature

The trends for days with meteorological frosts (minimum temperatures equal or less than 0,0 ºC) in this analysis are circumscribed to the central and southern mountain region in Peru (Figure 34). The trends with negative values, statistically significant, distributed over the high zones of Arequipa, differ from the ones in the adjacent zones north of the Titicaca Lake, which are statistically significant positive trends.

FIGURE 34

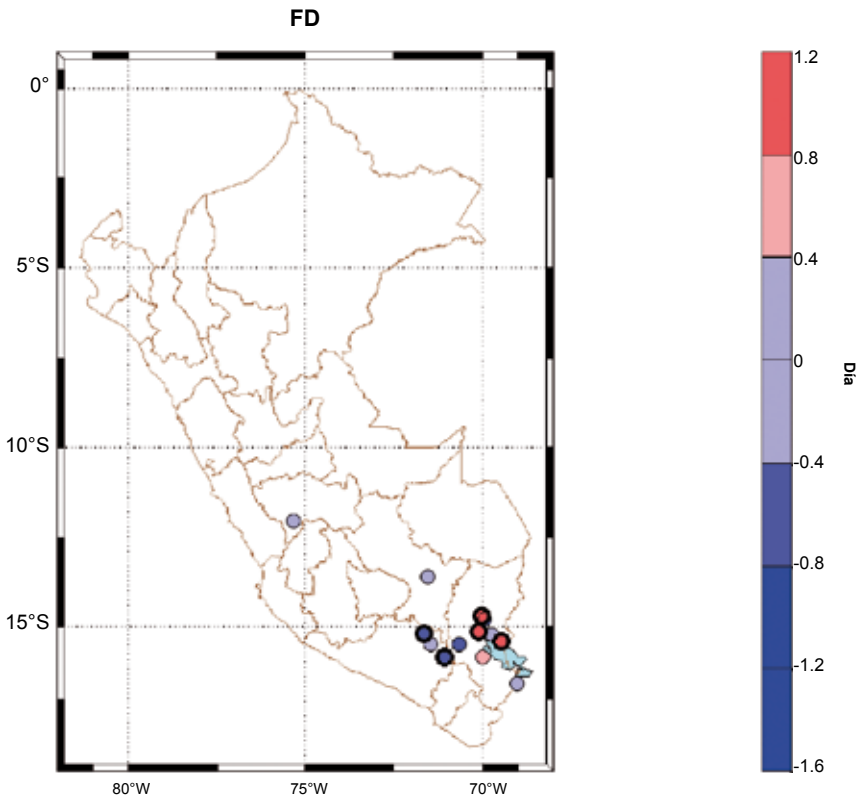

Spatial distribution of Extreme Climate Indexes trends for minimum temperature. Indexes of number of days with meteorological frost. The trends with statistical significance at 5% or less (Test Mann-Kendall) are indicated in black circles.

Everything seems to indicate that in the high zones of Arequipa and other isolated locations in the mountain region of Peru there is a significant decrease in the number of days with meteorological frost and an increase in the adjacent zones to the Titicaca Lake. The number of meteorological frosts in the high zones of Arequipa decreased at a ratio of up to 1,6 days/year (approximately in two months in the 42 years period). Similarly, in Puno they increased up to 1,2 days / year (very close to one month and a half). This apparently effect of the Titicaca Lake on this index needs to be verified by other studies, and if it happens to be truth, it could be relevant for the agrometeorological conditions for some kind of crops in these locations.

The trend in the spatial distribution of the number of cold nights (TN10p) and number of warm nights (TN90p), during the period of analysis, can be seen in Figure 35 a-b. The number of days with cold nights decreased in almost the whole country, except for some isolated stations, located in the central mountain region (Marcapomacocha) and the adjacent zones north of the Titacaca Lake (Figure 35 a). This indicates that each time the cold nights were gradually becoming warmer during the period of the present study. The negative trend values for the northern jungle (San Martin and TIngo Maria) and southern mountain and isolated location in the northern mountain and central coast are predominantly significant. One characteristic that strengthens the difference of decrease/increase of meteorological frosts between the central zone of Puno and the high zones in Arequipa is the polarity between the positive/negative trends of cold nights over these Andean zones. Also, it is worth mentioning, that while in the jungle region, central zone of Puno and central mountain region, the number of days with extreme temperatures decrease (TN10p), the number of cold days (TX10p) also show this same inverse behaviors from the one observed in the remainder part of the country.

FIGURE 35

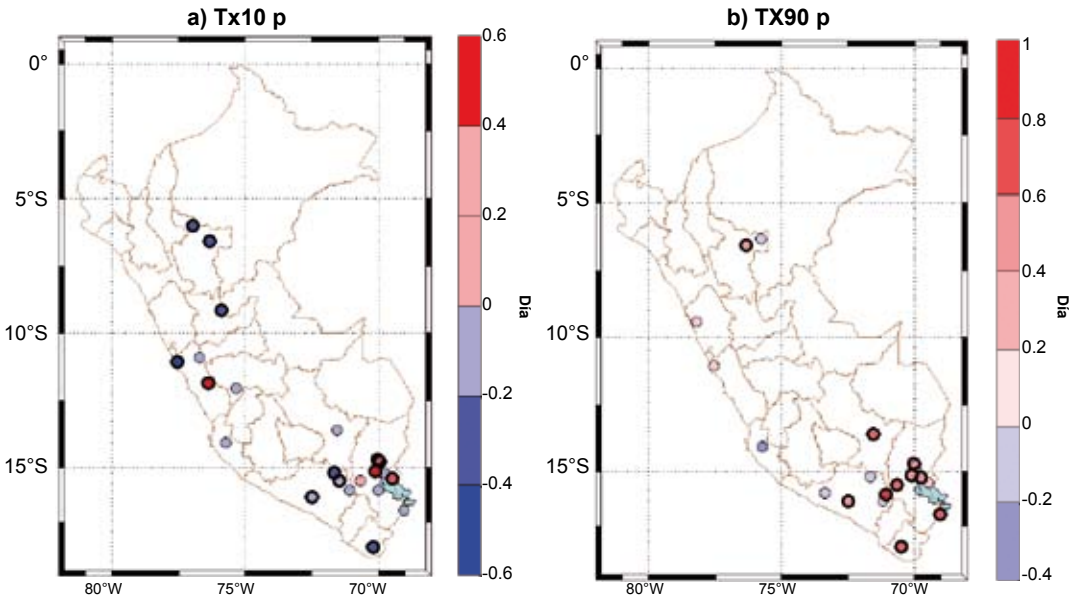

Spatial distribution of the trends of Extreme climate indexes for minimum temperature a) very cold nights (TN10p), percentile 10% and b) warm nights (TX90p) percentile 90% estimated for the period 1971-2000, based on the climatology of 1966-1995. The trends with statistical significance at 5% or less Test Mann-Kendall, are indicated in black circles.

The trend in the number of warm nights (Figure 35 b) shows an almost homogeneous pattern with positive values, statistically significant, over the high zones of Arequipa and Puno that seems to extend to Cusco. This pattern is inverse to the one observed for cold nights in the high zones of Arequipa, without the polarity observed in the trends in this areas and in the central part of Puno. On the contrary, the highest increase in the number of days with cold nights is registered west of Puno and mountain region in Arequipa (Imata and Pamapa de Arrieros). In the central coast there are some stations showing positive trends in Ancash and Lima and negative trends in the mountain region in Ica. Similarly, in the northern jungle (San Martin) there is a contrast in the trends, with a statistically significant positive value, followed by a very low negative value.

3.3.6. Drought analysis

A comprehensive the spatial/temporal analysis of drought in Peru, considering 64 temporal series of the SPI, is used a basis, on mean terms for the whole territory, to estimate a) temporal variability of the SPI

and the occurrence in terms of percentage, in the three categories for each one of the 3 different types of droughts: meteorological, hydrological and agrometeorological and; b) the spatial variability, where the frequencies of the different kind of drought for each one of the category of intensity: moderate, severe and extreme are estimated for each place (pluviometric station). This variability gives us the idea of the risk in case of the occurrence of drought in Peru. Also, in these distributions the cold (warm) events of the ENSO are highlighted, which are determined from negative anomalies lower (higher) than 1 ºC of the sea surface temperature in El Niño 3.4, a little bit different from what is recommended by Trenberth (1997), with the purpose to consider only the most intense events of the ENSO, since some experiments previously made do not show significant differences between both of them.

Then, the analysis of the temporal variability (%) of the occurrence of these three types of intensities in the three aforementioned categories shows the places or regions where there is a greater risk for each one of the categories of drought.

The teleconnections determined by the correlation analysis, serve as the source to recognize the large scale forcings that modulate the variability of precipitations at an annual and longer scales, and whose extreme events mainly produce droughts. At the end, the ACPs show the spatial/temporal patterns of drought in Peru and using as complement the OT analysis for the temporal series of these patterns, one will have a more comprehensive spatial/temporal knowledge on the occurrence of droughts in the Peruvian territory.

3.3.6.1. Analysis of the Standardized Precipitation Index (SPI)

a) Average temporal distribution of drought intensity

According to Figure 36 a-c, the temporal distribution (1965-2006) of the averages of the SPI from all the stations (64) is used in the present study for: the one-month scale (Figure 36 a) that is typical of meteorological droughts; for the three-month scale (Figure 36 b) typical of agrometeorological droughts, and one-year scale (Figure 36 c) typical of hydrological droughts. Additionally, the warm and cold phases of the ENSO events is shown.

One common characteristic in these three distributions is the high spatial variability, expressed in the standard deviations of each one of them that vary a lot through the years, apparently without any pattern. This indicated that drought events, a natural characteristic of climate, are regionalized and in very rare occasions, during the period of study, it has apparently occurred an event that involved all or most part of the country, as it seems to be the event occurred in 1991/1992. This event, besides involving most part of the country, it was very intense, causing a very intense hydrological drought.

During the present period of study, by means of the SPI method, it seems that there was no evidence of temporal trends, increase or decrease of drought occurrence in any of its three different types in Peru, because the mean value, during the whole time, oscillates around the SPI zero, in the three scales. This fact seems controversial; but, it can be explained because over the country, as a whole, the occurrence of drought or flood events are fundamentally regional or maybe local; partly due to the spatial/temporal complexity of precipitation in the Peruvian territory. At the same time, other distributions do not indicate a simultaneous compensation between regions with drought events and other regions with floods, as it may be assumed.

Among these three types of droughts we can distinguish the temporal variability, that is that month after month, related to the amount of accumulated precipitation in one month, quarter or year. The distribution of monthly SPI shows high interannual variability, it is even possible to observe some signs of intreseasonal variability. This variability becomes simultaneously more stable with the increase of the estimated temporal scale, as it is the case of the annual SPI.

FIGURE 36

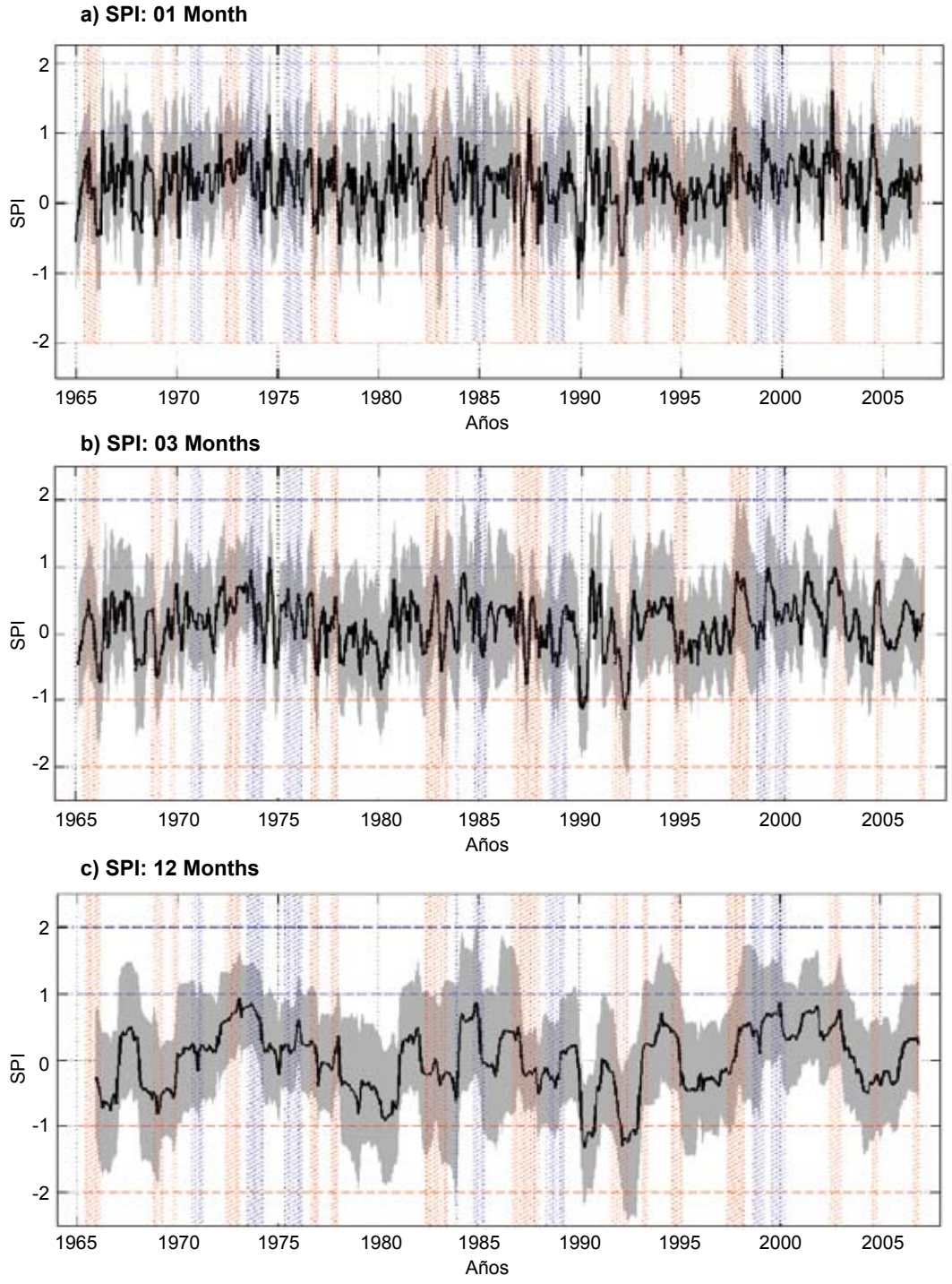

Temporal distribution of the Standardized Precipitation Index (SPI) average value for the period 1965-2006. a) meteorological droughts (monthly SPI), b) agrometeorological droughts (quarterly SPI) c) hydrological droughts (annual SPI). The shaded areas in grey indicate the standard deviation of the SPI. The shaded areas in red (blue) indentify the period of the occurrence of warm (cold) events of the El Niño phenomenon. El Niño/Southern Oscillation (ENSO)

Finally, in this graphics it can be observed the drought events over the Peruvian territory, in average, are not associated or are directly caused by all the warm events of the El Niño phenomenon / Southern Oscillation (ENSO), also it does not happen the contrary in the presence of cold events. But, it can be confirm that some of the very intense warm events of the ENSO, do caused some intense droughts, as

it was the case of the warm events of 1965/66, 1982/83, 1991/92. On the other hand, the cold event of 1999/2000 1999/2000 seemed to have caused some kind of persistence of heavy precipitations, favoring an SPI with a slight trend to positive values. Also, many drought events as: the one occurred at the end of the 1970's decade and beginning of 1980; starting of the last five years of the 1990's decade, a few years of the last five-year period of the 1960's decade, among other, are not associated to any kind of ENSO event; but, undoub- tedly, the circulation anomalies at large scale need to be studied, in case these patterns may occur again, since they are part of the natural climate variability.

From the three types of drought, the meteorological are the ones that show less intensity and are temporarily localized, but this characteristics intensify and involve a longer period of time, in accordance with an increase in the SPI scale, as it is observed in the SPI annual distribution (Figure 36 c). The duration of hydrological droughts goes beyond the ending of the event itself, probably . due to the accumulative effect of precipitation. In conclusion, this is due to the memory of the soil/climate system that is being affected.

b) Temporal distribution of the area affected by droughts in Peru

The distribution of the frequencies, in percentage, of the extreme, severe and moderate droughts registered in the whole territory (64 stations) during the period 1965-2006, is shown in Figure 37 a-c, for the three temporal scales (types) of drought (meteorological, agrometeorological and hydrological). Also it is shown the periods of occurrence of cold and warm events of the ENSO, with the purpose to associate the intensity and the area affected by the drought in each one of these types.

Also, it is observed that the distribution of the addition of the frequencies of the three different intensities of droughts in the meteorological scale shows a very high interannual variability with some discontinuous or occasional peaks, and a maximum value reaching 60% of the stations used, which was registered in the summer of 1989/90 and a maximum secondary value observed in the summer of 1991/92, as it is shown in Figure 37 a. In the other two scales the same maximum values are repeated; but, they are more noticeable in the hydrological drought scale (annual scale).

From the percentage of stations affected by the different types of drought intensities, it can be state that it decreases proportionally to the temporal scale of the droughts, as in the case of the hydrological drought (Figure 37 c). In the temporal distribution of the frequency of droughts, mainly at the hydrological scale (annual),it can be observed that there were stages in which occurred up to three drought periods in the majority of the analyzed locations; as it is the case that started in the last quinquennial of the 70's decade and it extended up to the middle of the 80's, and the last one occurred in the first quinquennial of the 90's decade. Also, periods in which occurred drought in very few locations is observed; such is the case of the first quinquennial of the 1970's and 2000.

The temporal distribution of these three types of droughts, proves the these are part of the normal climate and it strengthens the characteristics observed in the temporal distribution of the average SPI (Figure 36), at the same time, it shows that the high interannual variability of the meteorological and agrometeorological droughts can be interpreted as the most sensitive scales in response to any precipitation shortage.

On the other hand, it is observed that not all drought events are directly related to the warm events of the ENSO, since there are some indications that droughts, specially the meterological ones, occur in periods affected by cold events, such is the case of the summer 1973/74, 1984/1985 (meteorological (agrometeorological) droughts that reached 40% (20%) of the stations) . The warm events of the ENSO, such as the indicated in the previous item of 1965/66, 1982/83, 1991/92, seem to cause droughts over vast regions in Peru, specially the one of 1991/92, in which 60% of the locations under study, were affected by droughts between moderate and extreme, with a value that reached 20% (30%) of locations where agrometeorological (hydrological) droughts were registered. Other periods in which very intense

droughts were registered, particularly the hydrological ones, was between 1966/67, 1979/80 and 1990, that are not directly associated to any period of an ENSO event.

The characteristics of the temporal distributions of the percentage of stations (territory) affected by droughts, apparently show a modulation of a higher scale than just the interannual, which seems not to be directly related to the ENSO. The distribution of frequencies of the hydrological drought is very noticeable with intense periods that mostly include locates that were studied, and they are: the last quinquennial of the 1960's decade, between the end of the 1970's decade and the beginning of 1980 and the first quinquenniel of the 1990's decade, with some inserted periods showing low percentages of areas affected by droughts, such as the periods of the 1970/1975 and 1998/2004.

c) Spatial distribution of drought frequencies

The frequency of occurrence, percentage of occurrence in relation to the whole period of study, in the three drought scales (meteorological, agrometeorological and hydrological) and the three categories of drought intensities were considered independently for the 64 station distributed in the whole Peruvian territory. They were grouped depending on their intensity: moderate, (Figure 38 a-c) severe (Figure 39 a-c) and extreme (Figure 40 a-c).

In general, meteorological (monthly) droughts and agrometeorological (quarterly) droughts show spatial patterns with an occurrence percentage quite similar in each one of the three types of intensities, and they differ from the hydrological drought patterns (annual) in the spatial distribution, in the three scales, and specially, in the intensity of the occurrence frequency. This difference reaches higher values, as high as two times the frequencies registered in the other two temporal scales (meteorological and agrometeorological) in each one of the intensities and are restricted to isolated spots located in the western slope of the northern and southern mountain region.

Meteorological drought (monthly SPI) of moderate intensity show frequencies lower than 2% in all the coast and places in the mountain region located in the Pacific Ocean drainage basin (Figure 38 a) These droughts become more frequent in all the mountain region with values between 6% and 8% and values between 8% and 10% in the jungle, where some extremes between 10% and 12% are registered as in San Martin (Mayo river basin) and some disperse values in the central and southern mountain region.

Also, moderate droughts in the agrometeorological scale (Figure 38 b) show an spatial distribution similar to the meteorological scale (one month) with values lower than 2% in some locations in the coast and mountain region of Arequipa. Also frequency values between 6% and 10% are registered in the mountain and jungle region, and higher values, with a frequency between 10% and 12% were observed in most part of the northern jungle. The maximum frequency was observed in the location of Colquepata (Cusco), with a frequency between 16% and 18%. The distribution of frequencies of moderate hydrological droughts (Figure 38 c) show very low values (lower than 2%) in the northern and southern coast, while values between 6% and 12% are observed in the mountain and jungle. Also, there is no sign of any regional characteristic, as it is observed in the moderate droughts of the other two previous temporal scales. High frequencies of this type of drought are scarcely registered in the mountain region of Arequipa (Pampa de Arrieros), Cusco (Colquepata) and northern jungle (Juancito).

This type of drought intensity (moderate) in the temporal scale of one month and a quarter, show a clear difference in the occurrence frequency from 2% to 4%, although it is apparently small, in the regions located the western side of the Andes Mountains, and the rest of the mountain and jungle region of Peru. This difference in the whole Peruvian territory seems to be greater in the meteorological scale than in the agrometeorological, where the frequencies seem to be more homogeneous in most part of the stations. This difference practically disappear at the annual scale, in which, the frequent droughts of moderate intensity may occur with the same continuity in the whole territory , apparently more feasible in the high

FIGURE 37

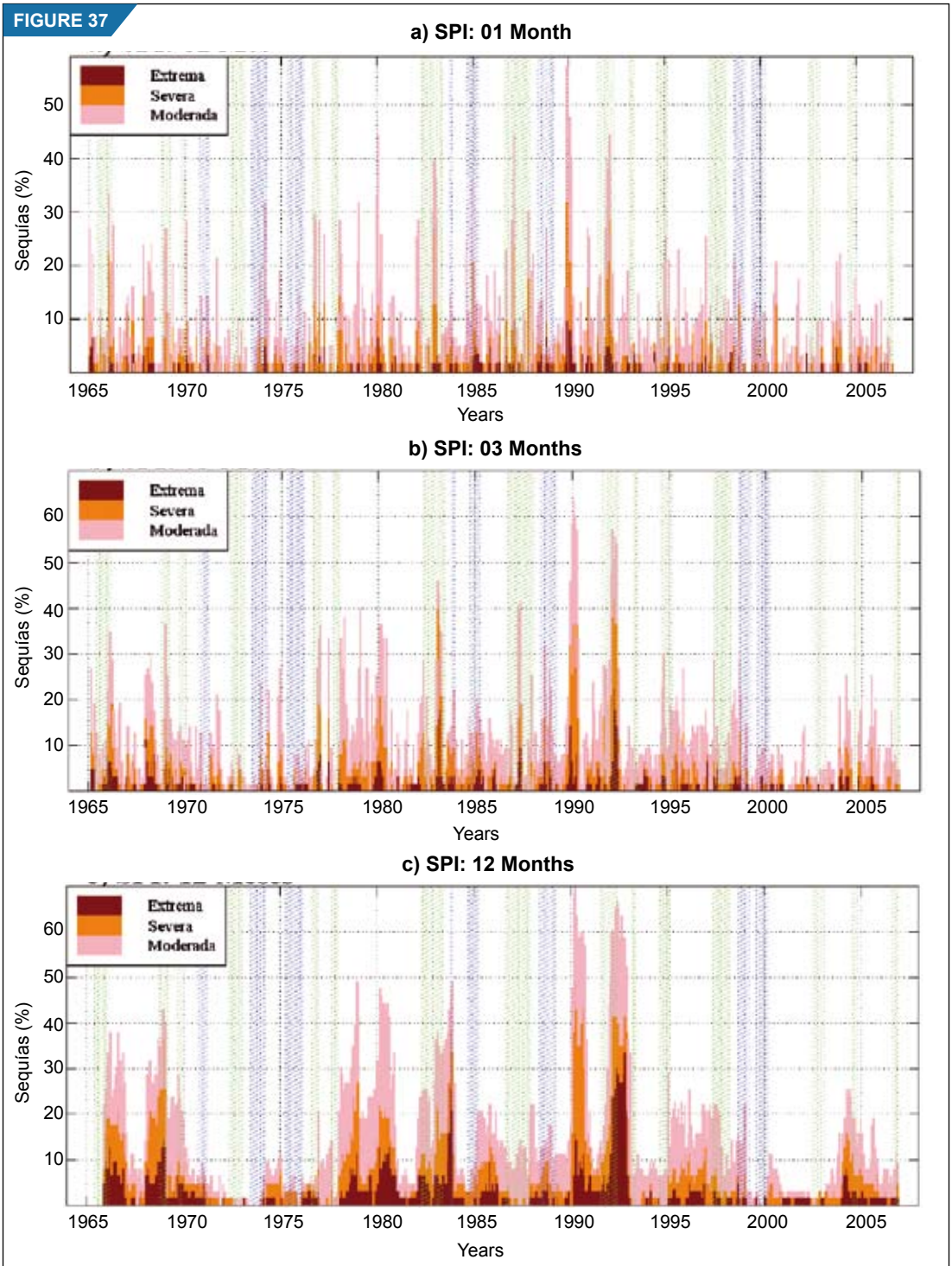

Temporal distribution of the area of Peru (percentage of 64 stations) affected by three categories of more intense droughts registered for the period 1965-2006. a) meteorological droughts (monthly SPI), b) agrometeorological droughts (quarterly), c) hydrological droughts (annual SPI). The shaded areas in green (blue) color identify period of occurrence of warm (cold) events of El Niño / Southern Oscillation (ENSO).

zones of Arequipa, some locations in the central zone of Puno and other higher parts of the mountain region, except for three locations in the mountain and jungle.

The distribution pattern of severe droughts at the temporal scales, monthly and quarter (Figure 39 a-b) follow the model of moderate droughts in the same temporal scales. The pattern of severe droughts

FIGURE 38

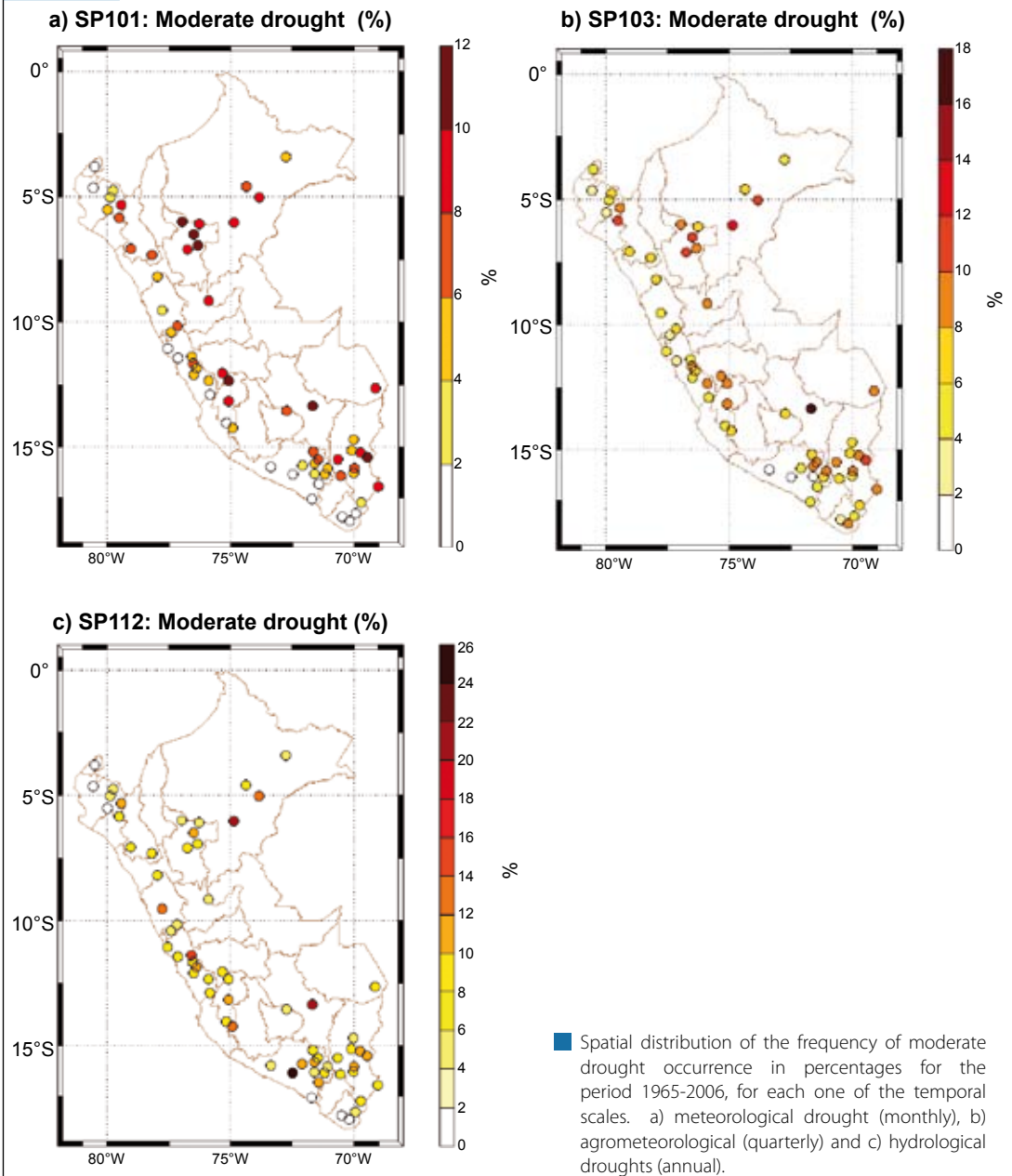

Spatial distribution of the frequency of moderate drought occurrence in percentages for the period 1965-2006, for each one of the temporal scales. a) meteorological drought (monthly), b) agrometeorological (quarterly) and c) hydrological droughts (annual).

in this intensity is very different from the model of hydrological moderate droughts (Figure 39 c). The minimum frequencies are restricted to the coastal region, at a higher ratio in the monthly scale (meteorological drought) than in the quarterly. The distribution of frequencies in the monthly scale (Figure 39 c) points out more precisely the contrast between the frequencies of droughts observed in the stations in the mountain region, over the western side of the Andes Mountains and the rest of the mountain and jungle region. These last two regions seem to be more prone to the occurrence of drought in this temporal scale especially in the northern jungle.

At the quarterly scale (Figure 39 b) the contrast observed in the previous scale intensifies, which originates a distribution of the frequencies slightly more homogenous in all the mountain and jungle region of Peru. Another important characteristic in the distribution of frequency of severe droughts in this scale (quarterly), is the apparently regionalization of the drought occurrence. These regions seem to group

FIGURE 39

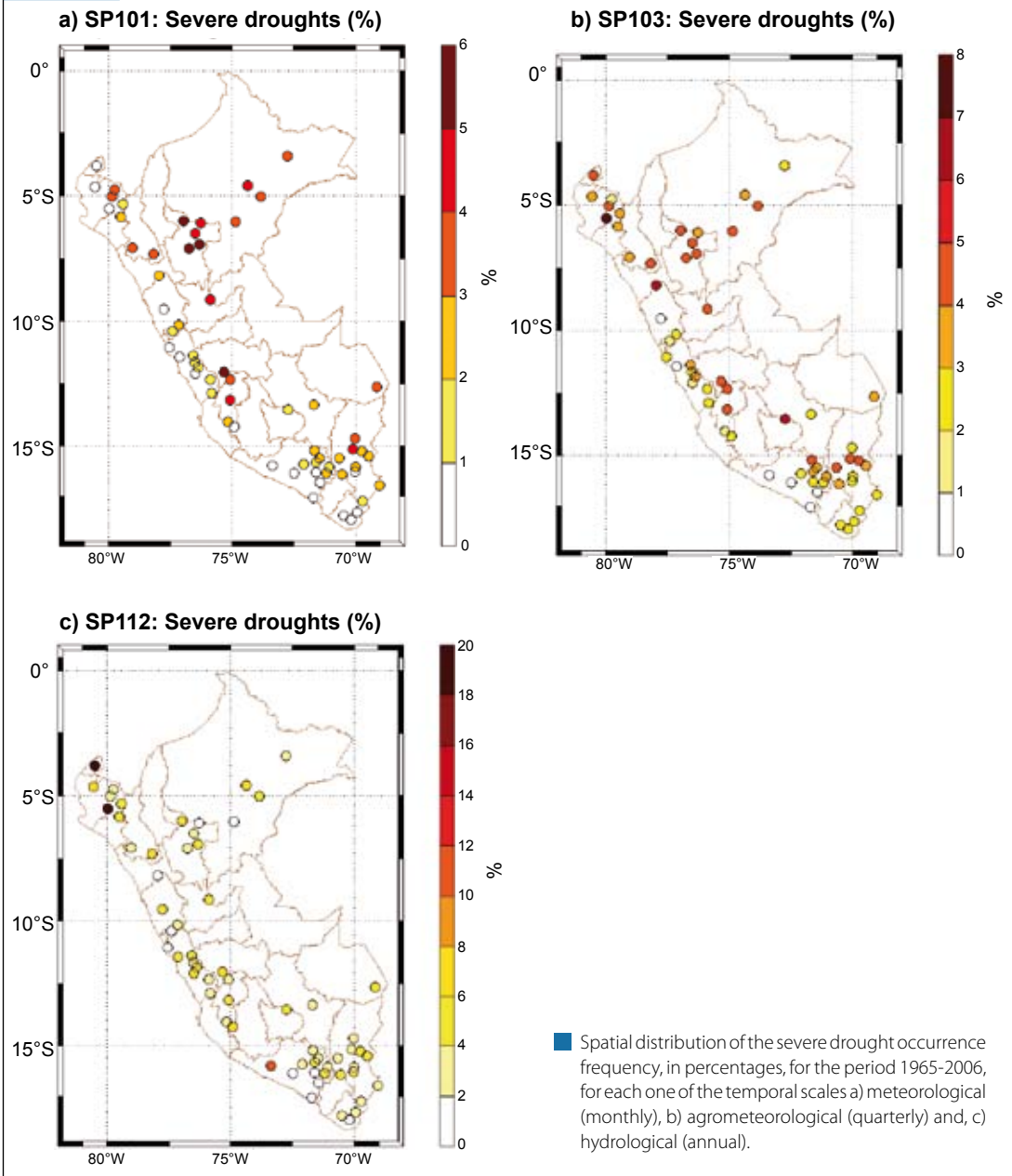

Spatial distribution of the severe drought occurrence frequency, in percentages, for the period 1965-2006, for each one of the temporal scales a) meteorological (monthly), b) agrometeorological (quarterly) and, c) hydrological (annual).

between Arequipa and Puno, and it extends to Huancavelica, Junin and Lima, and all the regions in the northern part of Peru. The values of the frequencies for the two scales are similar, which can indicate us that in this type of intensity there is a strong interdependence between the two. Finally, annual severe droughts (Figure 39 c) show low and homogeneous values of occurrence frequency in this type of drought. Also the extreme values are observed in the northern mountain region (Piura and Tumbes) and Arequipa. These values are possibly more associated to the aridness of these regions that to the variability of the rainfall period.

Extreme meteorological droughts (Figure 40 a-c) show that during the 42 years most of the locations registered drought frequencies lower than 1%, except for the northern jungle which registered values between 2% -3% with a maximum of 5% - 6%. This behavior differs from the other two drought intensities (moderate and severe), where the annual scale (hydrological) has a large number of stations that

show low frequency values. Another important characteristic observed in this type of drought intensity is putting together the stations with similar values, being the annual scale the most noticeable and with a higher number of stations (Figure 40 c). Meteorological droughts show two areas in Peru, where the stations with frequencies between 1% and 4% are more or less put together in groups. These stations are located in Arequipa and Puno, and the northern jungle, between San Martin and Loreto. At the three-month scale these areas are more prominent and another area appears in the central mountain region, between the southern part of Ancash and Andahuaylas. Finally, the annual scale (Figure 40 c) shows similar frequencies for the same areas, but a little more extended. To the south it includes the high zones of Arequipa, Puno and Tacna, in the central mountain region other stations are considered for the same area and, in the northern mountain region there is a slight increase in the number of stations and a decrease in Loreto. These spatial patterns of extreme drought indicate that in these places, its occurrence besides having regional characteristics, there is great possibility that a prolonged extreme event, as the hydrological drought occurs instead of a short event, such as the meteorological drought.

FIGURE 40

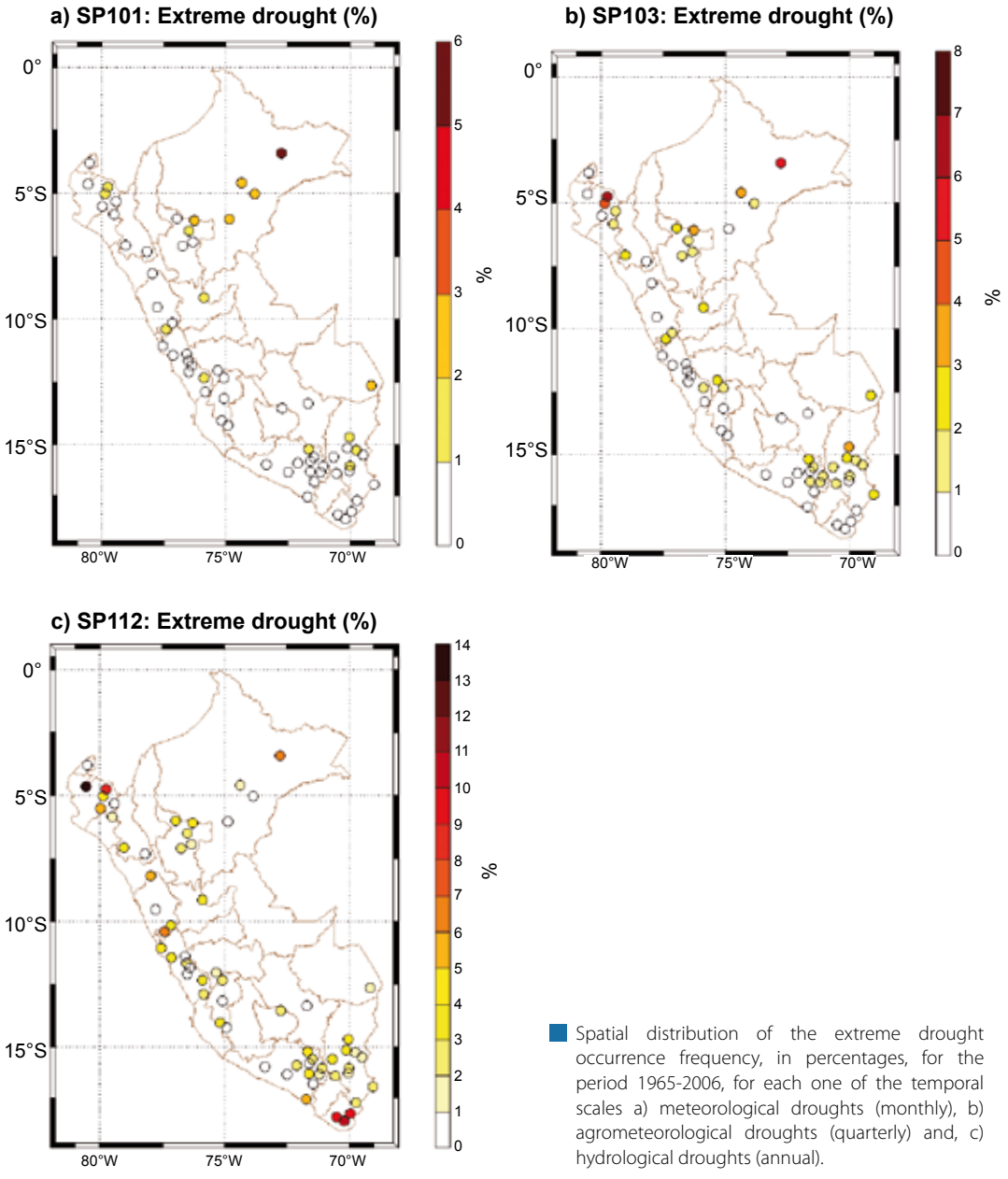

Spatial distribution of the extreme drought occurrence frequency, in percentages, for the period 1965-2006, for each one of the temporal scales a) meteorological droughts (monthly), b) agrometeorological droughts (quarterly) and, c) hydrological droughts (annual).

3.3.6.2. Tele-connections in drought distribution

In this part of the study, an analysis and discussion is made on the quarterly correlation analysis estimated for the three seasons that the rainy period for most part of the Peruvian territory consists of: (SON; DJF and MAM) and the indices of standardized anomalies of the SST of the El Niño 3,4 (Niño 3.4), the Pacific Decadal Oscillation (PDO); and the difference of sea surface temperatures between the South Tropical Atlantic and the North Tropical Atlantic (TSA-TNA), and the standardized anomalies of the SPI. This analysis may indicate us about possible teleconnections that exist between the temporal series of the monthly SPI (meteorological) and characteristics at a large scale, related to each one of these circulation patterns.

a) Correlation between the SPI and the Ocean/Atmospheric Indexes

The seasonal correlations between the standardized anomalies of the SST in the El Niño 3,4, an index that represents the ENSO phenomenon, and the Standardized Precipitation Index (SPI) monthly (meteorological scale) for each one of the 64 stations distributed throughout the country, for the rainy period (September- May) are shown in Figure 41 a-c. The distribution of the correlation coefficients (cc) with statistical significance at 95%, shows that they are very scarce, isolated and do not persist not even for two continuous astronomic stations, although the sign of the coefficients remain during the three stations, direct or inverse, and are located preferably over the mountain region.

An the beginning of the rainy period over most part of Peru (SON), the relation between the SPI and the ENSO events (Figure 41 a) seem to focus on three major regions of Peru that show opposite relations between them: the southern mountain region, consisting of the Departments of Puno and Arequipa apparently extending over the jungle; the northern regions of Peru that presents direct relations between both anomalies, and the central mountain zone between Ancash and Apurimac, that registers inverse relations and in some places they are very intense, but not significant. Even though the cc values are high and not statistically significant, this distribution indicates that during this season the occurrence of some warm event of the ENSO would cause positive anomalies in precipitation (excessive rainfall), specially over the southern mountain region and northern mountain and jungle region. The opposite is expected to happen over most part of the central mountain region, in the Departments of Apurimac, Ayucucho up to Ancash, where the cc between the SPI and the anomalies of the El Niño 3.4 are inverse, which suggests that warm events of the ENSO could favor the occurrence of droughts during the spring time (SON) in this region.

In the summer season (DJF) the spatial pattern of the cc between the anomalies of the SPI and the SST of the El Niño 3,4 (Figure 41 b) shows negative values over most part of the country, with predominance of lower values (lower than 0,2). Positive values are mostly limited to the western and northern mountain region and northern jungle, except for some locations in the mountain region of Piura and Lambayeque, eastern part of San Martin and southwestern part of Loreto. This distribution, although it is only observed in three locations that show statistically significant correlations, indicates that the warm events of the ENSO (positive anomaly of SST) affect directly by means of large scale circulation patterns that generate precipitation over most part of Peru, causing droughts and at the same time they generate positive anomalies over the northern region of Peru, possibly related to the direct effect of the Walker circulation.

The pattern of spatial distribution of the cc, observed during the summer (DJF), persists during the autumn months (MAM), in which cc values statistically significant are registered, at 95% in all the mountain region of Ancash. This reference clearly indicates that the ENSO events originate precipitation anomalies over this Department and at the same time, shows a division between the positive anomalies of precipitation in the northern mountain region and negative anomalies in the southern part of this Department. Thus, this two last distribution patterns indicate that the warm events of the ENSO could cause droughts in most part of the Peruvian territory during these months of maximum precipitation and at the end of the rainy station, which differs from what occurs at the beginning of the rainy period, especially in the

FIGURE 41

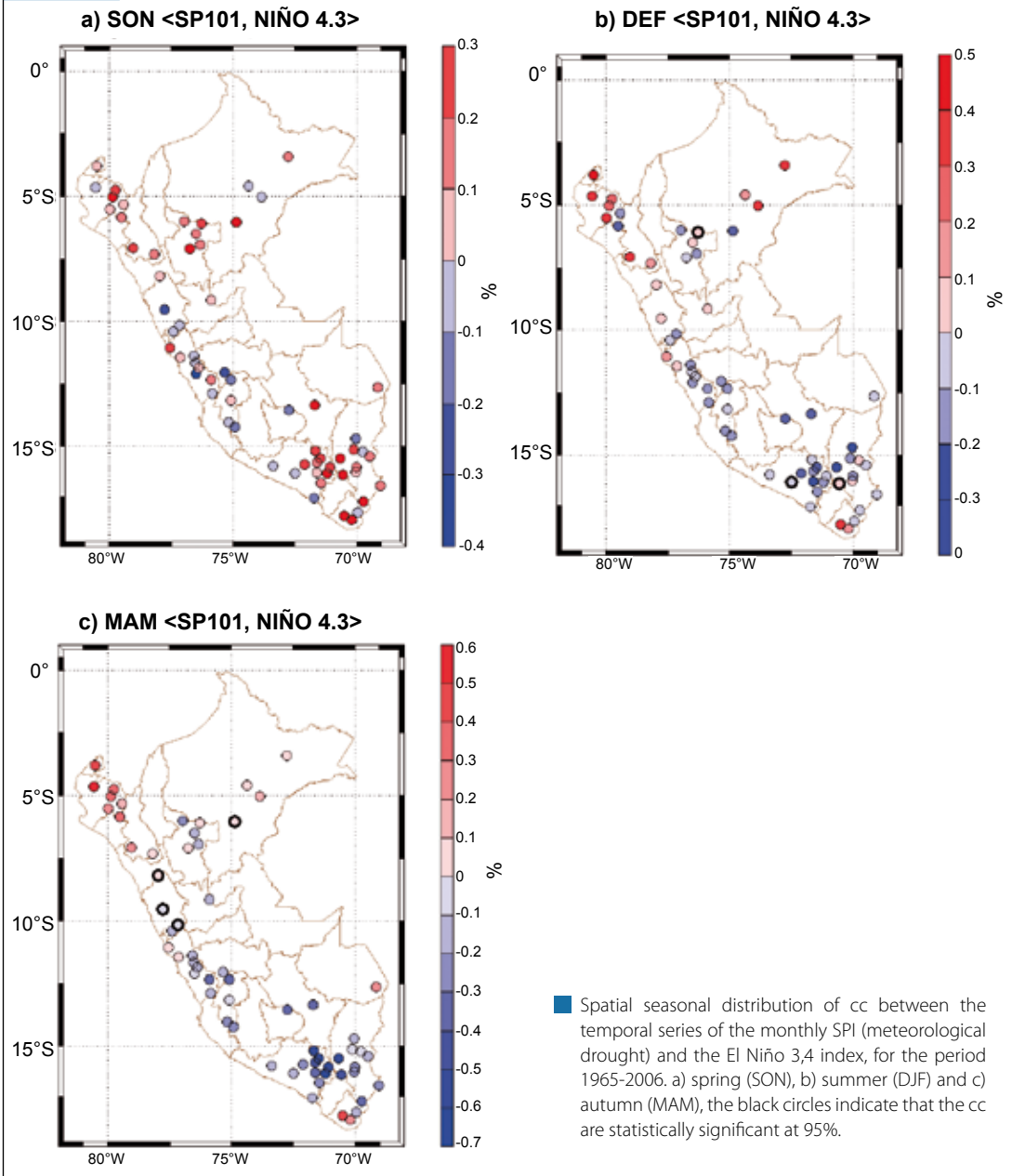

Spatial seasonal distribution of cc between the temporal series of the monthly SPI (meteorological drought) and the El Niño 3,4 index, for the period 1965-2006. a) spring (SON), b) summer (DJF) and c) autumn (MAM), the black circles indicate that the cc are statistically significant at 95%.

southern zone. Also, the direct relation continues in the northern coast and north-western mountain region, which indicates that in presence of an eventual El Niño phenomenon positive precipitation anomalies would be registered.

It is important to indicate that the persistent value of the cc, registered during the all the seasons in the locations of Tacna, indicate that the warm events of the ENSO favor the non-occurrence of droughts in these places.

The seasonal temporal distribution of the cc between the SPI and the PDO index (Figure 42 a-c) show that the seasonal patterns of spring and autumn are very similar to the seasonal models observed between the SPI and the El Niño 3,4 (Figure 41 a and c), specially in the southern and northern regions. The greatest differences are located in the north-western jungle (San Martin), where in both season inverse

relations are observed. On the other hand, the pattern of the summer season (Figure 41 b) is different from the correlation patterns with the SST of the El Niño 3,4, and predominance of cc positive values are observed, with some negative isolated values, mainly in the southern mountain region and northern jungle (San Martin), but none of the cc is statistically significant. This indicates that during the summer the PDO (positive phase) tends to cause positive anomalies of precipitation over most part of Peru.

The similarity of the two patterns of the cc of the SPI with El Niño 3.4 and the PDO at the beginning and at the end of the rainy period, indicates that the two phenomenon act in the same direction in each one of these seasons over the same regions of Peru. This means, that anomalies of the same sign for both indices caused the same effect over the same locations, but, since the oscillation period of this circulation patters varies (El Niño interannual, from 2-7 year and the PDO is decadal) it can be expected , depending

FIGURE 42

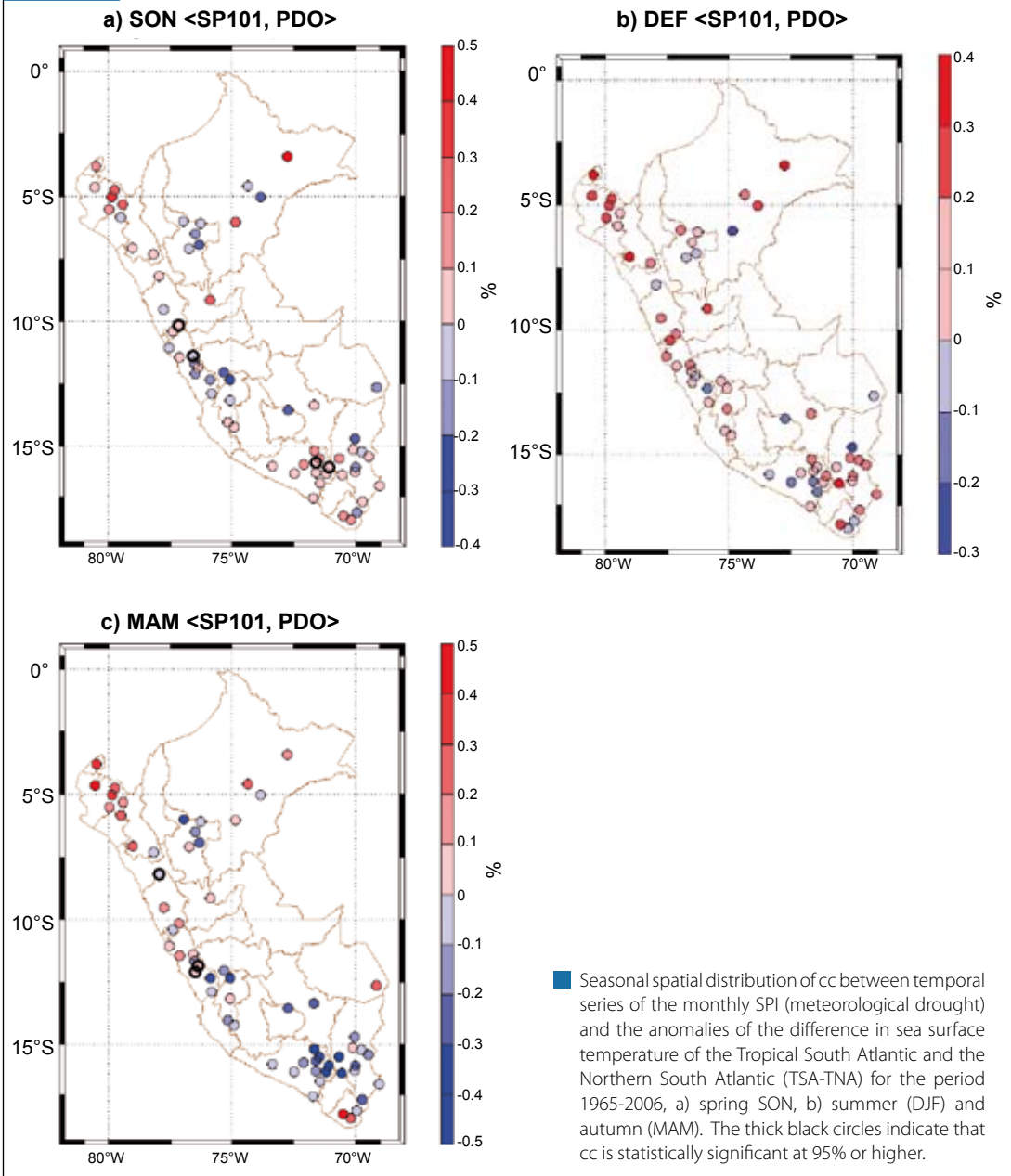

Seasonal spatial distribution of cc between temporal series of the monthly SPI (meteorological drought) and the anomalies of the difference in sea surface temperature of the Tropical South Atlantic and the Northern South Atlantic (TSA-TNA) for the period 1965-2006, a) spring SON, b) summer (DJF) and autumn (MAM). The thick black circles indicate that cc is statistically significant at 95% or higher.

FIGURE 43

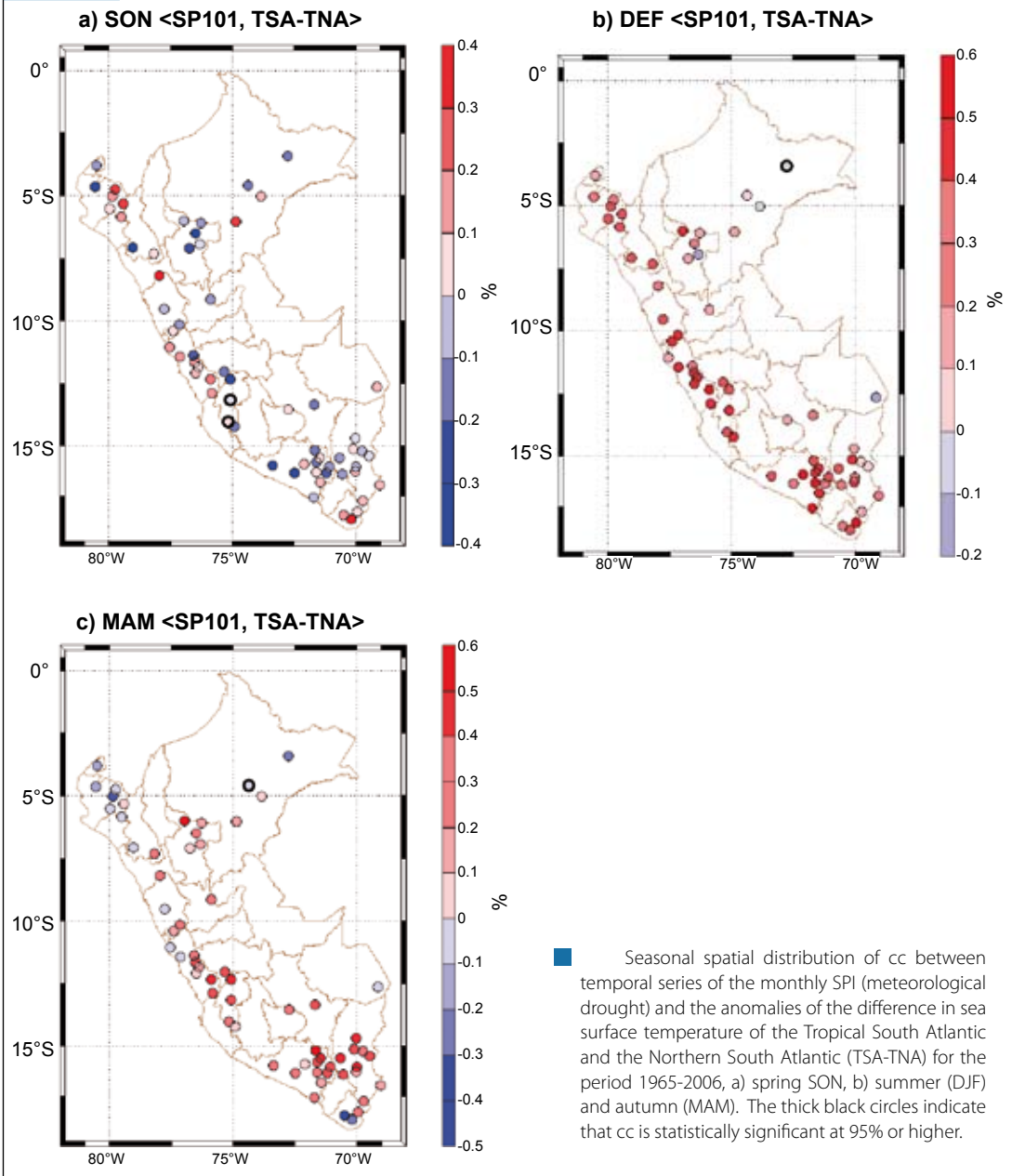

Seasonal spatial distribution of cc between temporal series of the monthly SPI (meteorological drought) and the anomalies of the difference in sea surface temperature of the Tropical South Atlantic and the Northern South Atlantic (TSA-TNA) for the period 1965-2006, a) spring SON, b) summer (DJF) and autumn (MAM). The thick black circles indicate that cc is statistically significant at 95% or higher.

on the modulation of these indices, that the drought periods may vary in intensity according to the phase in which they are, and it seems that the locations situated in the southern and central mountain are more sensible during the beginning of the rainy period (SON). In the summer season the opposite would occur for most part of Peru, where both phenomenon would oppose to each other, except for the coast and northern mountain region, where they would cause the same effect: floods, droughts depending on the phase of the ENSO or PDO.

The seasonal correlations between the SPI and the TSA-TNA (Figure 43 a-c) show cc patterns quite different in the rainy period. During spring (Figure 43 a), when the Intertropical Convergence Zone ITCZ, intrinsically related to the difference of the TSA-TNA, is localized in the northern hemisphere during the those months, the cc between the SPI and the TSA-TNA anomalies, show an apparent regionalization, with an inverse relation (negative values) over most part of Peru, with some exceeding positive values

specially in the northern mountain region, western slop of the central mountains, high zones of Arequipa and Tacna. This means that the positioning of the ITCZ (TNA>TSA) north of its normal position, the pattern becomes more favorable for the occurrence of positive anomalies of precipitation, and; therefore, inhibition of droughts over almost the whole country, preferable in the eastern part of the Andes Mountains and northern jungle. There is the possibility that the opposite thing might occur (droughts) in the northern and central mountain region (western slope) and the southern tip of the southern mountain region.

The spring pattern completely changes for the summer (DJF) and autumn (MAM) seasons. CC positive values for almost all the country are registered in the maximum rainfall period (DJF), with very high values over almost all the mountain region, although there is no statistically significant value. In autumn (Figure 43 3) when the position of the ITCZ reaches the southernmost part, the observed patterns in the summer change over the coast and northern mountain, they extend up to the central mountain showing inverse relations.

These patterns are the expected ones, because thecloser the ITCZ is positioned to the south during these two astronomic seasons, there is less probabilities to show rainfall shortage, except for the northern jungle and southern jungle, in the two seasons, and in the coast and north-western mountain during the autumn because it showed inverse relations. A possible explanation of this is that, the closer the ITCZ is to the south, mainly during the summer season, precipitation will be abundant in all the country, except for the jungle and northern region, due to the water vapor flux, facilitated by regional circulation. The areas of the northern jungle and possibly northern mountain , where there is a shortage in precipitation it is due to the subsidence produced by the position of the ITCZ, and the westerns slope of the central mountain, probablydue to subsidence conditions.

FIGURE 44

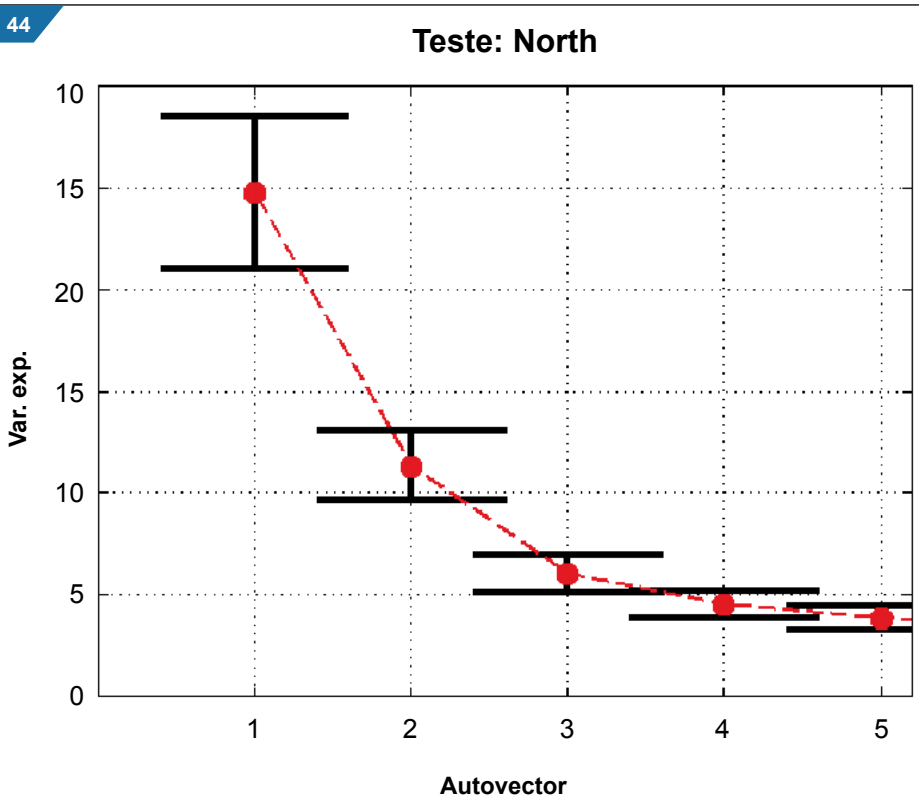

Distribution of the PCA autovectors of the SPI and the percentage explained variance by each one of them. The North Test indicates that the two first patterns are independents and starting the third component this some mixture of patterns.

b) Analysis of the principal components of the SPI

In the PCA of the SPI,using the North Test, it was determined that only two patterns are independent, as it is shown in Figure 44. Also these two patterns account for 36% of the total variance of the drought that occur here in Peru, according to the method used to make the estimates.

The spatial pattern of the first component of the Standardized Precipitation Index SPI (Figure 45-a) which accounts for 24.7% of the total variance, shows some positive values over almost all the Peruvian territory, except for two locations in Loreto and one in Tacna, with very small negative auto-values, over -0,05. The highest positive auto-values are located in all the mountain region, focusing the highest density of auto-values in the southern mountain region (Arequipa and Puno) and part of the central mountain region.

The amplitude of the time series of this first component (Figure 45 b) show very intense negative values during the summers of 1989/90 and 1991/92. Also, it has been registered high values in 1966, 1976, 1980, 1983, 1987. Similarly, high positive values are registered in 1974, 1984, 1990, 1997, 1999 and 2002. The result of the amplitude of these series with negative auto-values indicates the occurrence of drought with an intensity proportional to the result of both. Thus, the most intense droughts registered under this patter, in 42 years, occurred in the whole country, especially with more intensity in the central and southern mountain region, in the summers of 1989/90 and 1991/92, followed by the years that registered negative series. At the same time, this pattern also indicates the occurrence of high precipitations, mainly in the years 1974 and 1990.

The Wavelet analysis (Figure 45 c) suggests that the temporal series of this first pattern consists of very intense annual oscillations, contrasting and statistically significant, from the beginning of the period of study until the starting of 1990. These oscillations of the annual cycle are related to extreme values of the amplitude, either negative (very dry years), as 1966 and 1983 or positive (very humid) as 1974, 1984 and 1990. The very intense biennial oscillation (2-3 years), statistically significant, observed between 1989 and 1994, was responsible for causing extreme shortage of precipitations over the Peruvian territory in the summers of 1989/90 and 1991/92.

The annual oscillations observed during 1974 and 1994, which were intense and significant seem to be associated with an oscillation almost decadal with statistically significant values between 1975 and 1995. This oscillation seems to be related to the Pacific Decadal Oscillation (Mantua et al., 1997), that during those years was in its warm phase. The global spectrum of the wavelet shows that the annual oscillations are significant same as the almost decadal oscillation that shows a peak between 12/13 years. Also it is observed a less intense, but significant peak of 2-3 years, as a result of the oscillation occurred between 1989 and 1994, apart from weak oscillations observed at the end of the 1960's and 1990's decades.

The spatial and temporal distribution of the first component, as well as the wavelet analysis of the temporal series, indicate that the most intense droughts observed during all the period of the present study, are related to a biennial very intense oscillation, part of the oscillation spectrum of the ENSO, called by Barnett)1991) the high-frequency oscillations of ENSO (2-3 years) and modulated by almost decadal oscillations with periods of 12-13 years that apparently are a reflect of the Pacific Decadal Oscillation (PDO).

The second spatial pattern of the PCA accounts for the 11,3% of the total variance (Figure 46 a) and shows negative values over most part of the east-central and southern part of the mountain region, specially over Puno and the highest zones of Arequipa, where the highest values are observed, and it extends up to the jungle. In the other regions some positive values are registered with very intense values over the northern mountain and the western side of the central and southern mountains.

The temporal series of this component show high interannual variability with very intense positive values in: 1967, 1983, and 1997/1998 that combined with the values of the spatial pattern, means that in

FIGURE 45

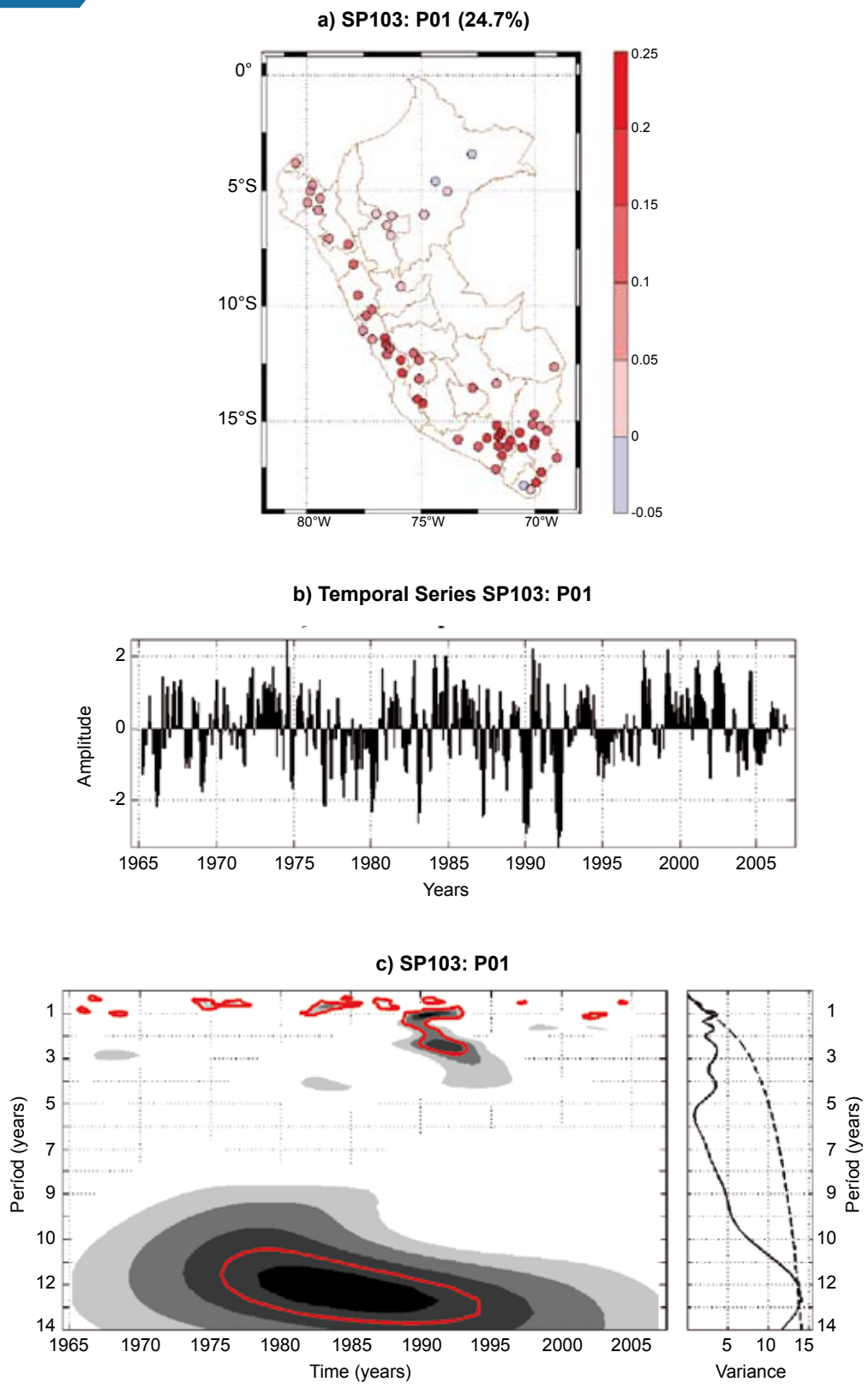

First component of the quarterly SPI a) spatial distribution of the autovalues, b) temporal series and , c) wavelet analysis of the temporal series (left side: spectral energy, right side: global spectrum . The red line in the wavelet analysis indicates statically significant values al 95%.

FIGURE 46

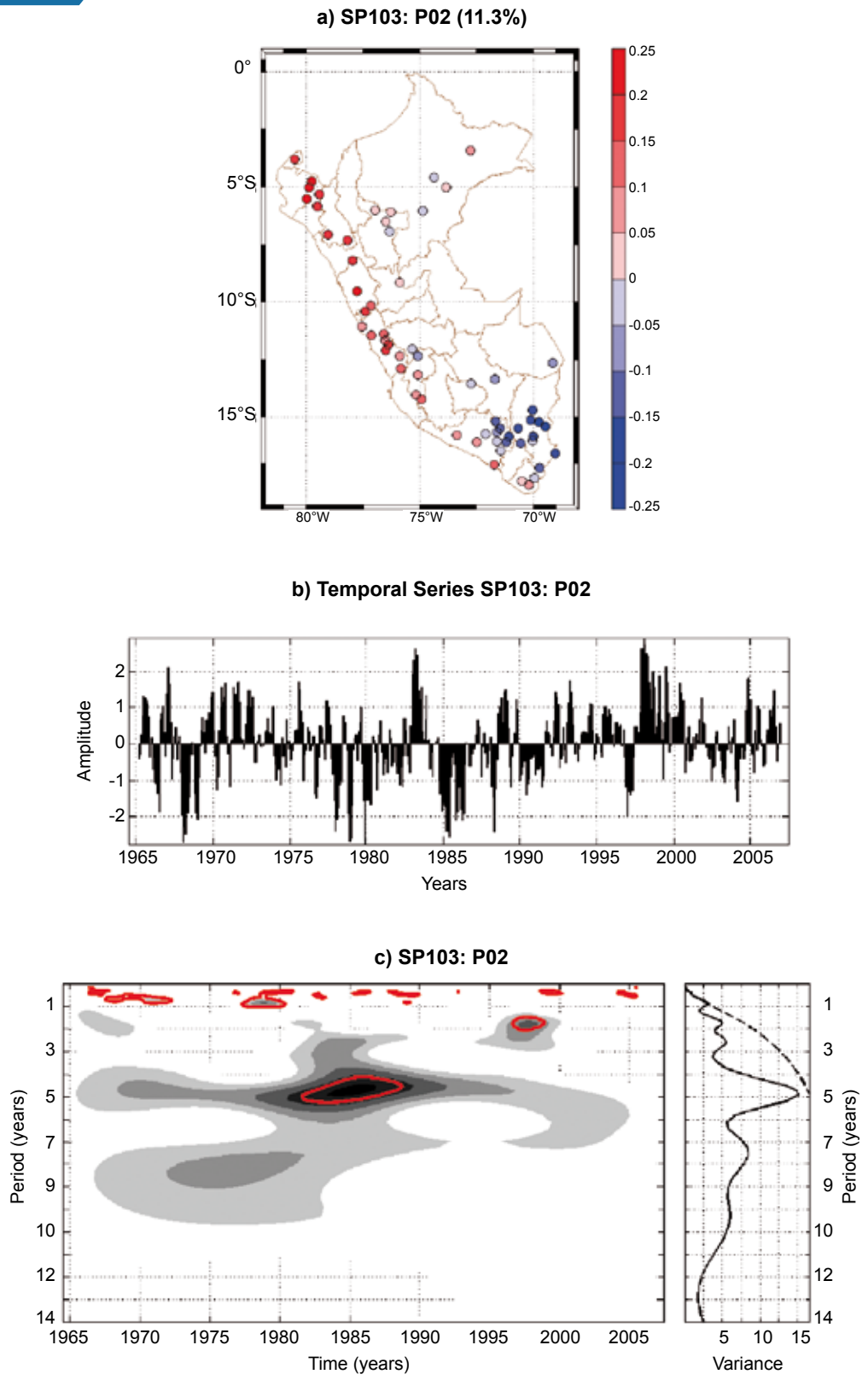

Second component of the quarterly SPI a) spatial distribution of the autovalues, b) temporal series and , c) wavelet analysis of the temporal series (left side: spectral energy, right side: global spectrum . The red line in the wavelet analysis indicates statically significant values at 95%.

those years very intense droughts that followed this pattern, were registered, mainly during 1983 and 1997/98 in the southern and central mountain region of Peru; and, high precipitation over the coast and northern mountain region. Also negative intense values were observed during 1968, 1978, 1979, 1985 and 1988, which indicates that the observed patterns during the periods with positive values reverse and positive anomalies of precipitation are registered in the southern and central mountain region and drought in the remainder part of Peru. From all these years, 1983 and 1987 are associated with the warm events of the ENSO and in 1985 is associated to a cold event.

The wavelet analysis of the temporal series of this second pattern (Figure 46 c), has an interannual oscillation with a period of 3 to 7 years, almost during the whole period of study and it is statistically significant throughout the 1980's decade. This oscillation is reflected in the global wavelet spectrum with a very intense peak of 4 to 6 years, but it is not statistically significant. Also, biennial oscillations are observed at the end of the 1960's and 19890's decade, associated to intense negative and positive anomalies in the temporal series, respectively.

In summary, the second pattern of the quarterly SPI represents the variability pattern of the ENSO low frequency events (Barnett, 1991), that modulates precipitation in Peru, with periods of oscillation between 3-7 years. This pattern persists throughtout the period of study, causing very intense droughts in the southern mountain region, that extends to the central mountain region and some places in the northern jungle. The typical spatial distribution was registered between 1982 and 1985, when some positive anomalies occurred between 1982/1983 and subsequently negative anomalies in 1984/1985, and the OT analysis indicates that these drought events followed by floods, are related to the 3-7 years oscillation, statistically significant, occurred in 1982 to 1989.

3.3.6.3. Seasonal distribution of droughts occurred during the warm events of the ENSO

The average quarterly behavior of the rainy period (September to March) of the SPI is described, during the occurrence of the most intense warm events of the ENSO occurred during the period of the present study. They are: 1982/83, 1991/92 and 1997/98.

The seasonal reconstruction of the SPI, using the first two principal components for 1982/83, caused by the ENSO at quarterly and annual scale , shows that in the spring season (Figure 47) high precipitation over almost all the country are registered, with maximum intensities over the high zones of Arequipa and Puno at the quarterly scale, similar to the correlations between the SPI and the anomalies of EL Niño 3.4, but with normal conditions, at the annual scale. In the department of San Maritn severe drought is observed during this station, which apparent alters the pattern over the national territory, possible due to local factores. Some signal of a drought event appears during the summer of 1982/83 (Figure 47 b) involving all the regions in the central and southern part of Peru, with moderate and severe droughts, focused in the Department of Puno (Arequipa) at a quarterly scale (annual), In the remaining regions it predominates the excess of precipitations focused in the coast and northern mountain region.

In the months of autumn (MAM) (Figure 47 c) droughts get intensified in the southern part of Peru, occurring extreme droughts in the Departments of Tacna and Puno, in the two scales, during this season of the year, and its expands towards the central mountain region and northern jungle. On the other hand, in both scales, high precipitations in the northern mountain region is observed that extends to the eastern slope towards the central mountain region.

During the ENSO event of 1991/1992, the distribution of the SPI (Figure 48 a-c) show at the quarterly scale, a very different pattern from the one observed in the 1982/83 event. In the spring of 1991, the distribution of the quarterly SPI shows severe and extreme droughts in isolated zones in the mountain and jungle regions, but the annual SPI registers a predominance of positive values in the southern par of Peru and extreme droughts in the northern jungle (Loreto). In the winter of 1991/92 drought starts

FIGURE 47

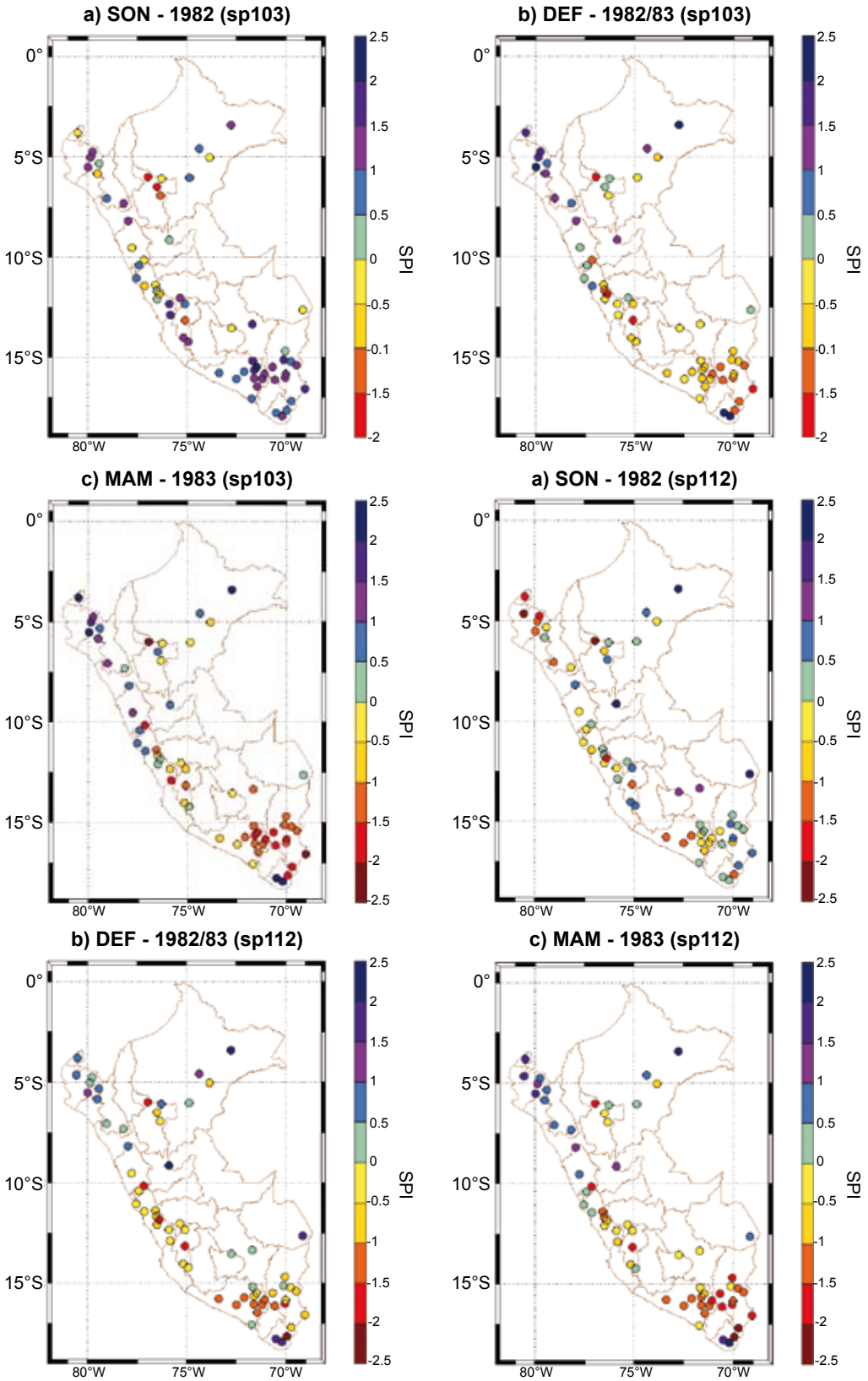

Reconstruction of the average SPI occurred during the ENSO of 1982/83 for the quarterly SPI (superior) and annual (inferior) a) spring 1982, b) summer 1982/83 and c) autumn 1983. The vertical bar indicates the intensity of the drought.

FIGURE 48

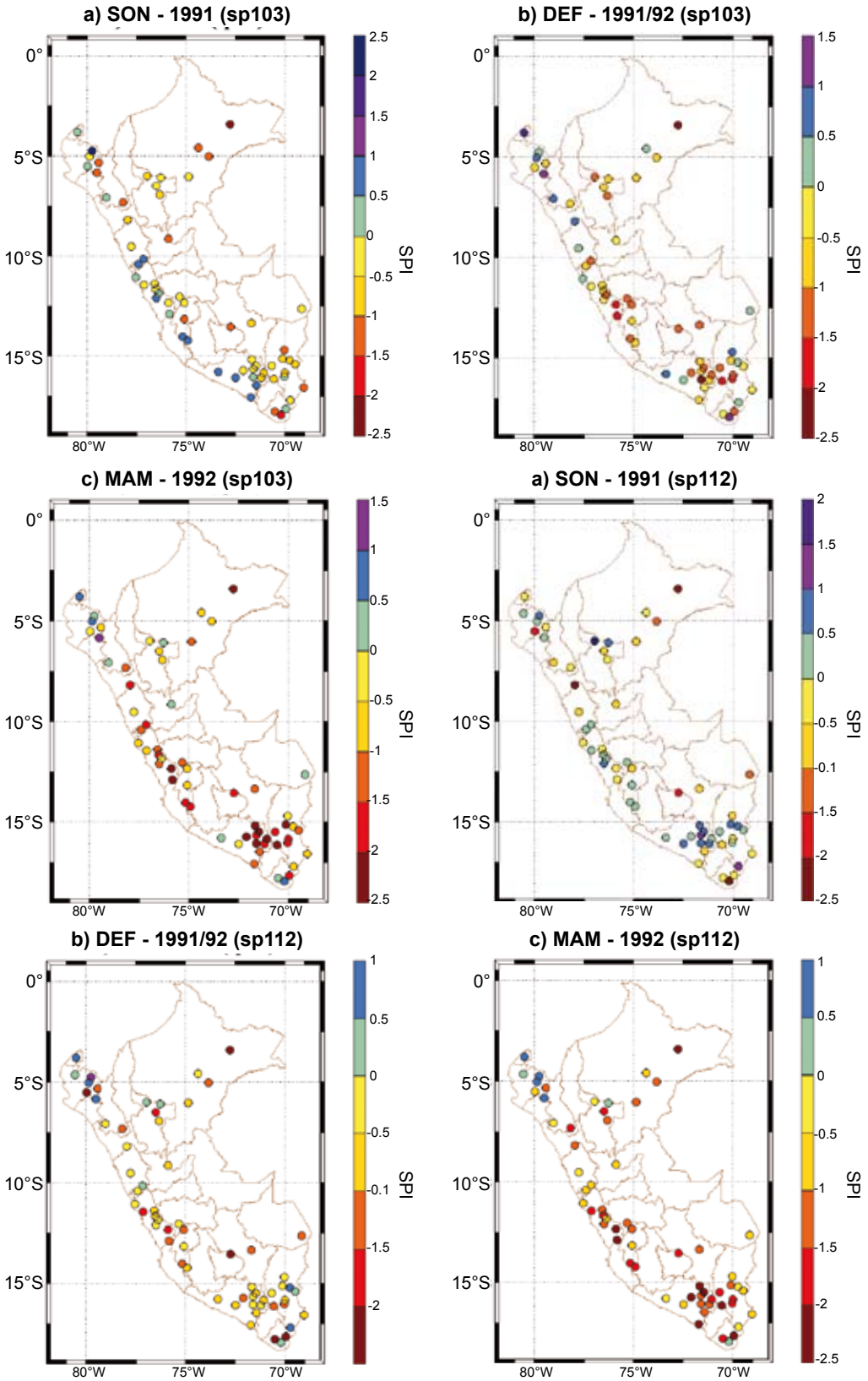

Reconstruction of the average SPI occurred during the ENSO of 1991/92 for the quarterly SPI (superior) and annual (inferior) a) September 1991 , b) summer 1991/92 and c) autumn 1992. The vertical bar indicates the intensity of the registered drought

FIGURE 49

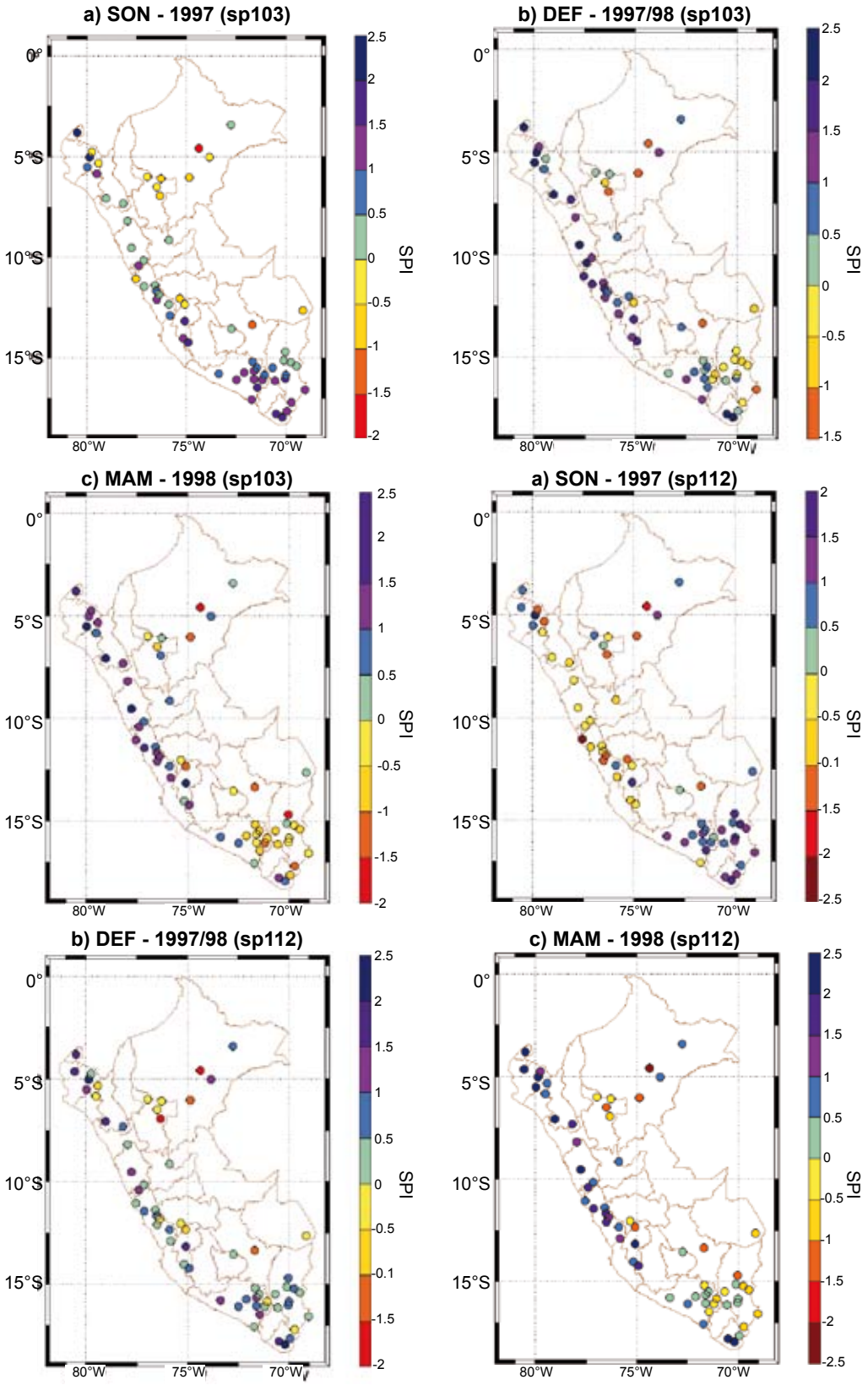

Reconstruction of the average SPI occurred during the ENSO of 1997/98 for the quarterly SPI (superior) and annual (inferior) a) September 1997, b) summer 1997/98 and c) autumn 1998. The vertical bar indicates the intensity of the registered drought.

and affects the whole country, with maximum values focused in the southern region (Puno) and central mountain region at a quarterly scale. At the annual scale, the pattern follows the same trend as in the quarterly scale, but with some low values (Figure 48 b).

In the autumn season, droughts intensify in most part of Peru at the two scales, focused on the same places that were observed in the summer in the southern and central mountain region.

During the warm event of the ENSO in 1997/98 (Figure 49 a-c) the spatial patterns of the quarterly SPI at the quarterly, annual are very different from the observed in the events of 1982/83 and 1991/92. During this event no drought was registered in the observed regions in the two previous events, in which extreme droughts were registered in the southern region of Peru and contrary conditions in the northern region. IN the spring of 1997, in some isolated points of the jungle, some slight droughts are observed, and in most part of Peru some positive values of the PSI is registered which means positive anomalies of precipitation. At the annual scale it can be distinguished moderate and severe droughts in the mountain and central and northern jungle, while in all the southern region positive values of the SPI are observed, almost exactly the opposite to the patterns observed in the previous events (1982/83, 1991/92).

In the summer months of 1997/98 the SPI patterns at the quarterly scale, in the southern region, change and they record moderate droughts in some isolated locations in Puno, as well as in some zones of the northern jungle; while in the rest of the country positive values intensify, being higher in the northern and central mountain region. At the annual scale, the SPI values over the southern region slightly decrease, with respect to the previous season, but they do not indicate any precipitation. The observed droughts in the central mountain region change into positive values and registered drought in the northern jungle continue occurring.

Then, during the autumn months, it appears some signs indicating the occurrence of a moderate to severe drought in the southern region in some isolated locations at both scales. Also, in the northern jungle a moderate drought persists, while in the rest of the country some small variations are observed in the intensity of the positive values, especially in the central and northern mountain region.

CHAPTER 4

CLIMATE SCENARIOS FOR THE DECADE 2020 - 2030

CLIMATE SCENARIOS FOR THE DECADE 2020 – 2030

The climate of a region is the result of a series of factors at different spatial scales, from the local forcings, such as topography, type of soil, vegetation coverage, etc., up to the large scale forcings, such as mesoscale circulation or teleconnections, that can determine the own characteristics of a region, for which reason they must be considered in the analysis of signals of climate change. However, this process might become extremely complicated and characterized for a high degree of uncertainty. Giorgi, 2008.

Climate scenarios that will be presented below, have been elaborated by means of the dynamical downscaling method, for the variables of precipitation and extreme temperatures. This process adds regional small-scale information to the climate signal of the global model, and this way the simulation of the climate spatial details is improved. Also, from the obtained scenarios, the projections of the climate extremes have been evaluated, such as the 95 percentile for precipitation and the 90 percentile for extreme temperature.

4.1 INTERCOMPARISON OF GLOBAL CLIMATE MODELS

Global climate models or General Circulation Models (GCMs) are mathematical algorithms that represent the main physical and dynamical processes of the climate systems, by solving the equations related the laws and principles on mass conservation energy and momentum, that rule such processes in each component of the system and in the interactions between mass and energy (Castro, 2007; SENAMHI, 2005; IPCC, 2001). This patterns are tools of fundamental importance in the simulation of current and past climate, as well as the generation of future climate scenarios, for which is necessary the use of computers that have great processing capacity.

When considering the importance of making studies on the potential impacts and vulnerability to climate change, it is necessary to make projections on the possible scenarios and trends of future climate, for this reason the GCMs are of great importance, because they are capable of simulating under different emission scenarios (3), feasible scenarios as how the climate can change in the future. In the present work six GCMs have been analyzed (see table 1), that are related to two trajectories of greenhouse gas emissions, defined in the Special Report on Emission Scenarios (SRES) of the IPCC (2007 a); they are the A2 (4), B2 (5) emission scenarios. The change in the emission of greenhouse gas effect (GHG) originating from energetic and/or industrialized sources, for the year 2030, show a consistent increase from 25 to 90% with respect to the year 2000, while for the year 2100 from 90% up to 250% (IPCC 2007).

(3) Trajectory of greenhouse gases emissions, defined in the Special Report on Emission Scenarios (SRES) IPCC, depending on socio-economic scenarios that describe the structure thought of population.

(4) A2: Describes a very heterogeneous world. Its more distinguished characteristics are the self-satisfaction and preservation of local identities. The birth rate the economic development is basically oriented to regions and the economical growth per person, as well as the technological change, are divided and are slower than in other evolution lines.

(5) B2 Describes a world in which local solutions prevail over economic, social and environmental sustainability. It is a world whose population increases progressively at a slower rate than in A2, with intermediate economic development levels and a technological change not as fast as the other and more diverse. Although this scenario is also oriented to the protection of the environment and social equity, it focuses mainly on local and regional levels.

The GCMs used by the IPCC and analyzed in the present study are listed in the following table (see more information in SENAMHI, 2005):

Table 3
General Atmospheric Circulation Models jointly used in the simulations done by the IPCC with the institutions in which they were processed.

Center	Country	Acronyms	Model
Max Planck Institute für Meteorology	Germany	MPIfM	ECHAM5/OPYC3
Hadley Centre for Climate Prediction and Research	England	HCCPR	HADCM3
Australia's Commonwealth Scientific and Industrial Research Organization	Australia	CSIRO	CSIRO-Mk2
National Centre for Atmospheric Research	EEUU	NCAR	NCAR-PCM
Canadian Center for Climate Modeling and Analysis	Canada	CCCma	CGCM2
Center for Climate System Research (CCSR) - National Institute for Environmental Studies (NIES)	Japan/EEUU	CCSR/ NIES	CCSR/NIES AGCM + CCSR OGCM
Geophysical Fluid Dynamics Laboratory	EEUU	GFDL	R30

In the present Chapter a comparison of the climatology of the models mentioned in Table 3 with the observed data or current climate from the Climate Research Unit (CRU) is made for the period 1961-1990 (New et al., 1999), aimed at detecting possible systematic errors or bias to be taken into account in dynamical regionalization or downscaling.

The difference between annual mean precipitation of the models and the observed climatology (CRU) in terms of percentage can be observed in Figure 50. All the models present a dry bias in the Andean region and the Amazon region in Peru it is particularly drier in the Andes region (90%).

At the level of the South American region, from the six analyzed models, the NCAR-PCM and the GFDL show more negative bias (dry) in most part of the region, however, it presents a more humid or more rainy bias in the western coast (70%). While the HadCM3 shows a dry bias of a low range in the Peruvian Amazon region and southern mountain region (15-30%). Similar results were obtained by Marengo et al., (2007), when he evaluated the global models for South America between the 1961 to 1990 period, showing that the CCSR/NIES, HadCM3 and CSIRO patterns had better skill in the presentation of rainfall over Peru, showing lower differences in precipitation between -1 to 1 mm day-1.

With reference to maximum temperature (Figure 51), the CCCma model shows a bias quite cold in most part of South America, specially in the tropics (4ºC), the CCSR/NIES shows a bias quite warm over the Peruvian Andes (5 ºC) followed by the CSIRO, this last one with a warmer bias in the southeastern border with Brazil. The NCAR-PCM show a cold bias restricted to a sector in the Peruvian Amazon region (3 ºC) and a warm bias in a sector of the central southern mountain region.
Concerning minimum temperature (Figure 52), the HADCM3 and the CCSR/NIES showed a bias warmer in the tropical region (5 ºC), while the CCCma and the CSIRO show cold bias east of the tropical Andes (5 ºC) and a warm bias over the Andes and adjacent western area (4 ºC). The NCAR-PCM model, in general, show a warm bias that gets stressed over the Andes and also shows a cold bias in the Peruvian-Bolivian Amazon (4 ºC).

The most outstanding feature about the CSIRO model is its predominant warm bias of maximum temperature in the sub-tropics and at the same time, a particularly cold bias, of minimum temperature over this same region.

FIGURE 50

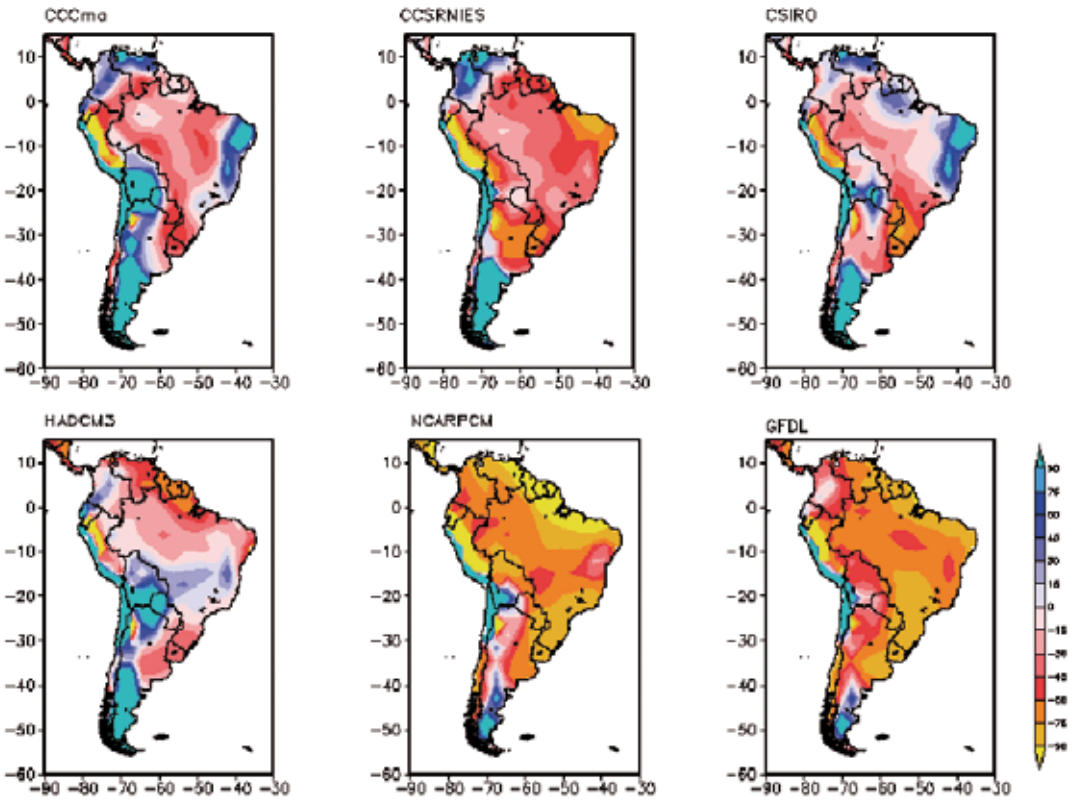

Difference between annual precipitation simulated by the CCCma, CCSR/NIES, CSIRO, HADCM3, NCAR-PCM and GFDL models, in relation to the mean observed climatology by CRU for the period 1961-1990. The units are in percentages.

All the models (except for the CSIRO), show warmer bias for minimum temperature in larger areas, with respect to maximum temperature, being the Andes region where positive bias for minimum temperature predominate, even in the CSIRO model. About the Amazon region, only the CCCma and the CSIRO show cold bias for minimum temperature (4 ºC), followed by the NCAR-PCM but in a lower degree.

4.1.1. Temperature projections for Peru to 2050, based on global models.

Figure 53 shows the projections on the increase of maximum and minimum air temperatures in five global models of the IPCC up to 2050, for the grid points over Peru in emission scenarios A2 and B2. The thick black line represents the mean or average temperature from all the 5 models.

The projections of the five global models, analyzed in this study, indicate, in average, positive anomalies which means, warming. According to these models it is expected and average increase in maximum temperature of up to 1 ºC to 2030, and up to 2 ºC by the end of 2050, in both scenarios. The HADCM3 model is the one that projects an extreme warming of up to 6 ºC in the extreme A2 scenario and up to 5 ºC in the B2 scenario, showing a larger dispersion starting in 2030. The NCAR-PCM model shows a cooling or at least lower values than the average in the A2 starting 2010 of up to -1 ºC. The CCCma model shows more stability, it almost follows an average projection, while the CSIRO and CCSR/NIES, compared to the other models they show high variability, that is to say, they fluctuate and project positive anomalies as well as negative (warming and cooling); however, the last mentioned model is the only one that reproduced the El Niño events 1972/73, 1982/83 and 1997/98, but only for the case of maximum temperature and in the A2 scenario.

Concerning minimum temperature, the average increase is similar to that of maximum temperature. The high variability showed by the HADCM3 model. The CSIRO model which show higher fluctuations, biased towards cooling in both scenarios. None of the models simulates the high temperatures detected during the El Niño years, except for the HADCM3 model, that with certain ability simulates the El Niño 1982/32, but only in the B2 scenario.

4.1.2. Projections of precipitation over Peru based on global models to 2030

The variation in the percentage of precipitation in Peru for the period 2025-2035 simulated by the global models is shown in Figure 54. All the models show different distributions throughout the country. Only in the northern coast all the models agree on increases of up to 15%, situation that is associated to the increase of the sea surface temperature (SST). Similar results found Marengo 2007 with a great intensity for the period 2041 to 2100.

The models of the mountain and jungle region do not agree, showing certain differences between them. Only two models out of the 6, show an increase of up to 15% prevailing the shortages that reach up to 45% over the western slope of the southern jungle region (model HADCM3). In the jungle 3 out of 6 models show increase of up to 15%.

FIGURE 51

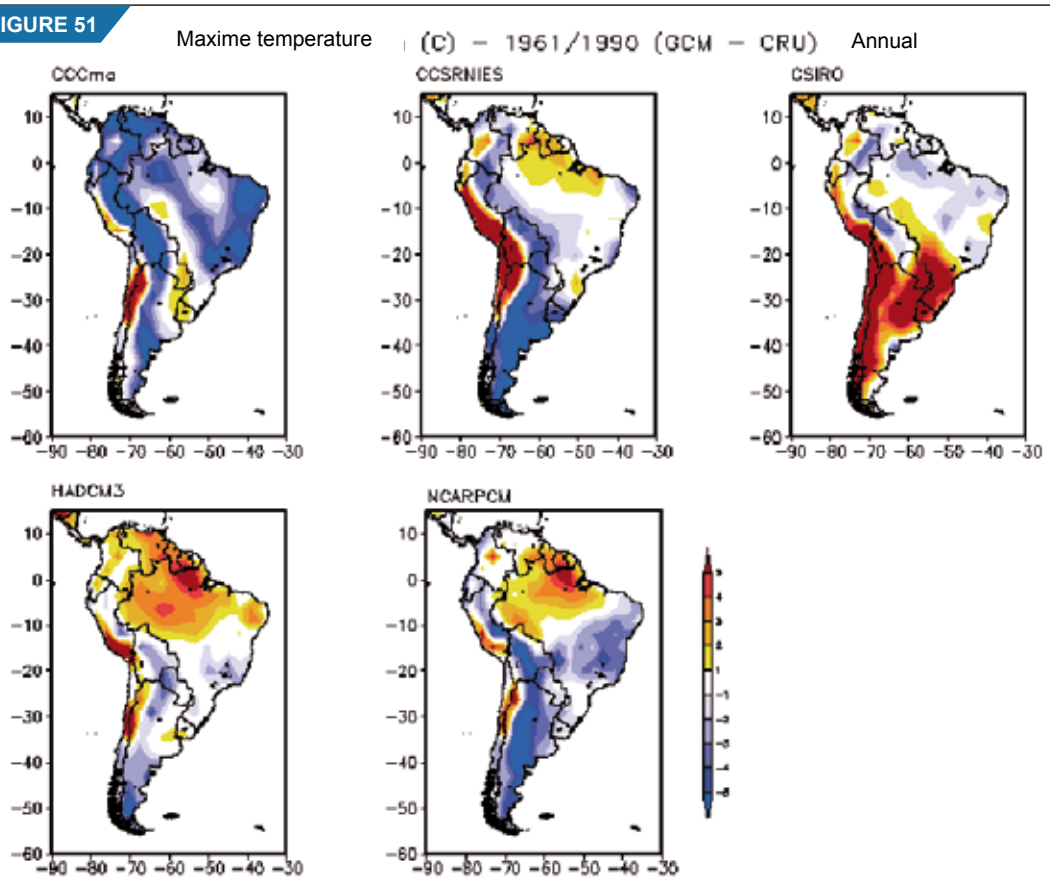

Difference between maximum temperature simulated by the CCCma, CCSR/NIES, CSIRO, HADCM3 and the NCAR-PCM models, in relation to mean climatology observed by CRU for the period 1961-1990. The units are in ºC.

FIGURE 52

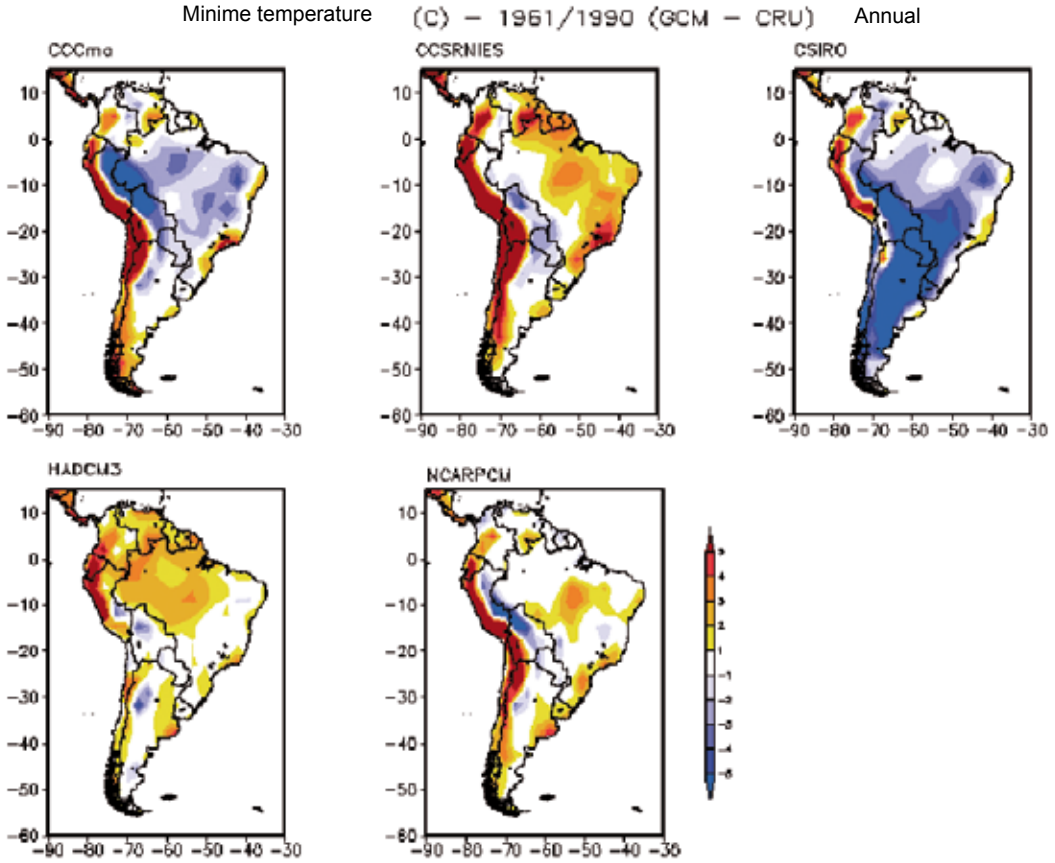

Difference between minimum temperature simulated by the CCCma, CCSR/NIES, CSIRO, HADCM3 and the NCAR-PCM models, in relation to mean climatology observed by CRU for the period 1961-1990. The units are in ºC.

FIGURE 53

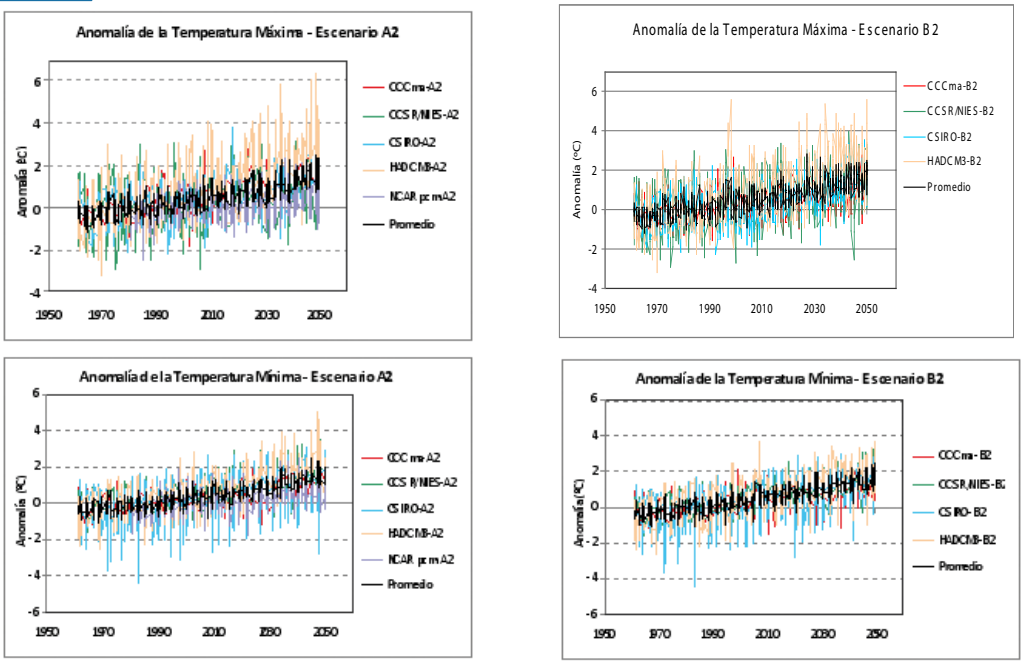

Anomalías de las temperaturas máxima (arriba) y mínima (abajo) en ºC, para los puntos de grilla sobre Perú en los escenarios extremos de emisión A2 y B2, para el año 2050.

FIGURE 54

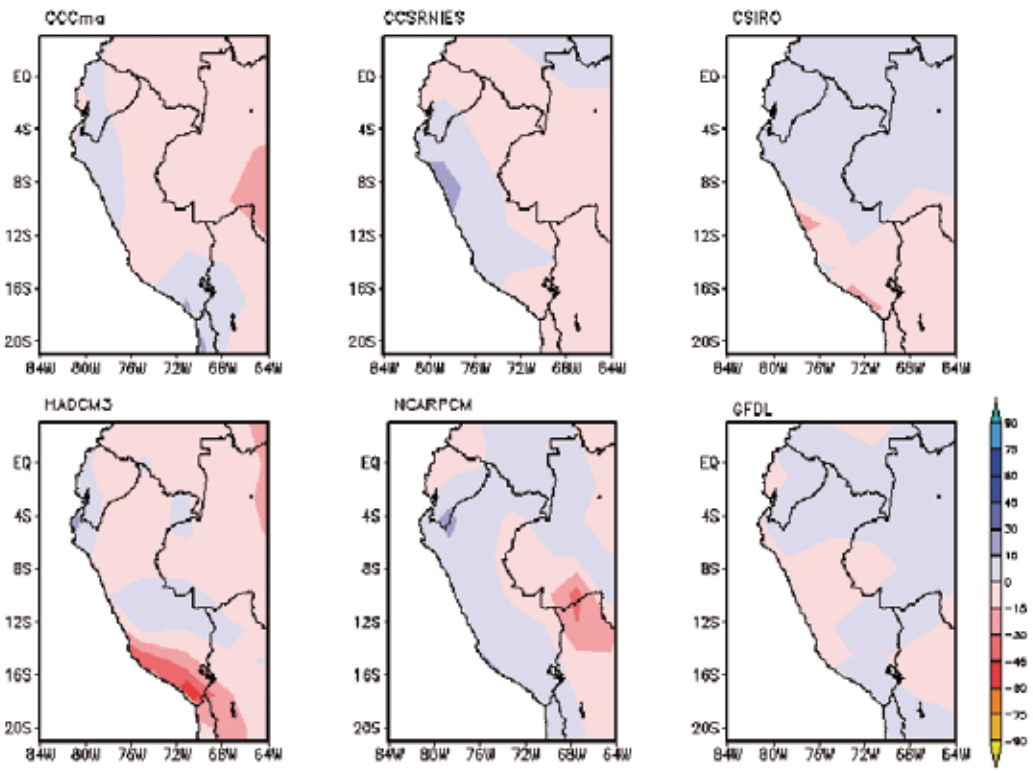

Variation in percentage (%) of annual precipitation simulated by the CCCma, CCSR/NIES, CSIRO, HADCM3 and NCAR-PCM models, for the 2030 decade in relation to the climatology 1961-1990

Although, it is truth that GCMs allow us to make projections on how the climate will be in the future, it is also truth that due to their low resolutions (normally between 300 and 500 Km) they do not allow us to know climate changes in areas like in the coast, high mountain regions, basins; in such case dynamical regionalization or dynamical downscaling is an alternative that it is used to simulate in a small-scale grid, the effects on the coastline, water and surface coverage in a local climate.

4.2 DYNAMICAL DOWNSCALING

Dynamical downscaling is an approach in which a regional pattern takes values from a thick-grid matrix model (boundary conditions and initial data from a GCM), and it solves the equations of the atmosphere and the ocean, related to the GCMs; but, on a fine grid, i.e., of a better resolution than the matrix grid. Besides, a regional model uses other surface variables such as topography, type of soil, etc.

En the present study, the dynamical downscaling was made using the regional RAMS model, which was forced from the NCAR global model, because it showed a better performance in the simulation of heavy rainfall in the northern coast of Peru, associated to the warm phase of the ENSO, a climate event that modulates the interannual variability in our country.

4.2.1 Preliminary data

The RAMS regional model was initialized using the NCAR-PCM T42 global model from the National Center for Atmospheric Research – NCAR of the United States of America (SENAMHI, 2005).

The data used for this study are files in a binary format corresponding to the Emission Scenarios A2 (Nakicenovic and Swart, 2000), with a six-hour frequency, previously processed for the PROCLIM project with the RAMS model, for Peru domain at a horizontal resolution of 60 Km (SENAMHI, 2005), divided in two periods: historical from 1983 to 2003, and a projection from 2004 to 2035.

4.2.2 Regional Simulation

In the present study, three domains were established for the simulation:

a) Peru domain: designed for the PROCLIM study (SENAMHI, 2005) with a resolution of 60 km, Figure 55.

b) Basin domain: carried out for two basins: Mayo and Santa, Figure NN, with a resolution of 20 km, the input data was the scenarios for Peru and a resolution of 60 km.

The characteristics of the simulation were:

- It was a nested unidirectional regional simulation, through which the information from the RAMS regional model does not return into the global model and this way small-scale regional information is added to the large-scale climate signal.

- The simulation period extended from 1983 to 2035 and the time step used by the RAMS model to integrate the equations of the atmosphere was 50 seconds.

- The sea surface temperature data (SST) were initialized every 10 days from the standard climate values of the RAMS model, that come from a monthly database at a global level.

- The soil humidity was initialized using a similar scheme, i.e., using the atmosphere initial condition of the large-scale model, (temperature and humidity) to initialize the soil humidity profiles.

- The nested domains 20 x 20 (over the Santa and Mayo basins), were re-initialized every 10 days in the internal grids, taking as an atmospheric and soil frontier the 60 Km domain of Peru (SENAMHI, 2005). This re-initialization would affect the first 1-2 days for each 10 days of simulation; so, the data were removed from the results.

- In this simulation sea surface temperature (SST) of the regional model was invariable, with appropriate values for the last half of the XX century (SENAMHI(, 2005).

FIGURE 55

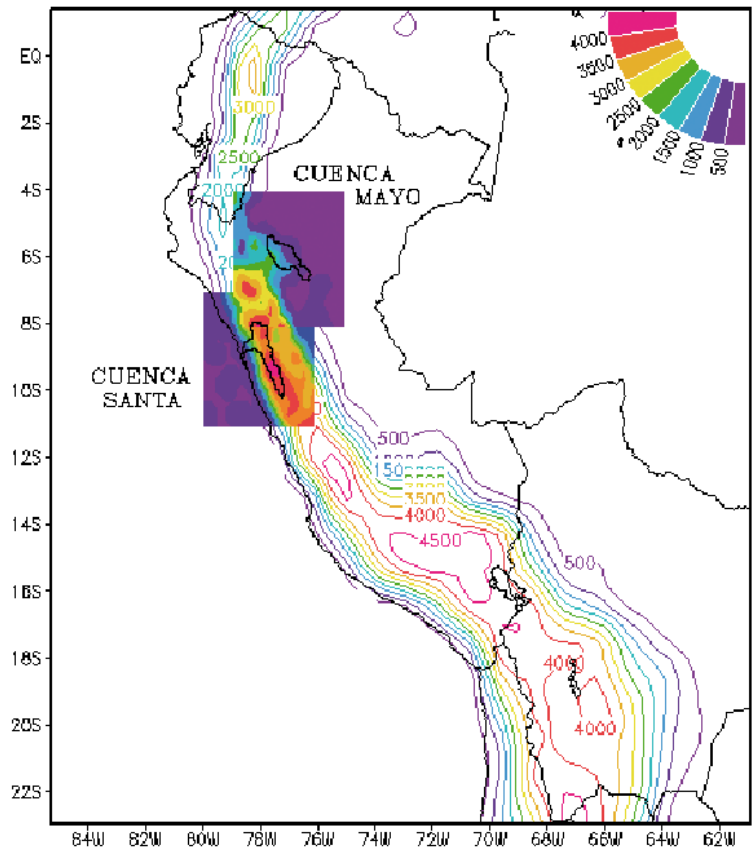

Representation of the simulation domains in the topography variable (meters)
Area of Peru at 60 Km and areas of the Santa and Mayo basins at 20 Km.

4.3 ANALYZED VARIABLES

Two variables were obtained: extreme temperatures (maximum, minimum) and accumulated precipitation, for the Peru domain y for the Santa and Mayo basins *. These variables after being averaged at daily basis and then at a monthly basis, they were interpolated at the station point, by means of the inverse distance interpolation method , then the bias of the model was eliminated (incorporation of seasonal climate variability) with the following relations:

MAP= CLIMOBS + VARSCENR – VARCLIM) For temperature and precipitation (Hulme et al., 2000)
MAP = CLIMOBS * (VARSCENR /VARCLIM) For precipitation in the costal region (Lenderkin, 2007)

Where:

MAP = Value of the model including climate variability

CLIMOBS = Monthly observed climatology during the period 1970-2000

VARSCENR = Monthly value of the scenario coming from the model

VARCLIM = Monthly climatology of the model during the period 1983-2003.

* The results of the studies are published separately from the present study.

The maps of the climate scenarios are shown per decades starting at the middle, (Hulme and Lu, 2000), and they correspond to the years 2015-2025 and 2025-2035 for the year 2020 and 2030, respectively. Also they are grouped in seasonal distributions throughout the year, annual averages and accumulated values, depending on the variables.

Also maps showing the anomalies to 2030, for extreme temperatures and in the case of precipitation, this is presented as percentage with respect to its climatological normal. Additionally, the 90 percentile is obtained for temperature and the 95 percentile, for precipitation to 2030, with respect to the observed climatology for each one of the meteorological stations, indicating changes with respect only to the intensity. (Hyndman, 1996).

Finally, all the maps were finished using the geographic information systems, and for the maps of extreme temperatures the interpolation was used, which related these variables with the altitude, while the precipitation maps were manually drafted and digitalized.

The descriptions were made annually and quarterly, using the regional climatological revision that is shown in Figure 56, carried out by SENAMHI, 2008 in which regions show similar hydrometeorological conditions. Figure 56 show the division per each geographical region, showing for the coastal region three zones denominated: north, central and southern, while in the mountain region there are 7 zones: north-western mountain, north-eastern mountain, central-western mountain, central-eastern mountain, south-western mountain, south-eastern mountain and the high plateau. In the jungle there are 4 zones: northern jungle, high central jungle, low central jungle and southern jungle.

4.4 SCENARIOS PROJECTED TO 2020 AND 2030

4.4.1 Maximum Temperature

On the subject about thermal evolution, one often resorts to mean temperature and its behavior in order to evaluate change trends. However, mean temperature by itself does not reflect other change trends, that may be hidden in other thermal parameters that do point out better those changes. (Miro et al., 2004).

Detailed projections on climate change over the South American Cordillera (Mountain Range) are seriously hindered by its own topography. Regional climate models that involve ocean-atmosphere coupled models and that are connected to hydrological and glacial models and even to ecological models are necessary to provide the adequate instruments to decision makers in order to make effective climate policy (Rauscher et al., 2008; Karmalkar et al., 2008; Urrutia and Vuille 2008, and others) quoted in: A Framework for a proposed IAI initiative ACCORD/CIMA initiative Members.

The increase in maximum temperature is expected to occur in the high mountains of Ecuador, Peru, Bolivia and northern part of Chile (Bradley et al., 2006). This change in temperature in the mountain regions of the intertropical zone; due to its population density, agriculture practices in the area and the existing glacial retreat; deserves an special attention of its potential climate change (Bradley et al., 2004). It is important to indicate that in the Southern Hemisphere the projected increase in temperature are >2.5 ºC for the mountain zone ~ 10 ºS (in Peru) passing across Bolivia up to ~ 40 ºS (in Chile/Argentina).

Thus, other analysis determine that variations in positive values of temperature toward the end of the century in the Pacific and South Atlantic will be 1,0 ºC and 2,5 ºC in the Andean region and central part of South America (report presented by Alves, L et al, 2008).

FIGURE 56

Regional climate division (SENAMHI, 2008)

In relation to the thermal impact on the Amazon region, in the study made by Ambrizzi et al., (2007), there was used three regional numerically integrated models for South America, using initial data from the Hadley Center global climate model, concludes that within the period 2071-2100, there will be the highest warming rate in the Amazon region with an increase in temperature between 4 to 8 ºC in the A2 scenario (pessimist) and between 3 to 5 ºC in the B2 scenario (optimist).

For what have been previously describe, it can be observed that many works on the detection of the behavior of temperature over South America are been done; although this is important to the country, we really need to know at what ranges are the aforementioned values finally evident; for this reason the present study includes the elaboration of future climate scenarios for the period 2020 – 2030 for Peru (0 ºS – 18 ºS, 82 ºW – 68 ºW) based on the mean climate from 1983-2003 and also the extreme climate is analyzed: temperature 90 percentile for the year 2030, the results are the following:

4.4.1.1 Annual projection

According to studies, in Tables 2, 3 and 4 annual projections and changes in maximum temperature are shown for the period 2020 to 2030 by regions at national level (see Maps 01 – 10 in Appendix 3), the values of variations are expressed in terms of ºC, this has only been made for the 2030 decade, since the results for the 2020 decade are similar; see Maps 01, 06, 11 in Appendix 3.

a) Coast

Regarding maximum temperature the most significant projected changes to 2030 in this coastal region mainly occur in the northern coast, they range form 0,4 to 1,2 ºC; while in the southern coast changes are not significant (see Table 4).

Table 4:
Maximum Annual Temperature projected to 2020 and 2030, and the change projected to 2030 in relation the current climate in the coastal region

Regiones		Annual average to 2020 °C	Annual average to 2030 °C	Projected changes 2030 °C	Main locations
Northern Coast	Top North	28,0 - 34,0	28,0 - 34,0	0,8 - 1.2	El Salto, Rica Playa, La Esperanza, Chusis, Reque
	North	22,0 - 32,0	24,0 - 32,0	0,4 - 1,2	Trujillo, Laredo, Buena Vista
Central Coast		20,0 - 28,0	22,0 - 28,0	0,0 - 0,4	Paramonga, Huayán, Lima, Callao, Cañete
Southern Coast		18,0 - 28,0	20,0 - 28,0	0,0 - 0,4	Ica, Ocucaje, Copará, Caravelí, Punta Atico, Pampa Blanca, Punta Coles, Sama Grande, Calana

b) Mountain

Between 2020 and 2030 maximum temperatures will not show any significant variations, thus, the analysis for the projected changes to 2030 oscillate between 0,4 and 1,6 ºC, being the north-eastern mountain region the one with the highest value, up to 1,6 ºC (see Table 5). Regarding the high plateau warming, it will range from 0,4 to 0,8 ºC to 2030.

Table 5
Maximum annual temperature projected to 2020 and 2030 and the projected change to 2030 in relation to the current climate in the mountain region

Regions 2020 °C		Annual average to 2030 °C	Annual average to to 2030 °C	Projected changes	Main locations
Northern Mountain	Westerb	18,0 - 28,0	18,0 - 28,0	0,4 - 1,2	San Pablo, Llapa, Salpo, Cachicadan, Callancas, Contumazá.
	Eastern	16,0 - 26,0	16,0 - 26,0	0,4 - 1,6	Weberbauer, San Marcos, Cajabamba, Celendín.
Central Mountain	Westerb	10,0 - 22,0	12,0 - 22,0	0,0 - 0,4	Sihuas, Recuay,Oyon, Huarochiri, Cusicancha, Santiago de Chocorvos, Huancayo, Marcapomacocha.
	Eastern	12,0 - 24,0	12,0 - 24,0	0,4 - 1,2	Huánuco, Tarma, Acobamba.
Southern Mountain	Westerb	14,0 - 18,0	12,0 - 18,0	0,4 - 0,8	Puquio, Coracora,Orcopampa, Cotahuasi, Chuquibamba, Arequipa, El Fraile,Omate, Yacango, Candarave,Tarata.
	Eastern	16,0 - 24,0	16,0 - 24,0	0,4 - 1,2	Curahuasi, Granja Kayra,Chalhuanca, Cusco.
High Plateau		12,0 - 18,0	12,0 - 18,0	0,4 - 0,8	Cuyo Cuyo, Progreso, Muñani, Ayaviri, Arapa, Huancane, Capachica, Puno, Sacuce, Mazo Cruz.

c) Jungle

For this region between 2020 and 2030, maximum temperatures do not show any significant changes, the projected change to 2030 is 1,6 ºC mainly in the northern jungle and temperatures up to 34 ºC in the northern and southern jungle (see Table 6).

Table 6
Maximum annual temperature projected to 2020 and 2030, and the projected change to 2030 in relation to the current climate in the jungle

Regions		Annual average to 2020 °C	Annual average to 2030 °C	Projected changes to 2030 °C	Main locations
Northern Jungle		20,0 - 34,0	20,0 - 34,0	0,4 - 1,6	Santa María de Nanay, San Ramón.
Central Jungle	Low	28,0 - 32,0	28,0 - 32,0	0,4 - 0,8	Pucallpa.
	High	20,0 - 30,0	20,0 - 30,0	0,0 - 0,8	Oxapampa, Satipo, La Merced, Tingo María.
Southern Jungle		20,0 - 32,0	20,0 - 34,0	0,0 - 0,8	Puerto Maldonado, San Gabán, Tambopata.

According to the estimation for the annual projections to 2030, maximum air temperature will be warmer up to 1,6 ºC compared to the current climate in almost the whole territory. With some values in the coastal region between 20 to 32 ºC and up to 34 ºC in the top northern part of the coast; in the mountain region it will fluctuate between 12 to 28 ºC and in the jungle it will vary between 20 to 34 ºC. Spatial configuration between the periods 2020 and 2030 shows more amplitude in the latter.

4.4.1.2 Seasonal projections

Maximum temperatures to 2020-2030 and their anomalies projected to 2030 in the coast, mountain and jungle region are show in Maps 12 to 15, Appendix 3 and in Tables 5, 6 and 7 at seasonal level.

a) Coast

The spatial distribution and values of maximum temperature projected on a seasonal basis to 2020 and 2030 in the Peruvian coast, would show more intense variation in the winter time (JJA) and spring time (SON), with values from 1,2 – 2,0 ºC and 1,2 – 1,6 ºC respectively; specially in the northern coast (top north). Conversely, there are not any significant changes in the summer time (DJF). (See maps 12 – 15 Appendix 3 and table 7).

Table 7:
Maximum seasonal temperature projected to 2020 and 2030, and the change projected to 2030 in relation to the current climate in the coast (ºC)

Regions			Summer		Autumn		Winter		Spring	
			Average	△	Average	△	Average	△	Average	△
North Coast	Top North	2020 2030	28 - 34 28 - 32	-0,4 - 0,0	26 - 32 26 - 32	-0,8 - 0,0	24 - 30 26 - 32	1,2 - 2,0	26 - 34 28 - 34	1,2 - 1,6
	North	2020 2030	26 - 34 26 - 32	-0,4 - 0,4	26 - 32 26 - 30	-1,2 - 0,4	24 - 28 24 - 30	0,4 - 2,0	22 - 34 22 - 34	0,4 - 1,6
Central Coast		2020 2030	22 - 28 22 - 30	0,0 - 0,8	20 - 28 20 - 30	0,0 - 0,8	18 - 26 18 - 26	-0,4 - 0,4	22 - 30 20 - 28	-0,4 -0,0
Southern Coast		2020 2030	22 - 32 22 - 34	-0,4 - 0,8	20 - 30 20 - 32	0,0 - 0,8	20 - 26 20 - 26	0,0 - 0,4	22 - 28 22 - 28	0,0 - 0,8

b) Mountain

According to analysis in Table 8, the largest variations are shown for the autumn (MAM) and winter (JJA) seasons, up to 1,6 ºC, mainly in the south-eastern mountain region in autumn and in the north-eastern mountain region and central-eastern mountain region during winter.

In the High plateau, variation are not very significant, except for autumn with values that reach 1,2 ºC.

9 Jungle

In the jungle the most intense variations are observed during the spring (SON), mainly in the northern jungle, with values up to 2,4 ºC, which agree with the studies made by Ambrizzi et al., (2007). Similarly, in this area of the northern jungle for the other seasons, projected variations show values up to 1,6 ºC. For the southern jungle, the periods with larger variations are the winter and spring, similarly, with values up to 1,6 ºC. In the central jungle, variations are not very stressed, except for the central low jungle during the summer time (DJF) with values that reach 1,2 ºC, see Table 9.

Table 8. Maximum seasonal temperature projected to 2020 and 2030, and the projected change to 2030 in relation to the current climate in the mountain (°C)

Regions			Summer		Autumn		Winter		Spring	
			Average	△	Average	△	Average	△	Average	△
Northern Mountain	Western	2020 2030	16 - 32 16 - 32	0,4 - 0,8	16 - 30 18 - 30	-0,4 - 0,4	18 - 24 18 - 26	0,8 - 1,2	20 - 26 20 - 26	0,8 - 1,2
	Eastern	2020 2030	14 - 24 14 - 26	0,4 - 1,2	14 - 24 16 - 24	0,4 - 1,2	16 - 26 16 - 26	0,4 - 1,6	16 - 26 16 - 26	0,4 - 1,2
Central Mountain	Western	2020 2030	10 - 24 12 - 24	-0,4 - 0,8	10 - 22 10 - 22	0,4 - 1,2	10 - 20 10 - 20	0,4 - 0,8	10 - 20 10 - 20	0,0 - 0,8
	Eastern	2020 2030	12 - 24 10 - 24	0,4 - 1,2	14 - 20 14 - 22	0,0 - 0,8	12 - 20 12 - 22	0,8 - 1,6	14 - 22 14 - 22	0,0 - 1,2
Southern Mountain	Western	2020 2030	10 - 22 10 - 22	0,4 - 0,8	12 - 20 12 - 20	0,4 - 1,2	10 - 18 10 - 18	0,4 - 1,2	12 - 18 14 - 18	0,0 - 0,8
	Eastern	2020 2030	12 - 22 20 - 22	0,4 - 0,8	14 - 20 14 - 20	0,8 - 1,6	14 - 18 14 - 20	0,0 - 0,8	14 - 20 14 - 22	0,0 - 1,2
High Plateau		2020 2030	10 - 18 10 - 18	0,4 - 0,8	12 - 18 12 - 18	0,4 - 1,2	10 - 16 12 - 16	0,4 - 0,8	12 - 18 14 - 18	0,0 - 0,4

Table 9: Maximum seasonal temperature projected to 2020 and 2030, and the projected change to 2030 in relation to the current climate in the jungle (°C)

Regions			Summer		Autumn		Winter		Spring	
			Average	△	Average	△	Average	△	Average	△
Northern Jungle		2020 2030	26 - 34 26 - 36	0,8 - 1,6	24 - 32 24 - 34	0,4 - 1,6	24 - 32 24 - 32	-1,2 - 1,6	26 - 34 28 - 36	0,4 - 2,4
Central Jungle	High	2020 2030	24 - 30 24 - 32	0,4 - 0,8	24 - 30 24 - 30	-0,4 - 0,0	22 - 30 22 - 30	0,4 - 0,8	28 - 34 28 - 34	0,0 - 1,2
	Low	2020 2030	30 - 32 30 - 34	0,8 - 1,2	28 - 32 28 - 34	-0,8 - 0,0	28 - 32 28 - 32	0,0 - 0,4	30 - 34 30 - 36	1,2 - 2,0
Southern Jungle		2020 2030	28 - 32 30 - 34	0,0 - 0,8	22 - 32 22 - 32	-0,8 - 0,0	22 - 32 22 - 32	0,0 - 1,6	22 - 34 22 - 34	0,4 - 1,6

4.4.1.3 Projection to 2030 of the 90 percentile of maximum temperature

According to studies in map 16 of Appendix 3, the extreme climate index, variation of the 90 percentile of maximum temperature is shown, for the year 2030. This index is associated to very warm days and it means that for the projected period, very warm days are increasing specially in the southern area of the national territory (south-eastern and south-western mountain region and the high plateau).

4.4.2 Minimum Temperature

Studies of future climate changes at regional scale in South America have been focused on two parameters: temperature and precipitation; but not on minimum temperature.

In the present item, the projections, resulting form the dynamical downscaling CCSM (NCAR)-RAMS (SENAMHI) to 2020 and 2030, are analyzed for minimum temperature, as well as the changes projected to 2030 at annual and seasonal level.

4.4.2.1 Annual projection

The results show that minimum temperature of air near surface to 2030 will increase in the country, with respect to the current climate between 0,4 and 1,4 ºC, mainly in the coast and northern jungle (Piura, Chiclayo and east of Iquitos) central region (Cerro de Pasco, Huancayo, Huancavelica) and part of the south Andean region (Ayacucho, Abancay).

Also, to 2030 in the jungle region, it is projected that the area of minimum temperatures 22 to 24 ºC will cover more spatial amplitude. In the coast, the area for 20 to 22 ºC will show a reduction, with respect to 2020. In the high plateau temperatures will increase up to 0,82 ºC with respect to 2020.

a) Coast

To 2020 and 2030 changes in the distribution of minimum temperature are projected, for the central and northern coast region , to range from 0.8 to 1,6 ºC. While in the south, changes are not too significant (see maps 17, 22, 27 in Appendix 3 and Table 10).

Table 10
Minimum annual temperature projected to 2020 and 2030 , and the projected change to 2030 in relation to the current climate in the coast

Regions 2020 °C		Annual average to 2030 °C	Annual average to 2030 °C	Projected changes to	Main locations
Northern Coast	Top North	16,0 - 22,0	16,0 - 24,0	1,2 - 1.6	El Salto, Rica Playa, La Esperanza, Chusis, Reque.
	North	12,0 - 22,0	14,0 - 20,0	0,4 - 1,2	Trujillo, Laredo, Buena Vista.
Central Coast		10,0 - 20,0	12,0 - 18,0	0,4 - 0,8	Paramonga, Huayán, Lima, Callao, Cañete.
Southern Coast		10,0 - 18,0	10,0 - 18,0	0,0 - 0,4	Ica, Ocucaje, Copará, Caravelí, Punta Atico, Pampa Blanca, Punta Coles, Sama Grande, Calana.

b) Mountain region

Minimum temperatures to 2030 are projected to be slightly warmer in relation to 2020, mainly in the central western and southern region of the country, and in the high plateau (see maps, 17, 22 in Appendix 3, and Table 20). To 2030, the sustained increase of minimum temperatures will be up to 1,22 ºC in the western region and mainly in the central Andean region, with respect to the current climate (see map 27 in Appendix 3 and Table 11).

The projection of the increase of minimum and maximum temperature in the mountain region is consistent as it was described by Alves, L et al., (2008) where it is determined that positive variations in temperature towards the end of the century would be 2,5 ºC in the Andean region.

On the other hand, the increase projected for maximum and minimum temperatures, on average, would be consistent with the current trend and with what Vuille and Bradley investigated (2000) who based on the recollection of 268 station between 1º N and 23 ºS (tropical Andes) observed a significant increase of air temperature close to surface between 0.10 – 0,11 ºC/decade in the last sixty years, from 1939, the most important increase occurred at the middle of the 70's decade between 0,32 – 0,34 ºC/decade. Also Mark (2002) and Mark and Seltzer (2005 a), who based on 29 stations at low and high altitude, observed that in the central region of Peru (9º - 11 ºS) the increasing trend of mean temperature is at a ratio of 0,35 - 0,39 ºC/decade between 1951 and 1999.

Table 11
Minimum annual temperature projected to 2020 and 2030 and the projected change to 2030, in relation to the current climate in the mountain region

Regions		Annual average to 2020 °C	Annual average to 2030 °C	Projected changes to 2030 °C	Main locations
Northern Mountain Region	Westernl	2,0 - 14,0	4,0 - 14,0	0,4 - 1,2	San Pablo, Llapa, Salpo, Cachicadan, Callancas, Contumazá.
	Eastern	4,0 - 16,0	6,0 - 16,0	0,4 - 0,8	Weberbauer, San Marcos, Cajabamba, Celendín.
Central Mountain Region	Westernl	-2,0 - 12,0	-2,0 - 12,0	0,4 - 1,2	Sihuas, Recuay, Oyón, Huarochiri, Cusicancha, Santiago de Chocorvos.
	Eastern	0,0 - 14,0	2,0 - 12,0	0,4 - 1,2	Huánuco, Tarma, Acobamba.
Southern Mountain Region	Westernl	-10,0 - 10,0	-6,0 - 10,0	0,4 - 0,8	Puquio, Coracora,Orcopampa, Cotahuasi, Chuquibamba, Arequipa, El Fraile, Omate, Yacango, Candarave, Tarata.
	Eastern	-8,0 - 12,0	-12,0 - 12,0	0,4 - 1,2	Curahuasi, Granja Kayra,Chalhuanca, Cusco.
High Plateau		14,0 - 4,0	14,0 - 6,0	0,4 - 0,8	Cuyo Cuyo, Progreso, Muñani, Ayaviri, Arapa, Huancané, Capachica, Puno, Sacuce, Mazo Cruz.

c) Jungle

Minimum temperatures to 2020 and 2030 will not show any significant increase, but they project an spatial amplitude much wider of temperature values from 20 to 22 ºC to 2020 and 22 to 24 ºC to 2030, mainly in the northern jungle (see maps 17, 22 Appendix 3 and Table 10).

The most important changes with respect to current climate are observed in the northern jungle, with anomalies of up to 1,6 (see map 27 Appendix 3 and Table 12).

Table 12
Minimum annual temperature projected to 2020 and 2030 and projected change to 2030 in relation to current climate in the Jungle

Regions		Annual average to 2020 °C	Annual average to 2030 °C	Projected changes to 2030 °C	Main locations
Selva Norte		18,0 - 24,0	20,0 - 24,0	0,4 - 1,6	Santa María de Nanay, San Ramón.
Central Jungle	Low	18,0 - 22,0	18,0 - 22,0	0,4 - 0,8	Pucallpa.
	High	16,0 - 22,0	18,0 - 24,0	0,0 - 0,8	Oxapampa, Satipo, La Merced, Tingo María.
Southern Jungle		18,0 - 20,0	18,0 - 22,0	0,0 - 0,8	Puerto Maldonado, San Gabán, Tambopata.

4.4.2.2 Seasonal Projection

In the autumn and winter seasons, to 2030 the most important changes in minimum temperature are projected, with increases reaching up to 2 ºC, with respect to current climate, mainly in Chiclayo, Chimbote and north-west of Iquitos. While in the spring, temperature would reach up to 1,2 ºC (Piura, Chiclayo and north-west of San Martin and east of Iquitos) and in the summer up to 1,6 ºC (top northern part of the coast, north-east of Moyobamba, central mountain region, Cusco and north-east of Abancay and south of Ayacucho).

a) Coast

To the year 2030, the most important changes in minimum temperature, will be observed in the northern coast in autumn and winter, up to 2 ºC above the current climate. While in spring in the central and southern coast, the increase would be around 0,4 ºC. In the summer, the changes in minimum temperature will range between values of - 0,8 and 0.8 ºC, in relation to the current climate (see maps 18-21, 23-25 and 28-31 in Appendix 3 and Table 13).

Table 13
Minimum seasonal temperature projected to 2020 and 2030 and the projected change to 2030 in relation to current climate in the coast (ºC)

Regions			Summer		Autumn		Winter		Spring	
			Average	△(°C)	Average	△(°C)	Average	△(°C)	Average	△(°C)
North Coast	Top North	2020 2030	16 - 24 16 - 24	0,8 - 1,6	16 - 24 20 - 24	1,2 - 2,0	14 - 22 16 - 22	0,8 - 2,0	16 - 22 16 - 22	0,4 - 1,6
	North	2020 2030	16 - 22 16 - 22	-0,4 - 1,2	12 - 22 12 - 20	0,8 - 1,6	12 - 20 12 - 18	1,2 - 1,6	12 - 22 08 - 18	0,4 - 1,2
Central Coast		2020 2030	16 - 20 16 - 22	0,0 - 0,8	12 - 20 12 - 18	0,4 - 1,2	10 - 20 08 - 18	0,8 - 2,0	12 - 20 10 - 18	0,0 -0,4
Southern Coast		2020 2030	10 - 18 10 - 18	-0,8 - 0,8	10 - 20 08 - 18	0,0 - 1,2	08 - 16 08 - 16	0,4 - 1,2	10 - 18 08 - 18	0,0 - 0,4

b) Mountain region

In most part of the Andean region, in autumn, minimum temperature will increase up to 2 ºC in relation to current values on seasonal basis. Except for the high plateau, the north-western and south-western mountain region where it will reach up to 1,6 ºC. While in spring, the increases will be lower between 0,4 ºC and 1,2 ºC in the high plateau, central-eastern and south-western mountain regions.

In the summer, increases of up to 1,6 ºC would be observed, in the central and southern mountain region, that would be associated with skies showing more cloudiness, but not necessarily rainfall in these regions. In the winter, (dry season in the Andean region), temperatures would increase and would be probably attributed to skies showing more cloudiness; this increase could be reflected in the diminish of meteorological frosts, in the zones higher than 4000 MASL, regions that have a strong daily thermal oscillation (see maps, 18-21, 23-25 and 28-31 in Appendix 3 and Table 14).

Table 14
Minimum seasonal temperature projected to 2020 and 2030, and the projected change to 2030 in relation to the current climate in the mountain region (ºC)

Regions			Summer		Autumn		Winter		Spring	
			Average	△(°C)	Average	△(°C)	Average	△(°C)	Average	△(°C)
Northern Mountain Region	Western	2020 2030	6 - 20 6 - 20	0,4 - 1,2	6 - 20 6 - 20	1,2 - 1,6	2 - 16 2 - 16	0,4 - 1,2	2 - 16 8 - 18	0,4 - 1,2
	Eastern	2020 2030	2 - 18 2 - 16	0,4 - 0,8	2 - 24 2 - 24	1,2 - 2,0	0 - 22 0 - 24	0,4 - 1,6	0 - 22 2 - 24	0,0 - 1,2
Central Mountain Region	Western	2020 2030	0 - 10 0 - 12	-0,4 - 1,6	2 - 12 2 - 12	1,2 - 2,0	-4 - 12 -4 - 12	0,4 - 1,6	-4 - 12 -2 - 12	0,0 - 1,2
	Eastern	2020 2030	0 - 12 2 - 12	0,0 - 1,6	2 - 12 2 - 12	0,8 - 2,0	2 - 12 -2 - 12	0 - 0,8	0 - 12 2 - 12	0,0 - 0,8
Southern Mountain Region	Western	2020 2030	-4 - 12 -4 - 12	0,4 - 1,6	6 - 12 6 - 12	0,4 - 1,6	-12 - 12 -14 - 8	0,4 - 1,2	-10 - 12 -8 - 10	0,0 - 0,8
	Eastern	2020 2030	-2 - 12 -2 - 12	0,4 - 1,6	2 - 12 4 - 12	0,8 - 2,0	-10 - 10 -8 - 10	0,4 - 1,2	-4 - 12 -4 - 12	0,4 - 1,2
Altiplano		2020 2030	-12 - 8 -12 - 8	0,4 - 0,8	-14 - 4 -14 - 4	1,2 - 1,6	-14 - 0 -14 - 6	0,4 - 1,2	-14 - 2 -14 - 8	0,0 - 0,4

c) Jungle

At seasonal level, minimum temperatures would increase in autumn and winter to 2030, mainly in the northern jungle of the country, up to 2,0 ºC in relation to current values. In the remaining part of the region, the increases would increase between 0,4 and 1,6 ºC. These increases in temperature could be associated to skies with more cloudiness and not necessarily rainfall in the jungle. (see maps 18-21, 23-25 and 28-31 in Appendix 3, Table 15.

Table 15:
Minimum season temperature projected to 2020 and 2030 and projected change to 2030 in relation to the current climate in the jungle (ºC)

Regions			Summer		Autumn		Winter		Spring	
			Average	△(°C)	Average	△(°C)	Average	△(°C)	Average	△(°C)
Northern Jungle		2020 2030	16 - 24 16 - 24	0,4 - 1,6	20 - 24 16 - 24	0,8 - 2,0	14 - 24 16 - 24	0,0 - 2,0	20 - 24 20 - 26	0,4 - 1,6
Central Jungle	High	2020 2030	16 - 20 16 - 22	0,4 - 0,8	16 - 22 16 - 22	0,4 - 1,6	14 - 22 10 - 18	0,4 - 1,2	16 - 22 16 - 22	0,0 - 0,8
	Low	2020 2030	18 - 20 16 - 22	0,0 - 0,8	16 - 24 18 - 22	0,4 - 1,2	14 - 22 14 - 22	0,8 - 1,6	18 - 22 18 - 22	0,4 - 0,8
Southenr Jungle		2020 2030	16 - 22 16 - 22	0,0 - 0,4	16 - 22 16 - 22	0,4 - 0,8	14 - 20 10 - 18	0,4 - 0,8	16 - 22 14 - 22	0,4 - 1,2

4.4.2.3 Projection to 2030 of the 90 percentile for minimum temperature

According to examinations, map 32 Appendix 34, shows the extreme climate index, variation of percentile 90 for minimum temperature for 2030, this index projects the variation of warm nights with minimum temperatures higher than percentile 90% and means that by 2030, warmer nights would show a

regionalized behavior in the country. This, in most part of the coast warm nights would tend to decrease and in the Andean region would sustainably increase, being this region consistent with the projections of positive changes in minimum temperature and confirmed with the current increasing trend of warm nights.

4.4.3 Precipitation

At present, rainfall shows a very complex behavior, mostly associated to topography. Future scenarios also show a distribution depending not only on topography, for which reason it is very difficult to summarize in one line, the distribution of rainfall at national level; but also on the fact that it shows increases and shortages in all the regions.

4.4.3.1 Annual projection

For both decades, it has been estimated that precipitations would have a behavior very similar to their climatology, both in their distribution and in their intensity. This, it has only been estimated the anomalies or variations in percentages for the year 2030, with respect to their climatological average.

The scenarios projected to 2030 show values between +10% and -10% over the mountain and jungle regions of the country, these are similar to the ones obtained by Marengo, 2007 about South America with global models, whose average of the 6 global models for the period 2010-2040 show anomalies for Peru of +-0,2 mm/day, representing approximately up to 15% of shortages or increases. In the analysis made in the previous chapter about global models, it is also observed some similar values, but there is not a common configuration about the distribution of rainfall in the mountain and jungle regions of Peru, except for the northern coast, where all the models are present and also the increases in precipitations; similar perspective show the regionalized scenarios with the RAMS model.

These scenarios register increases occurring in the eastern part of the jungle, and decreases mostly in the mountain region, which would be probably associated to a less transportation of humidity that only impacts on this area.

a) Coast

The coast would continue to be mostly a dessert with rainfall values that in both decades do not exceed 10mm/year between Ancash and Moquegua, 50 mm/year in Tacna and between 10 and 100 mm/year in La Libertad, Lambayeque and Piura. While in Tumbes it would have rainfall over 200 mm/year.

Variations in percentage of precipitations to 2030, in this region, show that there would be shortages from about 10% to 30% between La Libertad and Tacna. These shortages are not too large in number, since precipitations in the Peruvian coast are normally very low. It is estimated and increase of up to 20% above average in the Departments of Tumbes and Piura.

The description and variation to 2030, per zones in the coast, are shown in Table 16.

Table 16: Annual accumulated precipitation projected to 2030, and variation in percentage to 2030 in relation to the current climate in the coastal region

Regions	PP accumulated annually to 2030 (mm/year)	Projected changes to 2030 (Variation in percentage %)	Main locations
Northern Coast	5 - 200	Between +10 and +20 % - 10%	Most part of the northern part of Piura and La Libertad
Central Coast	5 - 50	Up to -30%	All the region
Southern Coast	5 - 50	Up to -20%	Ica and Arequipa

b) Mountain region

Also, in maps 33 and 38 it can be observed that precipitation will continue with the same behavior as it climate averages, i.e., more rainfall in the zones located in the eastern slope than in the western slope. In most part of the western slope, rainfall will amount between 50 to 200 mm/year, except for the high zones in Piura and Lambayeque, where rainfall would amount 1 000 mm/year. In the eastern slope rainfall would amount between 200 and 1000 mm/year.

Variation in the percentage of precipitations for the year 2030 does not show a similar trend; in general, there will be some shortages as well as some increases. Increases of 10% above normal values are projected in the north-western mountain region, southern part of the central-western mountain region (Lima, Ica and Huancavelica); southern part of the central-eastern mountain region (Junin) and southern part of the south-western mountain region (Arequipa, Moquegua and Tacna). Shortages of up to 10% would be in he north-eastern mountain region (Cajamarca), the largest shortages between 10% and 20% in the south-eastern zone (Ayacucho, Apurimac) northern part of central-eastern mountain region (Huanuco and Pasco).

The description and variation to 2030 per zones in the mountain region are shown in table 17.

c) Jungle

The total rainfall per year representing the years 2020 and 2030, is shown in the maps 33 and 38 respectively. These maps indicate that the nucleus of maximum rainfall would continue in this region.

Precipitations will amount 1 000 to 5 500 mm/year. Maximum annual quantities would be located in the southern jungle with 5 500 mm/year (jungle area in Puno and San Gabán), 4 000 mm/year over the boundaries of the Departments of San Martin and Loreto (Pongo de Caynarachi) and 3 500 mm/year over the north-eastern part of Iquitos 3 000 mm/year over the jungle of Huánuco and Ucayali and other nucleus of similar value in the southern zone of Ucayali. This last nucleus would show values above their climatological average.

With regard to the variation in percentages for the year 2030, map Nº 43, it is projected and increase up to10% in the southern jungle, part of the central area of the jungle, provinces of Moyobamba and Rioja of the Department of San Martin and southeastern zone of Loreto, Increases that exceed 10% in the high jungle of Puerto Maldonado, in the boundaries with the Department of Cusco. Also, there will be some shortages up to 10% in most part of the Department of San Martin, Huánuco, western and northern part of Loreto and the provinces of Padre Abad and Coronel Portillo in the central jungle.

The description and variation to 2030 per zones in the jungle are shown in Table 18.

Table 17. Annual accumulated precipitation projected to 2030, and variation in percentage to the year 2030 in relation to the current climate in the mountain region

Regions		PP accumulated annually to 2030 (mm/year)	Projected changes to 2030 (Variation in percentage %)	Main locations
Northern Mountain Region	Western	200 - 1000	Between +10 and 10%	All the region
	Eastern	500 - 1000	Up to + 10% - 10%	Over the eastern zone Over the western zone
Central Mountain Region	Western	100 - 1000	Up to - 20% Up to +20%	Northern part (Ancash-Lima and Pasco Southern Part: Junin, Lima and Huancavelica.
	Eastern	500 - 1000	Up to - 20% Up to 20%	Huánuco, Pasco. Junín and Huancavelica.
Southern Mountain Region	Western	100 - 500	- 20% + 20%	Northern part: Ayacucho, Arequipa. Southern part: Moquegua and Tacna
	Eastern	500 - 1000	- 20%	Apurímac and part of Cusco.
High Plateau		500 - 1000	Up to -10% + 10%	Southwestern part of the Titicaca Lake Northern part of the Lake

Table 18. Annual accumulated precipitation projected to 2030, and variation in percentage to the year 2030 en relation to the current climate in the jungle region

Regions		PP accumulated annually to 2030 (mm/year)	Projected changes to 2030 (Variation in percentage %)	Main locations
Northern Jungle		1 000 a 4 000	- 10% + 10%	Western part Eastern part
Central Jungle	Low	2 000 a 3 000	+ 10%	Ucayali Region.
	High	2 000 a 3 000	- 10% + 10%	Northern part: Huánuco and provinces of Padre Abad and Coronel Portillo in Ucayali, Pasco and Junin
Southern Jungle		1 500 a 5 500	- 10% + 10% y + 20%	Most part of the southern jungle, Madre de Dios and Cusco

4.4.3.2. Seasonal projection

Precipitation for each one of the seasons will be shown for Peru to the 2020 and 2030 and only the variation in percentage for the year 2030, because it a lot of similarity in the total amounts for each one of the quarters and in the spatial distribution in both decades.

The summary tables for the coast, mountain and jungle regions with regard to precipitation at seasonal level are the ones under numbers 19, 20 and 21 respectively.

4.4.4 Summer: Quarter December – February

In this quarter precipitations totalize the largest amounts, due to the interaction of the diverse atmospheric systems that generate rainfall (such as the Intertropical Convergence Zone, the Bolivian High, trade winds associated to the transport of humidity, etc.). Precipitation in the summer is significant at national level.

Future scenarios to 2020 and 2030 are shown in maps 34 and 39, while variation in percentage to 2030 is shown is map 44.

Precipitations in 2020 and 2030 are projected to be very similar in both decades at national level. Also, with similar amounts to their climatological values; but they have determined that for the 2030 decade, shortages in most part of the country, that includes specially the mountain region, it is necessar a larger amount of humidity in order to get saturated and originate rainfall, as the SACZ would be more intense, impacting over the central and southern jungle in Peru, with a lot of rainfall. Similar results found Marengo 2007, with the HADCM3 model for the period 2010-2040.

a) Coast

Precipitations in the southern and central coast are normally scarce, only in the northern coast precipitations amount between 50 and 100 mm/quarter. Projections to 2020 and 2030 indicate similar values to its climatology, i.e., between 5 to 10mm for the central and southern coast, and between 50 to 200 mm/quarter in he northern coast, especially over Piura and Tumbes, which shows values over their averages. These results would be associated to an increase in the SST near the coast, that would be contributing to increase in the frequency and intensity of rainfall.

Variations in percentages show deficiencies between 10 to 20% in the central and southern coast, while in the northern coast, only part of the Department of Piura and Tumbes show increases up to 10%, while the provinces of Paita and Talara show shortages between 10 to 20%.

b) Mountain region

Total precipitation to 2020 and 2030 in this quarter are very similar, in general, they show amounts that vary according to the altitudinal layers, especially over the western slope, registering between 100 to 500 mm/quarter. It shows three nucleus of maximum rainfall, located over the provinces of Ayabaca (Piura), Yauli (Junin) and between Vilcashuaman, Sucre (Ayacucho) and Andahuaylas (Apurimac) with rainfall exceeding 500 mm/quarter.

The variation in percentage to 2030 shows shortages in this region, except for the Departments of Junin and Huancavelica and the province of Yauyos (Lima), locations that would show an increase between 10 to 20% as well as the province of Ayabaca in Piura. Shortages would be up to 20% over the southwestern slope and the Department of Ancash.

c) Jungle

In this quarter total rainfall vary between 200 and 2 300mm/quarter for both decades. Maximum nucleus of rainfall will continue to occur over this region, this way, a nucleus of up to 2 300 mm/quarter in the boundaries of Madre de Dios and Puno (province of Tambopata and provinces of Carabaya and Sandia). Another nucleus of 1 500 mm/quarter, will also occur en the northeaster part of

the Department of Loreto, in the province of Maynas and Caballococha. Also, nucleus of 1 000mm/quarter will be located over the province of Alto Amazonas in Loreto, in the province of Padre Abad and the province of Coronel Portillo in Ucayali.

In the jungle, variation in percentage, map 44, it can be observed that the region does not show a defined trend, it does show some increases that do not exceed 10%, especially in the central jungle and in the northern par of the province of Maynas in Loreto (northern jungle) and some shortages that do not exceed 10% in the remainder part of the region. These increases and shortages could be considered as part of the normal variability during the rainfall period, but these projections are averages that represent a decade, which is really significant, especially the shortages. In San Martin and especially in the provinces of Huallaga, Mariscal Cáceres, Bellavista and Picota shortages will be moderate, exceeding 10%.

4.4.5. Autumn: Quarter March – May

Scenarios for the autumn season are shown in maps 35 and 40 for the decades 2020and 2030, respectively. Map 45 shows the variation in percentage for this quarter.

Both decades show values similar to their climatology, i.e., that the most intense rainfall concentrate in the jungle region, and less amount of rainfall in the mountain region. Scenarios indicate an increase in precipitations in most part of the country, maybe because the Intertropical Covergence Zone will be located further south, which generates instability and advection of moist air. Also, there is an increase of rainfall in the northern coast, associated to the increase of SST.

a) **Coast**

Scenarios agree with the climatology, that is to say, less amount of rainfall in the central and southern zone, only the northern coast will show a large amount of rainfall. Total accumulated in this quarter will be between 5 to 200 mm/quarter.

b) Mountain

To the year 2020 and 2030, rainfall will occur very similar in amount and distribution in all this region, except for the northwester mountain region (province of Ayabaca). The 2030 decade will be rainier that the 2020 decade. In the 2030 decade projections show rainfall of 700 mm/quarter, while in the 2020 they will only reach 500 mm/quarter. In all the region, rainfall in all the region will range between 50 to 200 mm/quarter, with higher values over the eastern slope.

c) Jungle

During this quarter, in relation to the climatology, rainfall will continue to be important for this region. This same behavior is projected for the years 2020 and 2030 in which rainfall will amount between 500 and 1 000 mm/quarter. Also, the nucleus of maximum rainfall continue to occur, with lower values in the zones of the previous quarter; thus, over the southern front-forest jungle, that includes the jungle region in the department of Puno and the province of Tambopata in Madre de Dios; rainfall will show a nucleus of up to 1 300 mm/quarter, over the province of Alto Amazonas, in the boundaries with San Martin and the province of Maynas; northeast of Iquitos a nucleus of 1 000 mm/quarter will be located.

In this quarter to 2030, precipitations will show and increase of up to 10% in the whole region, except for the zone between the provinces of Alto Mayo and Loreto; as well as in the eastern provinces of San Martin, that will show some shortages of up to 10%.

Variations in percentage indicate that there will be a significant increase of up to 30% for the 2030 decade in the northern coast and less in the southern coast (Arequipa and Tacna). Shortages will occur in the central coast.

4.4.6. Winter: Quarter June – August

Future scenarios for both decades have represented the climatology of the country, with very little precipitation in the coast, small amounts in the mountain and significant rainfall in the jungle region; but less amount than in the summer. Rainfall in this context will be mainly associated to the entrance of fronts with interactions of the mean atmosphere instability (trough) that will be more frequent because of a increased warming in the Pacific ocean, which will affect the southern part of Peru, which leads to an increase in rainfall over this zone.

According to investigations, maps 36 and 41, show that precipitations accumulated quarterly for the decades of 2020 and 2030, respectively, while map 46 shows the variation in percentage with respect to the year 2030.

a) Coast

Rainfall in the decades 2020 and 2030 will show amounts of up to 5 mm/quarter in all the coast; the values are slightly lower than its normal behavior.

With this spatial distribution shortages, in general, will be between 10 to 40%, especially in the northern coast (provinces of Sechura and Paita) and central coast (from Trujillo down to Ica). These values corresponding to shortages are not intense, since their normal values for this period are very small amounts, for which reason a certain decrease in rainfall shows high shortage values.

b) Mountain region

The decades show (maps 41 and 46) that rainfall will be more uniform with lower values with respect to the previous quarters. The amounts will be oscillating between 5 to 50 mm/quarter, the lowest values will be registered along the western slope.

In general, the variations in percentage of precipitation to 2030 will show some deficiencies, especially in the northern mountain region, while in the central and southern region, the spatial distribution is alternated with localized increases. Shortages will be between 10 to 30%, showing the highest values in the western slope.

c) Jungle

Rainfall in both decades will show values between 100 to 700 mm/quarter, maximum rainfall will occur in the southern front-forest jungle, the northern jungle in the province of Maynas (Loreto) and over the northern part of the province of Lams (San Martin).

Over the central and southern jungle, rainfall will be more uniform, showing values between 100 to 200 mm/quarter, the highest values will be registered in the high forest.

The variations in the percentage of rainfall for this quarter show some shortages in most part of the northern jungle, while in the central and southern part shortages will occur in the lower jungle and the increases will occur in the high forest. Shortages and increases will be between -10% to +10%.

4.4.7 Spring: Quarter September – November

In this quarter starts the rainy period, with regard to climate; especially in the mountain and rainfall will increase both in frequency and intensity in the jungle. Similar spatial distribution is shown in the scenarios shown in maps 37 and 42, which represent accumulated rainfall for the spring quarter in the years 2020 ad 2030, respectively.

Anomalies or variations in percentages to 2030 are shown in map 47.

a) Coast

Rainfall in this quarter will be between 0 to 5 mm/quarter in most part of the coast, showing values below its average values, during the decades 2020 and 2030. The northern coast, especially Tumbes during 2030 will show higher values of rainfall that will reach up to 10 mm/quarter, which indicates a rainy decade in this zone in relation to the 2020 decade.

Variations in percentages to 2030 in the central and southern coast will show some shortages that will register -20% over Ica. In the northern coast, shortages will be located in the southern part of Piura and Chiclayo with values of -30%. Tumbes will show some increases up to 30% over its average values.

b) Mountain region

Rainfall for both decades are similar in all the region, showing less amount of precipitations in the western slope, while in the eastern slope rainfall will amount higher amounts associated to the entrance or direct exposure to moisture over the slopes (orographic rainfall).

Precipitations will amount between 5 to 300 mm/quarter. Higher values will occur in the northern and central eastern jungle.

Variations in percentage to 2030 in this region are not uniform, increases and shortages occur in an alternated way, which indicates an irregular distribution or rainfall and that it will be localized and associated to the orography of the region. The variations range between -20 to +30%.

c) Jungle

Rainfall in both decades 2020 and 2030 will increase with respect to the winter season. The maximum nucleus of precipitation will be located in the southern front-forest jungle with 1 200 mm/quarter (province of Tambopata), 1 000 mm/quarter in the northern jungle (province of Alto Amazonas and Lamas), 800 mm/quarter in the central jungle (provinces of Leoncio Prado and Padre Abad) as well as in Maynas, (Loreto). On average, rainfall projections are between 200 and 1 200 mm/quarter.

In the year 2020 in the high central forest, rainfall will amount 700 mm/quarter, which are lower values than the ones that will occur in the year 2030. It is assumed that in the 2020 decade in the central jungle, rainfall will be under its average.

Variation in percentage for the year 2030, in this region, are not uniform, they show some shortages up to 10% over the western part of the northern jungle, the high forest zone in Huanuco and the eastern zone of the southern jungle. Increases will be up to 10% mainly over the central jungle.

4.4.8 Projections to 2030, 90 percentile for precipitation

A main problem in estimating the impacts of climate change are the potential changes in climate variability, for this reason the extreme events (or extreme climate) that may be associated to this climate change, become a fundamental piece to be analyzed. Tebaldi et al., 2006, says the in the observed data, as well as in the future projections, confirm that the changes in the tails of the distributions of precipitations and temperatures do not occur in the same proportion that the change with the mean (or average) do, especially with respect to precipitation.

In this sense, to evaluate extreme climate in relation to precipitation at national level, it has been made the estimate of the 95 percentile (p95th) of the observed precipitation for the meteorological stations, it also was estimated the p95th for the 2030 decade and the change in the intensity with respect to the observed climatology was analyzed per each meteorological station.

The variation in the 95 percentile for the year 2030, indicates us that maximum precipitations at national level have a decreasing trend with respect the maximum observed (average from 1971-2000), this distribution will be associated to the decreasing trend of average precipitations for this decade, according to what it is observed in map 48.

Positive variations that mean an increase in the maximum values of these precipitations will occur in an isolated way, especially in the provinces of Chupaca and Concepción (Junin), Castrovirreyna (Huancavelica), Huarochiri and Yauyos (Lima), some locations in Puno as in Lampa, Azángaro, Huaraya Moho y Yunguyo (Puno), as well as in zones of the northern jungle. These results agree with the ones found by Tebaldi, et al, 2006; in which in the average scenario from all the different global scenarios, for the zone of South America, especially in Peru, it shows increases in the 95 percentile, by the end of the XXI century; but, it has to be considered that these results from the global models have un thick resolution compared to the regional models, for this reason they cannot represent local characteristics, specially complex topography as there is in Peru. Additionally, Marengo 2007, says that a consensus among the models, with statistical significance, is difficult to be shown over tropical South America.

Table 19: Seasonal accumulated precipitation to 2030 and the variation in percentage projected to 2030 in relation to current climate in the coast (°C)

Regions	Summer		Autumn		Winter		Spring	
	Annual Acc PP	△(%)	Annual Acc PP	△(%)	Annual Acc PP	△(%)	Annual Acc PP	△(%)
Northern Coast	5 - 100	Up to - 20% over La Libertad, Lambayeque and the provinces of Talara and Paita + 10% over the provinces of Piura y Sechura	5 - 200	+ 30% specially in Piura	0 - 5	Up to - 40%	5 - 10	Up to - 30% over the western part of Piura and Chiclayo + 20% over Tumbes
Central Coast	5 - 50	Between -20% and 30% specially in Áncash	5 - 50	Between - 10% a - 20%	0 - 5	Up to - 40%	0 - 5	- 10%
Southern Coast	5 - 50	Up to - 20%	5 - 10	+ 10% over the province of Ica and from Camaná to Tacna - 10% over Chincha, Nasca and Caravelí	0 - 5	Up to- 40%	5 - 10	Up to - 20% over Ica + 10% over Moquegua and Tacna

Tabla 20: Seasonal accumulated precipitation projected to 2030 and the variation in percentage projected to 2030 in relation to the current climate in the mountain region (ºC)

Regions		Summer		Autumn		Winter		Spring	
		Annual Acc PP	△(%)	Annual Acc PP	△(%)	Annual Acc PP	△(%)	Annual Acc PP	△(%)
Northern Mountain	Western	100 - 500	+ 10% in Piura - 10% the remainder part of the zone	200 - 700	Between +10 and +20%	5-10	- 20%	5 - 100	- 20% over Cajamarca + 20% over La Libertad and Piura
	Eastern	100 - 500	Up to - 10%	200 - 500	Between + 10 and +20%	10 - 100	- 10% most part of the zone. Western part of Amazonas (+ 10%)	100 - 300	Up to -20% over Cajamarca and Amazonas. + 10% over La Liberttad
Central Mountain	Western	100 - 500	Up to -20% in all zone except for the Province of Yauyos - Lima (between +10 a +20%)	50 - 200	Up to -20% in all the zone, except for zones north and northeast of Huaraz and province of Yauyos (+10%)	5 - 50	Up to -30% in Áncash and northern of Lima +20% over central and southern Lima and Huancavelica	5 - 100	Up to -10% in Áncash and northern of Lima. +20% over central and southern Lima and Huancavelica
	Eastern	200 - 500	Up to -20% in Huánuco, Pasco and provinces of Yauli and Junín. +20% in the rest of the zone (Huancavelica)	100 - 500	+10% over most part of the zone. Up to -10% over the southern part of the province of Satipo	50 - 100	Up to 20% over Huánuco, Huancavelica and northern of Ayacucho +10% over Pasco and Junín	50 - 300	Up to +30% over Junín, Huancavelica and Ayacucho. Up to -10% in Huánuco.
Southern Mountain	Western	100 - 200	Up to - 20%	50 - 200	Up to -20% over southern of Ayacucho and Arequipa. Up to +40%, specially in Moquegua.	5 - 10	Up to -40% between Arequipa and Tacna. Up to +30% over southern Ayacucho and provinces of Aplao and Chivay	5 - 50	Up to 20% over middle part and -10% over the high parts of Moquegua and Arequipa.
	Eastern	200 - 500	Up to -20% over Apurímac and part of western Cusco +10% over eastern Cusco.	100 - 500	Up to 20% over Apurímac and provinces of Anta and western part of La Convención. +20% over Paucartambo and Cusco.	10 - 50	Increases of up to 30%	50 - 300	Increases up to 20%
High Andean Plateau		200 - 700	- 10%	100 - 700	Up to + 20%	10 - 100	-10% in all the zone except for zone in boundaries with Cusco.	50 - 300	-10% in the all the zone, except for zone in boundaries with Cusco (+10%)

Table 21: Seasonal Accumulated precipitation projected to 2030 and the variation in percentage projected to 2030 in relation to the current climate in the jungle (ºC)

Regions		Summer		Autumn		Winter		Spring	
		Annual Acc PP	△(%)	Annual Acc PP	△(%)	Annual Acc PP	△(%)	Annual Acc PP	△(%)
Northern Jungle		200 - 1500	Between -10% and -20% most part of the zone Up to +10% northern zone and southern province of Maynas and Requena.	200-1000	Up to +10% mostly in all the zone -10% over provinces of Loreto and Alto Amazonas and eastern part ofl San Martín.	100 - 700	Up to -10% in all the zone, except for provinces of Ríoja and Moyobamba (+10%)	200-1000	Up to -10% western zone +10% over eastern zone.
Central Jungle	LOW	200-1000	+10% province of Atalaya and southern part of province of Coronel Portillo -10% northern of Pucallpa and Purús province	200 - 700	+ 10 %	100 - 200	- 10%	500	+ 10%
	HIGH	200-1000	-10% in all the zone except for Junín (+ 10%)	500 - 700	+ 10%	100 - 200	- 10%	500 - 800	+ 10% over Pasco and Junín except for Huánuco (-10%)
Southern Jungle		500-2300	-10% in Madre de Dios +10% in province of La Convención in Cusco	200-1300	+ 10%	100 - 700	+10% over province of Manú, Madre de Dios and La Convención -10% in Tambopata and Tiahuamanú.	200-1200	+10% over province of Manú and high jungle. -10% over boundary zone with Brasil.

CHAPTER 5

CONCLUSIONS AND RECOMENDATIONS

CONCLUSIONS AND RECOMMENDATIONS

The present study was developed within the framework of the Second National Communication to the United Nations Framework Convention on Climate Change to support national efforts to develop and improve national capacities, facilitating the process of integrating climate change concerns into national development plans and reduction of poverty at national level. In the present chapter, the main conclusions on climate change in Peru are stated, based on the results obtained from the analysis of climate information, establishment of indices and climate trends in the last forty years and the future projections to 2020 and 2030, having elaborated for this purpose, precipitation and temperature scenarios using the dynamical downscaling approach. To this end, it was necessary to analyze the outputs of six global circulation models and the regional RAMS model, within the context of the extreme emissions scenario A2 of the IPCC. These methodologies have been developed in different studies by the work team of the Numerical Prediction Center at SENAMHI, within the framework of national and regional projects with the Ministry of Environment.

The generation of national climate scenarios, as well as the permanent coordination with researchers and specialists of international centers with a well-known background on climate change studies, such as CPTEC from Brazil, MPI from Germany, the MRI from Japan, among others, have provided our Service a the basis for the development and generation of future projections of regional climate as a fundamental tool for the analysis of vulnerability posed by climate change.

5.1 CONCLUSIONS

The conclusions are the following:

5.1.1. ABOUT CURRENT CLIMATE TRENDS

- One of the main limitations to obtain information, with a higher quality and reliability on climate change and climate extremes that are occurring in the last decades in Peru, is the lack of observational data, the ones that represent the complex interactions of climate system that has different variations with different occurrence periods. This shortage occurs because of the low spatial density of the stations across most part of the regions in Peru (few stations and a bad spatial distribution) and with relatively short information (limited to obtain a strong linear trends, in which the oscillations of long periods, such as decadal, are minimized), besides there is the need to temporarily select the data to homogenized the variability and not to obtain partial results, in which the analysis are restricted between 1965 and 2006 (42 years).

- Total annual precipitation shows stressed increases (positive trend) over the northern coast, while in the northern jungle it shows some decreases (negative trend) from the 1960's decade until the end of the last century. The temporal analysis of the last 40 years indicated that mechanisms of large scale circulation modulate precipitation in periods, mainly decadal or longer for these regions. In the case of the interannual variability, the ENSO events are responsible for it, but its influence is minimal, restricted to the most intense events of the ENSO. On the other hand, the central and southern mountain region show a very similar interannual variability, but with opposite trends, where the ENSO events seem to be the main dymanical source modulating these regions.

- Linear trends of annual and seasonal maximum mean temperature show a predominance of positive values (increase) over the entire territory with values of +0,2 ºC /decade, on average, and in general, these are statistically significant in the high areas of the southern part of Peru. Also, it is observed that maximum temperatures are affected by intense ENSO events, generating positive anomalies of different intensity across the country, determining interannual variability. In addition, there is evidence of a possible modulation of these temperatures due to larger oscillations than just interannual variability.

- Annual and seasonal trends of average minimum temperatures are mostly positive, with values between 0,1 and 0,2 ºC/decade, except for several stations that are located in the northern part of the Titicaca Lake. Temporal variations show that either increase or decrease of this variable is gradual (monotonic) in the whole period of the present analysis and it is clearly shown that these temperatures are modulated by larger oscillations than the interannual one, with more intensity than the observed in the maximum temperatures. Also, the temporal distribution of minimum temperature shows that these temperatures affected by the stages of the ENSO phenomenon, which alters interannual variability, depending on its intensity and the location of the place where the temperature is observed. It is important to highlight that minimum mean temperatures increased, on average, in a slightly less proportion than maximum temperatures.

- On average, the observed trends of maximum and minimum temperature in Peru for the 41 years (1965-2006) that were analyzed, is 0,1 ºC/decade to 0,2 ºC/decade. These values are within the range estimated for the whole planet by the IPCC AR4, between 1981 and 2005, which is 0,18 ºC/decade. As it was previously indicated, the temperature trends show very particular regional values that, possibly besides the anthropogenic influence there might be some others in some stations, such as the heat islands, due to the urban development and the alteration of the soil properties due to disturbance in the environment, such as deforestation, etc.

- Among the characteristics of the extreme precipitation indices, it is worth mentioning the trend of the precipitation average intensity index (SDII) in the central mountain region is the most homogeneous one with respect to the one of the northern and southern mountain region. Also it is observed that this index is influenced by the local prevailing geographical characteristics, as it can be proved in the distribution west of the northern jungle (San Martin). Similarly, the maximum temperature index registered for on day (Rx1day) shows that in the northern and central mountain region, the patterns observed continued in the trends of total precipitation. On the other hand, the index that indicates the amount of accumulated precipitation in five days (RX5day), shows that through the years, the central mountain region is the one that will be less prone to the occurrence of floods and landslides. Conversely, the northern and southern mountain region, especially the high zones in Arequipa and the central western region in Puno, are the ones that have the potential to become prone to this kind of hydroclimatic events, mainly in the northern region, because it shows an increase in the number of extreme rainy days.

- The trend of the dry periods index (DD) does not have a direction with regional coherent characteristics, it shows local patterns, restricted to small regions, where some places spread across the Peruvian territory, show significant positive values. On the other hand, the trend of the rainy periods index show a predominance of positive values in all the country; besides it shows regions with coherent trends, such as the northern mountain region. This would indicate that there is an increase in the number of rainy days, although it is not statistically significant, with days recording daily accumulated precipitation becoming heavier day after day; but with mean intensity that is quite scattered across the territory, because in certain places it decreased and on others it increased; possibly due to the orographic effects of the region.

- The indices of temperature climate extrems show a diminish in the cold days and an increase in the warm days in most of the stations indicated in the present study, except for the northern jungle, where this characteristics is just the opposite. The most outstanding characteristic of the trend of

number of days with meteorological frosts (FD) and cold nights (TN10p) is the presence of negative values (diminish of days with frosts) in the high parts of Arequipa, compared to the adjacent zones of the Titicaca Lake. This pattern indicates that the higher regions are becoming warmer which is a problem because it will cause the acceleration of the peak snow cap melting process in the highlands. This will first cause an increase of water amount in the rivers and then a drastic diminish that would affect agriculture and water for human consumption in many regions of Peru; where the main source of water are snow caps. On the other hand, the pattern of warm night index (TN90p) shows an increase with significant values in the southern mountain region, but, without characteristics of bipolarity observed between the adjacent zones to the Titicaca Lake and the high zones of Arequipa. Apparently minimum temperature values are affected because of the thermal effect of the Lake, On this matter, it is necessary to deepen on this matter doing some regional studies, where interannual and long-term variability of the lake's temperature needs to be considered.

- The droughts, one of the most complex hydrometeorological phenomena that have a harmful effect on society, are analyzed form a practical point of view, due to the limitations of information. The most intense droughts that occurred in the period of the present study (1965-2006) took place during the positive phase of the ENSO phenomenon, altering the normal distribution of precipitations over several regions of Peru. But, it is necessary to emphasize that there are several drought events that are not related to the ENSO events, such as the cases of 1980 and 1990, or some other like the warm event of the ENSO 1977/98 that didn't cause any droughts. These characteristics lead to the necessity to carry out some more comprehensive studies, emphasizing local characteristics, determining, if possible, circulation effects at regional scale and/or synoptic scale with the variability of large scale circulation. It must be emphasized that during the period of study no trends have been observed, neither increase nor decrease, of drought events, only fluctuations in their mean values with very little persistency.

- In the jungle region it is observed a very peculiar characteristic found in the drought analysis, where the highest frequency of moderate, severe and extreme drought at the meteorological and agrometeorological scales is registered. This is probably due to low variability of the hydrological cycle, with relatively high maximum precipitations in the monthly distribution, recording less dry periods and / or months with low precipitation, that after the adjustment to normal distribution, minimum values are considered as extreme. In the southern mountain region, the highest frequency of droughts, in all three scales, is the moderate one, followed by the severe drought. Droughts at the annual scale (hydrological) in the three intensities do not show regional patterns, only local characteristics that are distributed in the northern mountain region and the top end of the southern mountain region. These places may show this behavior because they are areas with very little precipitation that have certain characteristics similar to arid regions.

- The physical causes of the droughts determined for the rainy period (September – March) by means of teleconnections (correlations) between circulation patterns at a large scale (ENSO, PDO and TSA-TNA) and the precipitation indices for Peru, show a seasonal variation in the intensity, and at least in one station during a year, the correlation pattern changes signs at least in some regions. This characteristic is clearly seen in the correlation patterns with anomalies in the El Niño 3,4, in which, the summer and autumn are inverse to the spring (beginning of the rainy period) in the southern mountain of Peru, in the northern mountain the same sign persists. The characteristics of spatial distribution of the interaction between these teleconnection patterns allow to identify three regions with special features, for the occurrence of droughts, the southern mountain , focused on the high zones or Arequipa and Puno, that extend up to the central mountain, the northern coast and northern mountain region that in some cases prolonged up to the northern jungle and central mountain, which is considered a region of transition that has the influence of the other two regions.

- A summary of the behavior of the ENSO in the spatial/temporal distribution of precipitation can be described in the following way: at the beginning of the rainy season the positive anomalies of the El

Niño 3.4 produce heavier precipitation than normal over most part of Peru, except for the transition zone (central mountain region), then it reverses in the other two seasons and it follows a shortage pattern of precipitation in the southern mountain, that extends up to the central mountain region, while in the northern coast and mountain region precipitations are heavier than normal.

- The results of the multi-varied analysis of the Principal Component of droughts over the Peruvian territory show two spatial/temporal patterns of drought occurrence with very defined characteristics. A patterns that involves the whole territory, centered in the southern mountain region (Arequipa and Puno) and it extends over the central mountain region (Huancavelica and Lima) characterized for showing intense and prominent annual cycles, besides, biennial sporadic cycles (2-3years) that are part of the oscillation spectrum of the high frequency oscillation of the ENSO phenomenon, that are modulated by very intense decadal variations. An example of this pattern is the drought registered in 1991/92. The second pattern is characterized for presenting very intense droughts concentrated in the southern mountain region (Puno) and they spread towards the central mountain and northern jungle, while in the rest of the territory the behavior is just the opposite, with plenty of rainfall, concentrated in the northern mountain region, that extend through the western slope of the Andes mountain until it reaches the central mountain region. This pattern also has prominent annual cycles, apparently as a complement of the first pattern, some biennial oscillations not very intense and mainly an oscillation of 3 to 7 years (low frequency oscillation spectrum of the ENSO) during all the period of study, with intense values in the decade of the 1980's. The droughts occurred in 1982/83 were modulated by this pattern, and also, this pattern was associated to the biennial oscillation of 1997/98 that formed a warm event of the ENSO, but did not originated typical droughts of these events.

- The difference between the types of droughts and the intensity in which they occurred in the Peruvian territory during the period of the present study (1965-2006) reveals that the most intense droughts occurred in the rainy period 1991/92. A set of unfavorable characteristics seems that acted all together during this period, besides the occurrence of the warm phase of the ENSO, modulated by the Pacific Decadal Oscillation. It was also conditioned by the temperatures pattern of the Tropical Atlantic, which is adverse for the occurrence of rainfall over Peru. Also, during the rainy period of 1982/83, the agrometeorological and hydrological drought patterns were the most intense and the ones that occurred less frequently. Finally, the ENSO event of 1997/98, associated to a very intense biennial oscillation, with a weak modulation of the 3- to- 7- year cycle caused weak droughts in most part of the territory, except for some scattered places in the northern mountain and jungle regions, where droughts were moderate or severe. In conclusion, it is possible to detect the performance mechanisms of the different large-scale circulation patterns that generate droughts in Peru, particularly the ones related to the warm events of the ENSO, which is the main phenomenon that generates these anomalies. These mechanisms associated to different circulation patterns do not act independently, they act in a very complex way, because de amplitude and oscillation period of each one of them is different and their non linear interaction causes that these precipitation patterns over Peru have a different response for each ENSO event.

- The results, despite the problems of lack of information, are satisfactory and will serve as basis for further assessment studies on the risk and climate vulnerability, useful for planning processes and adaptation to climate change. Also, it is necessary to have with planned hydrometeorological observation network exclusively to make a permanent climate monitoring, which can improve the knowledge about many uncertainties about climate variability in Peru, at the different scales, both spatial and temporal.

5.1.2 About the climate projections to 2030

- Annual projections to 2030 for maximum temperature is 1,6 ºC, with respect to its current climatology in almost all the territory.

- From the seasonal point of view, maximum temperature over the coastal region to 2020 and 2030 will show positive variations, more intense in the winter period (JJA) and spring (SON) with values that range from +1,2 to 2,0 ºC and from +1,2 to 1,6 ºC, respectively; specially in the top northern coast . The most important variations in the mountain region will occur in the autumn season (MAM) and winter (JJA) of up to +1,6 ºC, mainly in the southeastern mountain region in autumn and in the northeastern mountain region and central eastern mountain region during the winter. In the High Andean plateau variations are not very significant, except in the autumn with values of up to +1,2 ºC. In the jungle region more intense variations will occur during the spring season (SON), mainly over the northern jungle, with values of up to 2,4 ºC, in the other seasons variations will show values of up to +1,6 ºC. In the southern jungle the periods with higher variations will occur in the winter and spring, with values of up to +1,6 ºC. In the central jungle variations are no very stressed, except for the low central jungle during the summer (DJF) season with values of up to +1,2 ºC.

- Minimum air temperature close to surface to 2030 will increase in the country, with respect to the current climate between 0,4 and 1,4 ºC, mainly in the coast and northern jungle (Piura, Chiclayo and east of Iquitos), central region (Cerro de Pasco, Huancayo, Huancavelica and part of the south Andean sector (Ayacucho, Abancay).

- To 2030 it is projected that in the jungle region the area of minimum temperatures from 22 to 24 ºC will show more spatial amplitude. In the coast, the area of 20-22 ºC shows a reduction, with respect to 2020. In the High Andean plateau, temperatures will increase up to 1,2 ºC to 2020.

- At seasonal level the largest changes in minimum temperature to 2030 are projected to occur during autumn and winter, with some important increases up to 2 ºC, with respect to current climate, mainly in Chiclayo, Chimbote and northeast of Iquitos. While in the spring season, they will reach 1,2 ºC (Piura, Chiclayo, northeast of San Marting and east of Iquitos) and in the summer up to 1,6 ºC (top north in the coast, northeast of Moyobamba, central mountain region, Cusco and northeast of Abancay and southern part of Ayacucho).

- To 2020 and 2030 there is not evidence of great changes in the spatial distribution of rainfall and they are very related to their climatology. Annual precipitations to 2030 show some shortages specially in the mountain region between -10 and -20% and in the northern and central jungle (High jungle) up to -10%. The most important increases will occur in the northern coast and southern jungle between +10% and +20%.

- At seasonal level there will be some irregularities in the behavior of rainfall, shortages will be very significant in most part of the country in the summer season, while in autumn rainfall will occur above its normal values. In the winter and spring some increases and decreases are intercalated in the spatial distribution between -30% and +20% above their averages.

- There will also be an stressed trend to the increase in the number of warm days at national level, being the most intense ones in the southern mountain territory. With respect to warm nights, there is not a pattern, but a regionalized behavior, where in most part of the coast there will be a diminish while in the mountain region there is a trend to increase, been consistent with the projections of positive changes in minimum temperature to 2030 and with a current trend to increase in the number of warmer nights, especially in the southern mountain. In the case of maximum precipitation to 2030 it tends to decrease in most part of the country and only in a localized way they will increase with respect to current values.

5.2 RECOMMENDATIONS

It is evident the lack of climate information in some important zones of the country; so, it is necessary to compile as much information as possible from some private stations with records corresponding to long periods of time; then, verify their quality in order to complement the analysis developed in the present study and explain in the most feasible way, the decadal and multi-decadal characteristics that modulate long-term climate in Peru; as well as to promote, at a medium term, the implementation of more stations that would allow us to have enough climate series to cover most part of the country. This will help to have a clear and better knowledge of the effect of these oscillations on current climate and in future climate scenarios. Also, the information of this system will allow to evaluate and improve understanding of the physical processes of climate and to identify the feedback processes, and in the near future it will serve as basis to determine, through climate models, the ratio of long-term variability attributed to anthropogenic effects in several regions of Peru.

A variable that needs to be evaluated without exception, as the other climate variables, is the time series of river discharge. This hydrological variable provides very important information within the limits of a basin, because discharges represent an indirect measure of precipitation in all the basin and also of the different hydrometeorological processes that take place in it. In addition, the changes occurred in the historical series of discharges, through the years, are an important source of information that involves anthropogenic factors of climate change such as the changes in the use of land in global terms for the whole basin. So, the analysis of this variable needs to be part of every study related to climate change, since it allows to generate important information on the subject of energy security in the country.

It is necessary to keep in mind that the results, obtained from the trends analysis and the indicators, are representative of the stations that were used and that they cannot be interpolated for smaller scales and presented as maps with distributions, these are obtained with a larger amount of information. This is because the mesoscale geographical characteristics at regional level (hundreds of kilometers) that modulate every day local and/or regional weather and climate conditions, are not able to reveal the real conditions of the places where there is no information; although these interpolations consider the altitude and longitude; simply because they do not have the most adequate physical information that considers the effects of the valleys orientation, mesoscale circulation, physical properties of soil, among other.

It is important to take the necessary measures and actions to decrease vulnerability of the areas that show occurrence of droughts, such as changes in the technologies and governmental policies. This is really indispensable to face the climate changes observed in the last forty years and that in this context vulnerability may extend to certain socio-economic sectors. The drought analysis in the northern jungle, identified as such by the methodology that was used, should be carefully examined, since its impacts on the socioeconomic activities is not perceived as such, and it could be causing some alterations at another level such as on the Amazon ecosystems.

When considering the limitations of the available historical information, and knowing also that there are some inherent uncertainties associated with the model and the climate projections; the results of the present study must be considered as an approximation to future climate, stressing the trends identified in the absolute values, which indicate the possible trends that extreme temperature and precipitation will take in the next decades; and based on these trends, evaluate the vulnerabilities to climate change and take preventive measures in view of the evident intensification of climate extremes as they are projected in the present technical document.

BIBLIOGRAPHY

Alves, L. M., Pesquero, J. F., Marengo, J. A., Nobre, C. A. (2008): Future changes in climate over Brazil as simulated by 20km mesh MRI-JMA (Meteorological Research Institute and Japan Meteorological Agency) AGCM. Informe presentado al MRI.

Avalos, G., 2008: Cambio climático y seguridad energética en el Perú. En: Chiri A. F. y Luyo J. E., La Seguridad Energética, un reto para el Perú en el Siglo XXI. Eds. Colegio de Ingenieros del Perú, 256 – 281.

Bradley, R. S.; Keimig, F. T.; Diaz, H. F. (2004): Projected temperatura changes along the American cordillera and the planned GCOS network. Geophys. Res. Lett., 31, L16210, doi: 10.1029/2004GL020229.

Bradley, R. S.; Vuille, M.; Diaz, H. F.; Vergara, W. (2006): Threats to wáter supplies in the Tropical Andes. Science, 312, 5781, 1755-1756.

Frich, P., Alexander L. V., Della-Marta P., Gleason B., Haylock M., Tank AMGK and Peterson T. 2002: Observed coherent changes in climatic extremes during the second half of the twentieth century. Climate Research, 19, 193-212.

Garreaud, R. D., Aceituno, P., 2007: Atmospheric circulation over South America: Mean features and variability. Chapter 2 in The Physical Geography of South America. Eds. Oxford University Press.

Hewitson, B.C. and R.G. Crane, 1996: Climate downscaling: techniques and application. Climate Research, 7, 85-95.

HIRSCH, R.M.; SLACK, J.R.; SMITH, R.A. (1982). "Nonparametric tests for trend in water quality". Water Resources Research, 18: 107-121.

Hulme, M. and Lu, X., 2000: How to factor interannual climate variability into Climate Scenaríos. A note prepared for the DETR Fast-Track Impacts Group.

Hyndman, R.J., y Y. Fan, 1996. "Sample quantiles in statistical packages". The American Statistician, 50, 361-367.

IPCC, 2001: Tercer Informe de Evaluación. Climate Change 2001: The Scientific Basis. J. T. Houghton et al. Eds., Cambridge University Press, UK, 881 pp.

IPCC, 2007: Cuarto Informe de Evaluación. Climate Change 2007: The Physical Science Basis. Alley, R. et al. Eds., Cambridge University Press, UK.

Kendall, M.G., 1975: "Rank correlation methods", 4th Ed., Charles Griffin, London.

Kousky, V., Higgins, R., 2007: An Alert classification System for Monitoring and Assessing the ENSO Cycle. Weather and Forecasting. 22, 353 -371.

Lenderink G.; Buishand A. y Deursen W., 2007: Estimates of future discharges of the river Rhine using two scenarío methodologies: direct versus delta approach. Hydrol. Earth Syst. Sci., 11(3), 1145-1159.

Mann, H.B., 1945: Non-parametric test against trend. Econometrica, 13: 245-249.

Marengo, J., Obregón, G. y Valverde, M., 2007: Elaboración de escenarios climáticos para la Región Arequipa. "Medidas Piloto de Adaptación al Cambio climático en el Perú". GTZ.

Mark, B. G., 2007: Tracing Tropical Andean Glaciers, over space and time: some lessons and transdiciplinary implications, Global Planet Change.

McKee, T.B.; Doesken, N.J. e Kleist, J. 1993. The relationship of drought frequency and duration to times scale. In: Conference on Applied Climatology, 8, Boston. American Meteorological Society, Boston: PREPRINTS, 1993. p.179 – 184.

Mckee, T.B.; Doesken, N.J. e Kleist,J. 1995. Drought monitoring with multiple times scales. In: Conference on Applied Climatology, 9, Boston. American Meteorological Society, Boston: PREPRINTS, 1995. Pp. 233 – 236.

Ministerio de Energía y Minas, 1998. Estudio de evaluación ambiental territorial y de planeamiento para la reducción o eliminación de la contaminación de origen minero en la cuenca del río Santa (Online).

Miro, J. J.; Estrela, M. J. (2004): Tendencia de la temperatura en los meses de julio y agosto en la comunidad Valenciana en las ultimas décadas: Cambio en la frecuencia de días calurosos. Asociación Española de Climatología y Universidad de Cantabria, Serie A, Nº 4, Santander, 389-398.

Morales-Arnao, B., 1998. Glaciers of Peru. In: Williams, R.S., Jr., and Ferrigno, J.G., eds., Satellite Image Atlas of Glaciers of the World: U.S. Geological Survey Professional Paper 1386 (Glaciers of South America).

Nakicenovic, N. and Swart, R., 2000. Emissions Scenaríos. 2000, Special Report of the Intergovernmental Panel on Climate Change. Cambridge University Press.

Nobre, C. A.; Sampaio, G.; Salazar, L. F.; (2007): Mudancas climáticas e Amazonia. Ciencia e Cultura (SBPC), v.59, p 22-27.

Obregón, G. O., Marengo J. A. 2006: Tendencias y Variabilidad de la Precipitación en el Perú. Variabilidad Climática y Cambio climático, Impacto en el loro de las metas del milenio. IV Encuentro RUPSUR 2006. Santiago de Cali, Colombia. 8-10 de noviembre de 2006.

Pielke et al., 1992. A Comprehensive Meteorological modeling System RAMS. Meteorol. Atmos. Phys. 49, 69-9.

Ponce de León, R. G. 2000: Perú: visión global y de síntesis. Auge Editores SA. Lima – Perú.

Pouyaud, B., Zapata, M., Yerren, J., Gómez, J., Rosas, G., Suárez, W., and Ribstein, P. (2005). Avenir des ressources en eau galciaire de la Cordillère Blanche. Hydrological Sciences - Journal - des Sciences Hydrologiques 50, 999-1021.

Quinn, W. H. y Neal, V. T. 1992. The Historical record of El Niño events. in Climate since AD 1500, R. S. Bradley, P. D. Jones, Eds. (Routledge, London, 1992), pp. 623-648.

Rajagopalan, B., Y. Kushnir, and Y. M. Tourre (1998), Observed Decadal Midlatitude and Tropical Atlantic Climate Variability, Geophys. Res. Lett., 25(21), 3967–3970

Sanabria, J., y Zevallos L, 2006: tendencias térmicas y pluviométricas indicadores de un cambio climático en la sierra sur y zonas costeras del Perú de 1960 al 2006 (estudio diagnóstico). Estudio técnico del Servicio Nacional de Meteorología e Hidrología del Perú – SENAMHI, s/p.

Sen, P.K. (1968). "Estimates of the regression coefficient based on Kendall´s tau". Journal of the American Statistical Association, 63: 1379-1389.

SENAMHI y OSE, 1986. Boletín Agroclimático del Perú. Proyecto PADI – EIA. Características climáticas por departamentos.

SENAMHI, 1988: Mapa de Clasificación Climática del Perú. Método de Thornthwaite. Eds. SENAMHI Perú, 50 pp.

SENAMHI, 2005: Climate change scenaríos in Peru to 2050: Piura river basin. Autores: Rosas G., Díaz A., Ávalos G., Oria C., Acuña D., Cornejo A., Metzger L., Fano G., Carrillo M., Miguel R., PROCLIM. Eds. SENAMHI Perú, 170 pp.

SENAMHI, 2007: Escenarios de cambio climático en la cuenca del río Mantaro para el año 2100. Autores: Ávalos G., Díaz A., Oria C., Acuña D., Metzger L., Rosas G. y Miguel R., PRAA. Eds. SENAMHI Perú, 124 pp.

SENAMHI, 2008: Escenarios climáticos en el Perú para el año 2030. Autores: Obregón G., Díaz A, Rosas G., Ávalos G., Acuña D., Oria C., Metzger L., Llacza A. y Miguel R., Eds. SENAMHI – MINAM, Perú, 100 pp.

Trenberth, K.E., P.D. Jones, P. Ambenje, R. Bojariu, D. Easterling, A. Klein Tank, D. Parker, F. Rahimzadeh, J.A. Renwick, M. Rusticucci, B. Soden and P. Zhai, 2007: Observations: Surface and Atmospheric Climate Change. In: Climate Change 2007: The Physical Science Basis. Contribution of Working Group I to the Fourth Assessment Report of the Intergovernmental Panel on Climate Change [Solomon, S., D. Qin, M. Manning, Z. Chen, M. Marquis, K.B. Averyt, M. Tignor and H.L. Miller (eds.)]. Cambridge University Press, Cambridge, United Kingdom and New York, NY, USA.

Vincent, L.A., T.C. Peterson, V.R. Barros,M.B. Marino, M. Rusticucci, G. Carrasco, E. Ramirez, L.M. Alves, T. Ambrizzi, M.A. Berlato, A.M. Grimm, J.A. Marengo, L. Molion, D.F. Moncunill, E. Rebello, Y.M.T. Anunciação, J. Quintana, J.L. Santos, J. Baez, G. Coronel, J. Garcia, I. Trebejo, M. Bidegain, M.R. Haylock, D. Karoly: Observed trends in indices of daily temperature extremes in South America 1960-2000. Journal of Climate, 18: 5011-5023. 2005.

Vuille, M., 2007: Climate change in the Tropical Andes – Impacts and consequences for glaciation and water resources. Part I, II and III. A report for CONAM and the World Bank.

APPENDIX 1

HYDROMETEOROLOGICAL NETWORK
RELIEF MAPS AND CLIMATE CLASSIFICATION

Map N[a]	Name of the Map
Map N° 1	Hydrometeorological network map at national level
Map N° 2:	Relief map
Map N° 3:	Climate classification map

APPENDIX 2

MULTIANNUAL AVERAGES MAPS

EXTREME EVENTS AND CURRENT TRENDS

Map Nª	Name of the Map

APPENDIX 3
CLIMATE SCENARIOS MAPS
TO 2020 AND 2030

Map Nª	Name of the Map

APPENDIX 4

CONCEPTS AND BASIC TERMS

In order to better understand this document it is necessary to know certain terms and definitions related to the subject. This glossary is based on the last report of the IPCC (2007).

Climate change
It is an important variation of climate that persists for a prolonged period of time. Such variation occurrs at different time scales and affect all the climate parameters: temperature, precipitations, cloudiness and others. It is due to natural causes and, in the last centuries, to human activities.

Climate model
Numerical representation of the climate system based on the physical, biological and chemical properties of its components, in its interactions and that gathers all or some of its properties.

Climate scenarios
They are possible descriptions of how cliamte may change in the future. The methodology used to elaborate these scenarios varies according to the evaluation purpose. For many years, the scenarios have been used by the governments in business and military fields, for strategic planning. These socio-economic scenarios provide the basis as how the future may be.

Climate variability
It's the natural variability of the climate system, particularly at seasonal time scales or longer, it is preferably subject to certain spatial and temporal scales, because of the dynamical characteristics of the atmospheric circulation and the interactions with the land and ocean surface. Such patterns are known also as the regimens, modes or teleconnections.

Drought
Whilhite and Glants (1985) found more than a hundred definitions of drought, which were classified in four groups: meteorological, hydrological, agricultural and socio-economic. Also they defined the meteorological drought as an expression of the deviation of precipitation with respect to the mean during a determined period of time. On the other hand, managing and planning water resources systems involves the different hydrological processes, such as floods, shortages and droughts. (Salas et al., 2005).

Environment
It is where all the processes and agents that participate in daily life get together; they can be natural or anthropogenic. The interaction among these agents aims at attaining balance and harmony.

Glacier retreat
It is the fusion of snow as a consequence of temperature increase. One of the main causes is global warming that is rising temperature year after year and that is causing glacier melting of the ice caps, of glaciers, which is originating several problems such as the loss of sweet water for human consumption.

Global warming
Is a generalized phenomenon as consequence of the greenhouse effect at global scale, showing an increase in the Earth's temperature. This phenomenon causes a warming in some zones and a cooling in others; it is the main cause of climate change.

Global Warming Potential
It is a referential value that allows to compare the power that have the greenhouse gases with respect to the carbon dioxide CO2, which has a proportional value of global warming power equal to 1 and CH4 to 25, which means the CH4 has 25 times the power of warming the earth with respect to CO2.

Greenhouse effect
It is a phenomenon through which the greenhouse gases effect trap part of the energy coming form the surface after it heats up due to solar radiation and it prevents the sun energy from returning immediately to space,

Greenhouse gases
They are the ones that contribute to the greenhouse effect, due to their physical properties and their interaction with infra-red radiation.

Pollution
It is the presence of any agent (physical, chemical or biological) in the environment or the combination of them in places, in the different forms and concentrations, in such a way that may be harmful to health, security or welfare of the population or that may be harmful to animal or vegetal life. It is also the incorporation of solid, liquid or gaseous substances into receptive bodies, that adversely alter their natural conditions, or that may affect health, sanitation or welfare of people.

Predictability
It is the capacity to predict the future condition of a system knowing its current and previous state. The knowledge of the current and previous conditions of the climate system is usually faulty or imperfect, and the climate system is essentially non-linear and chaotic, which makes predictability essentially limited; even though models and precise observations are used, there are some limitations concerning predictability of a non-linear system as it is climate.

Uncertainty
It is the expression of the lack of knowledge of a determined value (for example the future state of the climate system). It can be due to the lack of information or a disagreement with respect to something that is known.

Vulnerability
It is the measure in which a system is able or unable to face the negative effects of climate change, even climate variability or extreme episodes. Vulnerability depends on the magnitude, the conditions and the index of climate variability to which a systems is exposed to, its sensibility and its capacity of adaptation.

Ministry of Environment - MINAM
Av. Guardia Civil 205, San Borja, Lima - Peru
Telf.: (511) 2255370
www.minam.gob.pe
minam@minam.gob.pe

National Meteorology and Hidrology Service - SENAMHI
Jr. Cahuide 785, Jesús María, Lima - Peru
Telfs.: (511) 6141414
www.senamhi.gob.pe